UNIVERSITÉ DU QUÉBEC

VARIATIONS SPATIALES ET TEMPORELLES DE LA SÉDIMENTATION SOUS LA ZONE EUPHOTIQUE DANS LE SECTEUR CANADIEN DE LA MER DE BEAUFORT

THÈSE

PRÉSENTÉE À

L'UNIVERSITÉ DU QUÉBEC À RIMOUSKI

comme exigence partielle

du programme de doctorat en océanographie

PAR

THOMAS JUUL-PEDERSEN

Décembre 2007

UNIVERSITÉ DU QUÉBEC

SPATIAL AND TEMPORAL PATTERNS OF SEDIMENTATION BELOW THE EUPHOTIC ZONE IN THE CANADIAN BEAUFORT SEA

THESIS

PRESENTED TO

L'UNIVERSITÉ DU QUÉBEC À RIMOUSKI

in partial fulfillment of the requirements of the

Doctorate Program in Oceanography

BY

THOMAS JUUL-PEDERSEN

December 2007

AVANT-PROPOS

"So throw off the bowlines, sail away from the safe harbor. Catch the trade winds in your sails. Explore. Dream. Discover" (Mark Twain). What started a few years ago with a flight across the Atlantic Ocean soon became a voyage of exploration and learning. I will forever be indebted to my parents, Marian and Holger Juul-Pedersen, and my brother, Lars-Henrik Thorngreen, for always encouraging me to explore new horizons, while providing a profound sense of stability and unwavering support – always a safe harbor. A warmhearted thanks to my new-found Canadian friends for making me feel so welcome.

My Arctic journey started in Greenland where, during my second visit, I had the privilege of working with Dr. Christine Michel, as arranged by my Master of Science supervisor Dr. Torkel Gissel Nielsen. This meeting facilitated my involvement in a field project in Resolute Passage, Canadian Arctic, and led to a Ph.D. collaboration with Drs. Christine Michel and Michel Gosselin. I will always remain grateful to Christine and Michel for accepting me as their student. Christine and Michel contributed greatly to this thesis and I would like to acknowledge all their guidance and hard work. Christine, thank you for always taking time to discuss the thesis and instilling a strong scientific professionalism. I really appreciate our friendship. Michel, I would like thank you for your

always insightful and constructive input. I have enjoyed all the good times we spent in the field, at meetings and during my stay in Rimouski.

This project has greatly benefited from the support and assistance of numerous collaborators. To our team, C. Michel, M. Gosselin, A. Niemi, B. LeBlanc, M. Różańska and M. Poulin I send a special thanks for your invaluable efforts and friendship. I am also grateful for the support of our collaborators, S. Brugel, K. Lacoste, M. Lizotte, W. Moskal, L. Seuthe, A. Tatarek, J. Wiktor, M. Zajaczkowski and many more. I would like to acknowledge the assistance provided by K. Proteau, K. Wilson, K. Cherewyk, D. Bérubé, M. Simard and J. Ferland in the processing of samples. This project was part of the Canadian Arctic Shelf Exchange Study (CASES) and I would like to convey my gratitude to the CASES project organizers and the coast guard officers and crew onboard the CCGS *Amundsen*, for making this research possible.

I wish to thank Dr. A. Rochon (Université du Québec à Rimouski, UQAR) for being part of my thesis and evaluation committees and Dr. J.-É. Tremblay (Université Laval) for being part of my thesis committee. I am also very grateful that Dr. P. Wassmann (Norwegian College of Fishery Science, University of Tromsø) agreed to be the external member of my evaluation committee. Finally my gratitude goes to the students and staff at the Institut des sciences de la mer de Rimouski (ISMER) and UQAR who assisted in maintaining my long-distance study from Winnipeg.

This project was supported by grants from the Natural Sciences and Engineering Research Council (NSERC) of Canada and from the Department of Fisheries and Oceans Canada (DFO). Funding was also provided by the International Joint Ventures Fund of the Canada Foundation for Innovation and the Fonds québécois de la recherche sur la nature et les technologies (FQRNT). My involvement in this Ph.D. program was made possible by post-graduate scholarships from ISMER and UQAR (Exemptions des frais majorés pour étudiants étrangers).

This research is a contribution to the research programs of CASES, the Freshwater Institute (Fisheries and Oceans Canada), ISMER and Québec-Océan. The results presented in this thesis have been presented at the CASES general meetings in Montréal, QC (October 2004) and Winnipeg, MB (February 2006), the Gordon Research Conference on Polar Marine Science in Ventura, CA (March 2005), the American Society of Limnology and Oceanography (ASLO) summer meeting in Victoria, BC (June 2006) and the Arctic Science Conference in Fairbanks, AK (October 2006). The three main chapters of this thesis will be published in scientific journals. The first chapter is currently in press in *Marine Ecology Progress Series*, the second chapter has been submitted to the CASES special issue in *Journal of Marine Systems* and the third chapter will be submitted to an international journal.

RÉSUMÉ

La sédimentation de la matière particulaire a été étudiée sous couvert de glace de première année et en eau libre dans le secteur canadien de la mer de Beaufort. Les patrons saisonniers d'exportation verticale de la matière particulaire ont été étudiés pendant toute la période de production des algues de glace, de la fin de l'hiver à la fonte printanière, en ciblant la couche de surface près de la base de la glace (jusqu'à une profondeur de 25 m). En eau libre, les variations spatiales de l'exportation verticale de la matière particulaire sous la zone euphotique ont été étudiées en fonction des caractéristiques particulières de cette région, i.e., l'influence du panache du fleuve Mackenzie et de la polynie du Cap Bathurst.

L'étude réalisée sous la glace de première année de la baie de Franklin a montré une étroite relation entre l'augmentation de la biomasse des algues de glace et la sédimentation du matériel algal au printemps, avant la fonte de la glace. De plus, nous avons observé une importante contribution de matériel non-algal à l'exportation verticale du matériel. Cette étude a mis en évidence une transformation significative du matériel algal qui sédimente, dans les 25 premiers mètres de la colonne d'eau. La fonte printanière a mis fin à la période de production des algues de glace, tel que montré par une augmentation importante de la sédimentation du matériel organique associée avec la libération de la biomasse présente dans la glace. Il est généralement considéré que la sédimentation de matériel provenant de l'interface glace-eau est liée à la fonte de la glace. Nos résultats remettent ce principe en question, bien que le maximum de sédimentation ait été observé pendant la période de fonte.

L'étude spatiale en eau libre a montré que l'étendue saisonnière des taux de sédimentation du matériel organique particulaire était comparable dans la région influencée par le fleuve Mackenzie et dans la polynie du Cap Bathurst. Nous avons observé une diminution saisonnière de la sédimentation du matériel organique particulaire de l'été à l'automne, dans toute la région d'étude. Cette étude a aussi montré qu'une succession d'espèces phytoplantoniques, à même le matériel qui sédimente, prévaut dans le secteur canadien de la mer de Beaufort, malgré les différences spatiales et interannuelles entre les stations d'échantillonnage. Une étude comparative de l'exportation verticale du matériel à une station de glace de rive, en présence de couvert de glace et en période libre de glace, a mis en évidence l'importance de l'exportation verticale de la matière organique particulaire sous la glace, notamment au cours de la période de fonte.

ABSTRACT

The sedimentation of particulate material was assessed under first-year sea ice and in open waters in the Canadian Beaufort Sea. Seasonal patterns of particulate material sinking export were studied throughout the ice algal productive period, from late winter to spring melt, targeting the upper water column near the bottom surface of the sea ice (down to 25 m). In open waters, spatial patterns in the sinking export of particulate material from the euphotic zone were related to key features of this region, i.e. the influence of Mackenzie River and the Cape Bathurst Polynya.

The underice component of this study showed a close coupling between the increasing ice algal biomass and the sedimentation of algal material in spring, prior to the onset of ice melt. In addition, we observed a large contribution of non-algal material to the sinking flux of material. This research also showed significant transformation of the sedimenting algal material in the upper 25 m of the water column. Spring melt induced the termination of the ice algal productive period, as shown by a strong increase in the sedimentation of organic material associated with the release of ice biomass. Passive sinking export of material across the ice-water interface is generally considered to be related to ice melt. Our results challenge this view, even if the spring melt period showed maximum sedimentation.

The spatial investigation during ice-free conditions revealed comparable seasonal ranges of sinking export of particulate organic material between the region influenced by the Mackenzie River and the Cape Bathurst polynya. A general seasonal decrease in the sinking export of particulate organic material was observed from summer to fall throughout this study. This research also found that a strong seasonal phytoplankton species succession prevailed in the Canadian Beaufort Sea, regardless of the spatial and interannual differences between sampling stations. A comparison of the sinking export of particulate organic material at a landfast station, during the ice covered period and subsequent ice-free conditions, emphasized the importance of underice sinking export of particulate organic material, particularly during spring melt.

TABLE DES MATIÈRES

LISTE DES TABLEAUX

CHAPITRE 1:

SEASONAL CHANGES IN THE SINKING EXPORT OF PARTICULATE MATERIAL, UNDER FIRST-YEAR SEA ICE ON THE MACKENZIE SHELF (WESTERN CANADIAN ARCTIC)

CHAPITRE 2:

INFLUENCE OF THE MACKENZIE RIVER PLUME ON THE SINKING EXPORT OF PARTICULATE MATERIAL ON THE SHELF

CHAPITRE 3:

SINKING EXPORT OF PARTICULATE ORGANIC MATERIAL FROM THE EUPHOTIC ZONE IN THE EASTERN BEAUFORT SEA

LISTE DES FIGURES

INTRODUCTION GÉNÉRALE

CHAPITRE 1:

SEASONAL CHANGES IN THE SINKING EXPORT OF PARTICULATE MATERIAL, UNDER FIRST-YEAR SEA ICE ON THE MACKENZIE SHELF (WESTERN CANADIAN ARCTIC)

CHAPITRE 2:

INFLUENCE OF THE MACKENZIE RIVER PLUME ON THE SINKING EXPORT OF PARTICULATE MATERIAL ON THE SHELF

CHAPITRE 3:

SINKING EXPORT OF PARTICULATE ORGANIC MATERIAL FROM THE EUPHOTIC ZONE IN THE EASTERN BEAUFORT SEA

INTRODUCTION GÉNÉRALE

The Arctic Ocean

In recent decades it has become more apparent that the global climate is changing and that a warming trend is at the center of this change. The global mean surface temperature has increased by ca. 0.7°C over the last 100 years (from 1906 to 2005), increasing at a rate of 0.1°C per decade over the last 50 years (IPCC 2007). Although the basis for the present global warming trend is still debated (e.g. Oreskes 2004), there is growing evidence that increasing atmospheric concentrations of the so-called green-house gases, particularly carbon dioxide and methane, play a key role (IPCC 2007). The present atmospheric concentrations of carbon dioxide and methane are the highest reported from ice core records dating back 650,000 years (379 ppm and 1774 ppb, respectively, in 2005), reflecting a significant increase since the pre-industrial era (280 ppm and 730 ppb, respectively, in 1750; IPCC 2007).

Nowhere has the observed temperature increase been more pronounced than in the Arctic, with land-surface temperatures increasing by 0.4°C per decade over the past 40 years (ACIA 2005). The extensive sea ice cover, permafrost areas and glaciers make the Arctic highly susceptible to increasing temperatures. In addition, reduction of the sea ice cover triggers a positive feed-back mechanism for temperature increases in the Arctic

(Johannessen et al. 2004), due to the reduction in surface albedo associated with a shift from sea ice to open water conditions (ca. 80 and 20 % of incident solar radiation, respectively; Kerr 1999). Altogether, the Arctic is considered an early indicator of climate change, particularly increasing temperatures (ACIA 2005, IPCC 2007).

Sea ice in the Arctic Ocean is already showing signs of the ongoing warming trend, as the annual average sea ice extent has decreased by ca. 3 % per decade between 1978 and 2005 (IPCC 2007). The summer minimum sea ice cover, i.e. the multi-year sea ice concentrated mainly in the central Arctic Ocean, is showing the highest rate of decrease, at ca. 7 % per decade between 1978 and 2005 (IPCC 2007). The reason for the different loss rates is that multi-year sea ice is being replaced by first-year sea ice in some areas, thus increasing the seasonal ice zone (Comiso 2002). In addition, the seasonal first-year sea ice cover in the Arctic Ocean is predicted to show earlier ice break-up in spring, delayed refreezing in fall and larger and more widespread flaw lead systems and polynyas (ACIA 2005, Lukovich & Barber 2005). Consequently, areas of permanently and seasonally ice-free conditions are projected to expand in size and duration, particularly on the continental shelves of the Arctic Ocean (ACIA 2005, IPCC 2007).

Increasing precipitation is another projected consequence of the warming trend in the Arctic, with a projected increase in the freshwater runoff to the Arctic Ocean by up to ca. 15 % at the end of this century (ACIA 2005). The Arctic Ocean already receives the highest freshwater runoff of any ocean relative to its size, since it receives 11 % of the global

runoff but represents only 1 % of the world ocean water (Shiklomanov 1998). Arctic rivers generally display a high discharge of organic material (Dittmar & Kattner 2003), which is likely to increase with the projected increasing runoff and melting permafrost (ACIA 2005). The already strong riverine discharge of freshwater and material (Gordeev & Rachold 2004), may therefore extend further onto and beyond the Arctic shelves.

Arctic continental shelves

The continental shelves are key regions of the Arctic Ocean, comprising more than half of its total surface area (53 %; Jakobsson 2002) and displaying the highest annual primary production (between ca. 170 and 323 Mt C y^{-1}; Sakshaug 2004, Michel et al. 2006). In two recent reviews, the Arctic shelves were categorized in terms of their exchange of water with the Atlantic or Pacific oceans (Fig. 1); as inflow, outflow or interior shelves (Carmack & Wassmann 2006, Carmack et al. 2006).

This study focuses on the Canadian sector of the Beaufort Sea Shelf (Fig. 1), categorized as a narrow interior shelf (Carmack & Wassmann 2006). This region includes a shelf plateau bordering the Canada Basin in the Arctic Ocean, covering ca. 530 km alongshore and ca. 120 km offshore (ca. 6.0 x 10^4 km^2; Carmack et al. 2004). This shelf receives freshwater from the Mackenzie River, which is the fourth largest river entering the Arctic Ocean in terms of annual freshwater discharge (from 249 to 333 km^3; Dittmar & Kattner 2003). Along with the high freshwater discharge, occurring mostly between May to

September, the Mackenzie River shows the highest discharge of inorganic sediments of all the Arctic rivers (ca. 127 Mt y^{-1}; Macdonald et al. 1998). Also considered part of the Canadian Beaufort Sea Shelf is the Amundsen Gulf, extending east from the Beaufort Sea to the Canadian Arctic Archipelago, and covering ca. 8.7 x 10^4 km^2 (Bélanger et al. 2006). The Amundsen Gulf is characterized by the Cape Bathurst Polynya, which generally starts forming in May from a flaw lead system separating landfast first-year sea ice from the offshore drifting pack-ice on the shelf (Barber & Hanesiak 2004). Sea ice continues to retreat, during summer, generally leaving the Canadian Beaufort Sea Shelf completely free of sea ice by September (Carmack & Macdonald 2002).

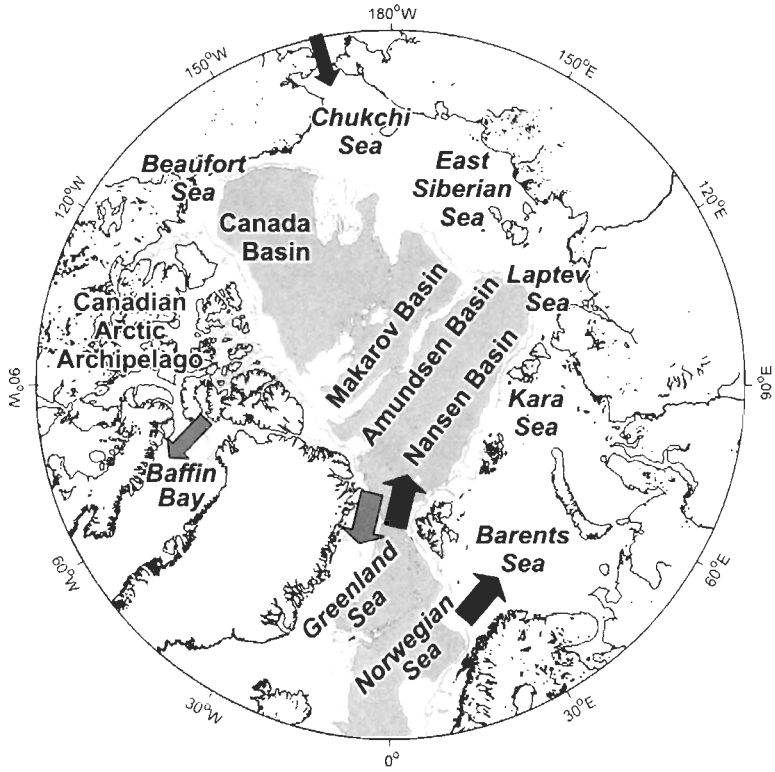

Fig. 1. The Arctic Ocean with its shelves and basins. The black arrows indicate places and strength for the inflows of Atlantic and Pacific Waters and the grey arrows indicate the outflows of Arctic Water (redrawn after Carmack & Wassmann 2006)

Most Arctic shelves show a strong seasonal freshwater influence from melting first-year sea ice and terrestrial runoff, in spring and summer (Köberle & Gerdes 2007, Dickson et al. 2007). The resulting stratification of the water column influences the seasonal pelagic primary production on these shelves; initially promoting phytoplankton production above the halocline, while later limiting the replenishment of nutrients to the phytoplankton community, as described later. Still, pelagic phytoplankton production dominates the total annual primary production on Arctic shelves, comprising an estimated ca. 75 to >97 % of the integrated ice algal and phytoplankton production (Subba Rao & Platt 1984, Legendre et al. 1992, Gosselin et al. 1997).

Seasonal primary production and sinking export

Primary production in the Arctic Ocean is governed by the extreme annual cycle of sunlight and the low angle of the sun above the horizon, at high latitudes; along with the reduced light penetration in the water column during the sea ice covered period (Carmack et al. 2004, 2006, Sakshaug 2004, Hill & Cota 2005). Yet, algal cells, mainly pennate diatoms (Michel et al. 1996, Gosselin et al. 1997, Gradinger 1999, von Quillfeldt et al. 2003), entrained in the newly formed ice at the time of its formation (Garrison et al. 1989, Gradinger & Ikävalko 1998, Riedel et al. 2007), initiate an ice algal bloom during early spring (Michel et al. 2006). Variable ice thickness and snow cover on top of first-year sea ice produce spatial patchiness in ice algal biomass on Arctic shelves (Gosselin et al. 1986, Mundy et al. 2005). Ice algae in first-year sea ice are considered a seasonally important

food source for some pelagic copepods (Runge & Ingram 1988, Conover & Siferd 1993, Michel et al. 1996, Hattori & Saito 1997) and amphipods (Werner 2000), and also support sympagic micro- and meiofauna (Nozais et al. 2001, Michel et al. 2002).

Ice algal blooms are usually terminated during ice melt in spring, often resulting in an abrupt export of ice bound material to the underlying water column (Tremblay et al. 1989, Michel et al. 1996, 2002, Fortier et al. 2002, Lalande et al. 2007). Since the timing of the ice melt and break-up may vary significantly between years (e.g. Barber & Hanesiak 2004), the sinking export of ice algal material may not parallel the annual cycle of pelagic herbivorous zooplankton (i.e. "mismatch" scenario; Wassmann 1998), notably calanoid copepods in Arctic waters (Dawson 1978, Hirche & Mumm 1992, Richter 1995, Hirche 1997, Madsen et al. 2001). Under such a scenario, the sinking export of ice algae may represent a seasonally important input of organic material to the benthic communities (Carey 1987, Renaud et al. 2007b).

Unimpeded light penetration to the water column after the ice break-up, a stratified water column formed by melt water and high nutrient concentrations following winter mixing, generally promote a pelagic diatom bloom in spring, i.e. ice edge bloom (Sakshaug & Skjoldal 1989, Strass & Nöthig 1996, Head et al. 2000, Rat'kova & Wassmann 2002). This intense primary production event often leads to nitrate or silicic acid depletion in the surface mixed layer on Arctic shelves (Tremblay et al. 2002a, 2006a, Carmack et al. 2004, Hill & Cota 2005), accompanied by increased sinking export of primary-produced material

(Wassmann et al. 2004 and references therein). Yet, herbivorous grazing activity may be considerable during spring phytoplankton blooms reducing the sinking export of primary-produced material (Andreassen & Wassmann 1998, Olli et al. 2002, Juul-Pedersen et al. 2006, Tremblay et al. 2006b).

Phytoplankton production in summer on Arctic shelves generally remains limited by nitrate and silicic acid, following the spring diatom bloom (Tremblay et al. 2002b, Carmack et al. 2004, Hill & Cota 2005). Nutrient depletion in the surface mixed layer often leads to a seasonal phytoplankton succession, from a diatom dominated spring bloom to a dominance of flagellates, which have no requirement for silicic acid and higher nutrient affinity than diatoms, during summer and fall on Arctic shelves (Bursa 1963, Heiskanen & Keck 1995, Booth & Smith 1997, Rat'kova et al. 1998, Lovejoy et al. 2002, Hill et al. 2005).

Calanoid copepods are abundant during summer on Arctic shelves and shelf-slopes (Madsen et al. 2001, Pasternak et al. 2002, Ringuette et al. 2002, Hirche & Kosobokova 2003, Riser et al. 2007), while copepod nauplii and protozooplankton may become dominant towards the fall. At that time, various species of adult copepods descend to depth to overwinter, as seen in Disko Bay, Greenland (Madsen et al. 2001). Zooplankton may therefore utilize much of the phytoplankton biomass in summer. A phytoplankton bloom may occur in the fall due to vertical mixing with deeper nutrient-rich waters during increased wind activity (e.g. Klein et al. 2002, Arrigo & Dijken 2004). According to predicted climate-change scenarios, a retreating multi-year sea ice cover may expose the

shelf-break to seasonally ice-free conditions and increased wind effect, thus promoting upwelling of nutrient-rich waters from the central Arctic basins onto the Arctic shelves (Carmack & Chapman 2003).

Ice algae initiate the primary production season in response to increasing light levels, after winter, on the Canadian Beaufort Sea Shelf (Carmack & Macdonald 2002). Horner & Schrader (1982) reported an increase in ice algal production and biomass from March until the onset of ice melt in early-June 1979 (reaching ca. 63 mg C m^{-2} d^{-1} and >26 mg chlorophyll *a* m^{-2}, respectively), with ice algal production comprising about two-thirds of the total primary production (i.e. ice algal, phytoplankton and benthic microalgae). An increase in the sinking export of particulate organic carbon (POC) during ice melt in May and June was observed during two separate studies in 1987 and 2004 (O'Brien et al. 2006, Forest et al. 2007). Phytoplankton production, after the ice break-up, was reported to increase until late-July (reaching ca. 200 mg C m^{-2} d^{-1}), when nitrogen became limited in the surface mixed layer (Carmack et al. 2004). Subsequent summer phytoplankton production (between ca. 40 to 100 mg C m^{-2} d^{-1}) was concentrated deeper (20 to 40 m), where nutrient concentrations were higher (Carmack et al. 2004). The presence of the Mackenzie River plume, in summer, has been shown to induce higher sinking export of POC near the river outlet (ca. 80 mg C m^{-2} d^{-1} at 213 m; O'Brien et al. 2006). Satellite images of the Cape Bathurst Polynya, in the Amundsen Gulf region, showed occurrence of two distinct phytoplankton blooms (Arrigo & Dijken 2004). A spring bloom followed the

sea ice retreat, while a later and often stronger phytoplankton bloom was reported in fall, though timing and intensity of the blooms varied interannually (Arrigo & Dijken 2004).

Pelagic-benthic coupling

Gravitational vertical export, i.e. sinking export, of organic material is the principal transport pathway linking pelagic primary production with the benthos. Yet, a multitude of biogeochemical transformational processes affect the organic material during its transport, heterotrophic degradation generally being the most pronounced (Boyd & Trull 2007). As such, sinking algal cells may be subjected to bacterial degradation (Smith et al. 1995, Grossart & Simon 2007) and viral cell lysis (Suttle 2005) but, often more importantly, to zooplankton grazing (Turner 2002 and references therein). Transformation of the sinking organic material during sinking generally follows a non-linear trend with depth, often explained by a power law function (Buesseler et al. 2007), as first described by Martin et al. (1987). High abundance and activity of zooplankton and bacteria in the surface and subsurface layer, along with differential solubilisation of organic material (Smith et al. 1992, Hoppe et al. 1993), are considered the main reasons for the exponential attenuation in sinking export of organic material with depth (Boyd & Trull 2007 and references therein).

The residence time of the sinking material within the pelagos determines the time available for transformational processes to affect the material in transit (Schnack-Shiel & Isla 2005, Riser et al. 2007). Aggregation of ice algal (Riebesell et al. 1991) and

phytoplankton (Kiørboe et al. 1996) cells is a key process that may increase their sinking velocity, and is often enhanced during high cell concentrations and in the presence of transparent exopolymeric particles (TEP) (Engel 2003, Grossart et al. 2006). Yet, these aggregates may at the same time improve the availability of organic material to mesozooplankton, by increasing the size of food particles (Kiørboe 2001).

The copepod dominated mesozooplankton community, in Arctic waters, generally congregates within the euphotic zone where the phytoplankton cell concentrations are highest during spring and summer (Richter 1995, Madsen et al. 2001, Pasternak et al. 2002, Astthorsson & Gislason 2003, Hirche & Kosobokova 2003, Riser et al. 2007). Fecal pellets may at times comprise a significant fraction of the organic material sinking from the euphotic zone towards the benthos in Arctic waters (González et al. 1994, Riebesell et al. 1995, Urban-Rich et al. 1999, Riser et al. 2002, Sampei et al. 2004, Juul-Pedersen et al. 2006). Although fecal pellets represent the waste product of zooplankton grazing activity they may have a high organic content, particularly during periods of high food availability (Penry & Frost 1991, Turner 2002). Still, herbivorous grazing translates into a loss of primary-produced organic material to assimilation (Conover 1966, Landry et al. 1984, Møller et al. 2003) and leaking of dissolved organic material to the surrounding water (Strom et al. 1997, Møller & Nielsen 2001, Møller et al. 2003). In spite of the generally high sinking velocity of fecal pellets, i.e. a short residence time in the pelagos (Turner 2002), their ingestion (coprophagy) and/or fragmentation (coprohexy) may be effective in

reintroducing egested material into the pelagic food web (Sampei et al. 2004, Riser et al. 2007 and references therein).

Advective processes may disrupt the pelagic-benthic coupling in a particular area, by horizontally exporting or importing material. As such, benthic and intermediate nepheloid layers, i.e. particle-rich layers, are important in transporting resuspended and sinking material from the continental shelves onto the continental slopes (McPhee-Shaw 2006 and references therein). Cross-shelf transport has been reported during long-term studies of sinking export on the Canadian Beaufort Sea Shelf (O'Brien et al. 2006, Forest et al. 2007). While these advective processes for the most part occur below the stratum studied in this study, they are part of the pelagic-benthic coupling and will influence the sequestration of material. Nevertheless, the sediments on the Canadian Beaufort Sea Shelf still retain a clear signal of input from the Mackenzie River (Macdonald et al. 1998, Carmack & Macdonald 2002). Moreover, a tight pelagic-benthic coupling was suggested during a study of the benthic carbon demand on the Canadian Beaufort Sea shelf/slope, indicating that the carbon demand of the sediment communities accounted ca. 60 % of the annual new primary production, i.e. primary production based on allochthonous nutrients, in this region (Renaud et al. 2007a).

Research objectives

Due to the challenges posed by ongoing climate change and the need to understand the sequestration of organic material in the ocean, much effort has gone into studying long-term time series of sinking export at depth. Consequently, processes affecting the sinking export of particulate material in the mesopelagic zone are not as well understood nor quantified (e.g. Boyd & Trull 2007). Yet, sinking export in this part of the water column will most likely be strongly affected by the predicted increase in pelagic primary production due to climate change. It is therefore imperative to obtain a better understanding of the biogeochemical processes affecting the organic material in transit through the mesopelagic zone towards the benthos.

As part of the Canadian Arctic Shelf Exchange Study (CASES), "an international effort under Canadian leadership to understand the biogeochemical and ecological consequences of sea ice variability and change on the Mackenzie Shelf" (http://www.cases.quebec-ocean.ulaval.ca), the main objective of this study was to assess the sinking export of particulate material from the euphotic zone in the Canadian Beaufort Sea. This has only been investigated once before in this area, using short-term deployments (5 d) of particle interceptor traps moored just above the bottom (at ca. 10 m) on the Alaskan Beaufort Sea Shelf (Carey 1987). The only other sedimentation studies in this area have focused on long-term sinking export of particulate material at depth on the Canadian Beaufort Sea shelf and slope (O'Brien et al. 2006, Forest et al. 2007).

The first chapter focuses on seasonal changes in the sinking export of particulate organic material under first-year sea ice, throughout the productive season of ice algae, from late winter to spring melt. The objectives of this chapter were three-fold. Our first objective was to estimate the sinking export of particulate material under first-year sea ice, at a landfast station, prior to ice algal production (late winter), for the duration of the productive season (early spring) and during spring ice melt. Our second objective was to evaluate changes in the magnitude of the sinking export and in the composition of the sinking organic material, after its release from the ice and during descent to depth. Our third objective was to quantify the daily loss of the standing biomass in the bottom sea ice and upper part of the water column through sinking. It was hypothesized that the sinking export of organic material would increase during spring melt and that ice algal material would dominate the organic material exported from the sea ice.

In the second chapter, the influence of the Mackenzie River on the sinking export of particulate material and on the composition of this material on the adjacent shelf was evaluated. In order to tackle the influence of the Mackenzie River on the sinking export of particulate material, we studied the layer immediately under the surface halocline as well as the sedimentation signal recorded at deeper depths (down to 150 m) along two separate transects under the influence of the river plume. It was hypothesized that the river plume would induce higher sinking export of particulate organic material and would affect the composition of the sinking material.

The third chapter examines the sinking export of organic material from the euphotic zone in the Canadian Beaufort Sea. The objectives of this chapter were to assess spatial variations in the magnitude of the sinking export of particulate organic material in this area. A second objective was to characterize any patterns in the cell composition of the collected sinking material. The third objective was to make a comparison between the magnitude of sinking export of particulate organic material during the sea ice covered and subsequent ice-free periods at a landfast sea ice station. It was hypothesized that the Canadian Beaufort Sea would display spatial and seasonal differences in the sinking export of particulate organic material. It was also hypothesized that the comparative assessment at the landfast sea ice station would show higher sinking export of particulate organic material during ice-free conditions, when phytoplankton material may be exported from the euphotic zone.

CHAPITRE 1

SEASONAL CHANGES IN THE SINKING EXPORT OF PARTICULATE MATERIAL, UNDER FIRST-YEAR SEA ICE ON THE MACKENZIE SHELF (WESTERN CANADIAN ARCTIC)

RÉSUMÉ

La sédimentation du matériel particulaire a été étudiée sous couvert de glace de première année, de la fin de la période hivernale à la fonte printanière, sur le plateau du Mackenzie, dans l'Arctique canadien. Des pièges à particules à court terme ont été déployés à 1, 15 et 25 m sous la glace, à 16 occasions consécutives entre le 23 février et le 20 juin 2004. Des analyses de chlorophylle *a* (chl *a*), phaeopigments, carbone particulaire total (TPC), carbone et azote organique particulaire (POC et PON) et silice biogénique (BioSi) ont été effectuées sur le matériel collecté dans les pièges. Les flux verticaux de chl *a* et de BioSi ont augmenté de façon consistante entre le 19 mars et le début de la fonte printanière (26 mai). Par la suite, ces flux ont augmenté considérablement (maxima de 2.0 et 90.4 mg m^{-2} d^{-1}, respectivement). La contribution des cellules de grande taille (>5 µm) à la sédimentation de la chl *a* totale a aussi augmenté après le 19 mars (passant d'environ 60 % à 90 %), reflétant une augmentation de la contribution des diatomées à l'exportation verticale du matériel algal. En accord avec ce résultat, une relation linéaire significative entre le taux de sédimentation de la chl *a* à 1 m et la biomasse chlorophyllienne dans la glace, a été observée. En moyenne, près de la moitié (46 %) de la chl *a* exportée à 1 m a été perdue dans les 25 premiers mètres de la colonne d'eau. Le POC constituait la composante principale des flux de TPC (91 %) pendant toute la durée de l'étude. Les flux de POC, relativement stables jusqu'au début de la fonte printanière (valeurs médianes de 21.0 et 24.6 mg m^{-2} d^{-1} à 1 m), ont par la suite augmenté considérablement (maximum de 522 mg m^{-2} d^{-1}). Les rapports POC:chl *a* étaient élevés (étendue de 75.8 à 3474 g:g à 1 m), indiquant une contribution significative de matériel non-algal aux flux verticaux de POC. Les taux quotidiens de perte par sédimentation de la chl *a*, du POC et du PON, présents dans la glace et à l'interface glace-eau (premier mètre de la colonne d'eau), ont varié de façon saisonnière et étaient plus élevés pendant la période hivernale. Au cours de la période de quatre mois couverte par cette étude, les flux verticaux de chl *a*, POC et PON, mesurés à 1 m sous la glace, étaient de 31.3 mg m^{-2}, 7.2 mg C m^{-2}, et 1.3 mg N m^{-2}, respectivement. Les résultats de cette étude montrent que la matière organique est exportée de façon continue de la glace de première année, de l'hiver jusqu'à la fin du printemps.

ABSTRACT

The sinking export of particulate material under landfast first-year sea ice was studied from the winter period to spring melt on the Mackenzie Shelf, western Canadian Arctic. Short-term particle interceptor traps were deployed at 1, 15 and 25 m under the ice on 16 consecutive occasions from 23 February to 20 June 2004. The sinking material was analysed for chlorophyll *a* (chl *a*), phaeopigments, total particulate carbon (TPC), particulate organic carbon and nitrogen (POC and PON) and for biogenic silica (BioSi). The sinking fluxes of chl *a* and BioSi increased steadily after 19 March and until the onset of spring melt (26 May), after which these sinking fluxes increased considerably (maxima of 2.0 and 90.4 mg m^{-2} d^{-1}, respectively). The contribution of large algae (>5 μm) to the total chl *a* sinking flux also increased after 19 March (from ca. 60 % to 90 %), reflecting an increasing contribution of diatoms to the sinking export of algal material. Accordingly, chl *a* sinking fluxes at 1 m showed a significant linear relationship with bottom ice chl *a* biomass. On average, almost half (46 %) of the chl *a* exported at 1 m was lost in the upper 25 m. POC was the main component of the TPC sinking fluxes (91 %) throughout the study. POC sinking fluxes remained fairly stable until the onset of spring melt (median values of 21.0 and 24.6 mg m^{-2} d^{-1} at 1 m), after which a considerable increase was observed (maximum of 522 mg m^{-2} d^{-1}). High POC:chl *a* ratios (ranging from 75.8 to 3474 g:g at 1 m) indicated a significant contribution of non-algal material to the sinking POC. The daily sinking loss rates of chl *a*, POC and PON from the sea ice and interfacial layer (top 1 m of the water column) varied seasonally and were highest during the winter period. Over the 4-month duration of this study, underice sinking fluxes of chl *a*, POC and PON at 1 m were 31.3 mg m^{-2}, 7.2 g C m^{-2} and 1.2 g N m^{-2}, respectively. These results illustrate the continuous downward sinking export of organic material under landfast ice, from winter throughout late spring.

1.1 Introduction

The sinking export of organic material at the termination of phytoplankton blooms is a key process by which primary-produced material from surface waters is transferred to the benthos (e.g. Turner 2002). In ice-covered seas, where sea ice primary production precedes the phytoplankton bloom, the sinking of organic material from the sea ice may provide an early source of material for benthic communities (e.g. McMahon et al. 2006). In the Arctic Ocean, most sea ice primary production takes place in first-year sea ice, which is primarily found on shelf areas. Arctic continental shelves make up more than half (53 %; Jakobsson 2002) of the total area of the Arctic Ocean and adjacent seas. On these shallow shelves, higher annual primary production (phytoplankton and ice algal production) is found compared to the central Arctic Ocean (e.g. Gosselin et al. 1997). Ice algal chlorophyll *a* (chl *a*) biomass in the bottom layer of Arctic first-year sea ice may vary considerably between areas, and may reach concentrations of 250 mg m^{-2} (Smith et al. 1990). Although light and nutrient conditions have been observed to limit ice algal production (e.g. Gosselin et al. 1990), the production period of ice algae typically extends until they are released from the sea ice at the time of spring ice melt (e.g. Michel et al. 1996).

Ice algal communities in the Arctic have been shown to be directly grazed upon by pelagic copepods and amphipods (e.g. Werner 2000, Fortier et al. 2002) and, to a lesser extent, by sympagic fauna (Nozais et al. 2001, Michel et al. 2002). Still, the bulk of the ice algal biomass is mainly released into the water column at the time of spring ice melt (Tremblay et al. 1989, Michel et al. 1996, 2002, Fortier et al. 2002). Melnikov (1998) did,

however, suggest an export of material from the sea ice during ice growth, as a result of episodic brine drainage. Based on this study, Lavoie et al. (2005) applied a continuous export of ice algae from the sea ice throughout the period of ice algal development, when modelling ice algal growth and decline in Arctic first-year sea ice.

Primary-produced particulate organic material (POM) may either sink directly as intact algal cells or be diverted to the pelagic heterotrophic food web (e.g. Wassmann 1998, Turner 2002), which affects the composition of the sinking material. The sinking of intact algal cells may result in better preservation of the sinking POM (e.g. Turner 2002), though some loss usually occurs during sinking (e.g. release of dissolved material and dissolution). Algal cells released from the sea ice may either sink as intact cells or form aggregates, which may increase their sinking velocities and therefore decrease their residence time in the pelagic zone (e.g. Wassmann 1998). The other export pathway, through the heterotrophic food web, affects both the quantity and composition of the sinking particulate organic material (e.g. Turner 2002), and a considerably reduced amount of the ingested carbon may be reintroduced to the water column as fecal material (e.g. Møller et al. 2003). The efficiency of the heterotrophic food web in utilizing the sinking material is thought to depend largely on the timing and rate of release of the material from the sea ice in relation to the seasonal presence of grazers (e.g. Michel et al. 1996, Fortier et al. 2002). In northern Baffin Bay, ca. 75 % of the bottom first-year sea ice carbon biomass was observed sinking as intact algal cells (at 1 m under the sea ice; Michel et al. 2002), while ca. 60 % of the ice algal production was estimated to be channelled through pelagic herbivores in Resolute

Passage, Canada (Michel et al. 1996). Sinking ice algae are believed to provide a seasonally important food source for the pelagic (e.g. Michel et al. 1996, Werner 2000, Fortier et al. 2002) and benthic (e.g. McMahon et al. 2006) communities.

The Mackenzie shelf in the western Canadian Arctic covers an area of ca. 60 x 10^3 km^2 (defined by the 200 m isobath) and generally experiences a landfast inshore first-year sea ice cover from December to May-June and drifting pack ice on the outer-shelf during winter (Carmack & Macdonald 2002). Primary production on the Mackenzie shelf has been estimated at 12 to 16 g C m^{-2} y^{-1} (Carmack et al. 2004), and ice algae are estimated to account for < 15 % of the annual primary production (Horner & Schrader 1982, Macdonald et al. 1998). Ice algae have been observed forming dense mats on the under-surface of the sea ice on the Mackenzie Shelf, which were later dislodged from the sea ice during spring melt and sea ice break-up (Macdonald et al. 1998). These events could result in a large proportion of organic material reaching the benthos unutilized, if exceeding the grazing capacity of the pelagic heterotrophic food web. Indeed, Seuthe et al. (2007) showed that the underice copepods in Franklin Bay on the Mackenzie Shelf increased their grazing activity from March to May 2004. Studies of sinking fluxes under the sea ice on the Mackenzie Shelf are from long-term sediment trap moorings (O'Brien et al. 2006, Forest et al. 2007). From these studies, the annual particulate organic carbon (POC) sinking flux was estimated to vary between 1.7 - 5.8 g C m^{-2} y^{-1} (deployment depths ranging from 118 - 213 m; O'Brien et al. 2006) and 1.0 - 1.7 g C m^{-2} y^{-1} (depth of 200 m; Forest et al. 2007) on the Mackenzie Shelf.

The present study investigated the seasonal changes in the sinking flux of particulate material under first-year sea ice on the Mackenzie Shelf during late winter and spring 2004. Our first objective was to estimate underice sinking fluxes of particulate material during the period of ice growth and prior to the period of ice algal production, in contrast to the later productive season and the period of ice melt. The duration of this study ensured that the entire productive season of ice algae was covered, and that a complete seasonal time-series of underice sedimentation, from late winter to spring melt was obtained. Our second objective was to evaluate depth-related changes in underice sinking fluxes of organic material and in the composition of the sinking material, after its release from the ice into the water column. Our third objective was to quantify sinking export processes with respect to the standing biomass of chl *a*, POC and particulate organic nitrogen (PON) in the bottom sea ice and the upper part of the water column.

1.2 Materials and methods

1.2.1 Sampling

Underice sampling was conducted at a landfast first-year sea ice station (ca. 250 m water depth) in Franklin Bay, western Canadian Arctic (Fig. 1). This study was carried out onboard the Canadian research ice-breaker CCGS *Amundsen* during the overwintering period of the Canadian Arctic Shelf Exchange Study (CASES). From 23 February to 20 June 2004, sinking fluxes of particulate material from the sea ice were studied using particle interceptor traps deployed at 1, 15 and 25 m from the under-surface of the ice. Two

identical particle interceptor trap arrays, fixed to a tripod on the sea ice, where deployed in relatively close proximity (ca. 50 m) on 16 consecutive occasions (Table 1). The ice holes through which the sediment traps were deployed were covered by wooden plates and snow to prevent increased light penetration. During the initial part of the study, from 23 February to 13 April, the deployment time was, on average, 7.8 ± 0.8 days (n = 6). From 13 April to 20 June, the deployment time was reduced to an average of 6.2 ± 0.4 days (n = 8), in response to higher sinking fluxes, except for two deployments of 4.0 and 15.2 days on 26 May and 30 May, respectively. The particle interceptor traps were constructed of PVC (Polyvinyl Chloride) cylinders closed at one end, with an internal diameter of 10 cm and an aspect ratio (height:diameter) of 7. The sampling with particle interceptor traps was carried out in accordance with JGOFS protocols (Knap et al. 1996) and recommendations by Gardner (2000). Prior to deployment, the particle interceptor traps were filled with 0.22 μm filtered seawater previously collected at 200 m, to ensure that the higher density particle free water would remain within the traps during deployment. No preservative or poison was added to the filtered seawater prior to deployment. Upon recovery, the entire sample volume of the particle interceptor traps was transported back to the laboratory onboard the CCGS *Amundsen* for chl *a*, phaeopigments, total particulate carbon (TPC), POC, PON, and biogenic silica (BioSi) analyses.

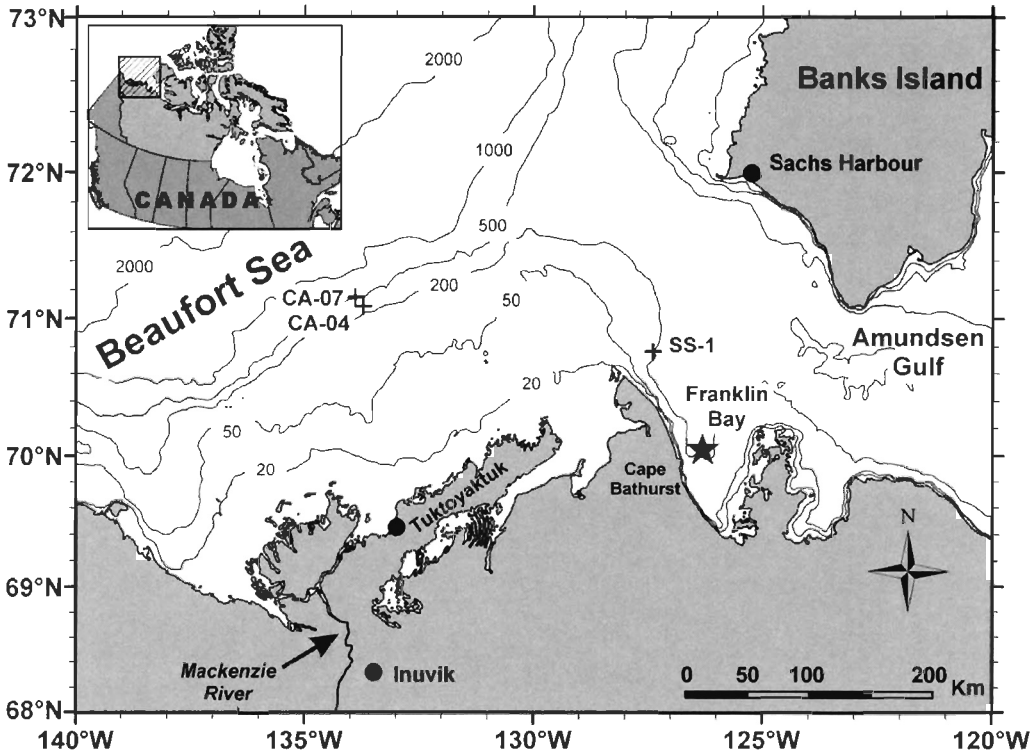

Fig. 1. Location of the sampling station (indicated by star) in Franklin Bay on the Mackenzie Shelf, western Canadian Arctic. For comparison, the positions of sediment trap moorings CA-04 and CA-07 of Forest et al. (2007) and SS-1 of O'Brien et al. (2006) are shown. Water depth is in meter

Surface water samples were collected at 1 m using a 5L Niskin bottle. During a parallel study on sea ice microbial communities in the same area, the bottom 4 cm of ice cores were collected using a Mark II manual ice corer (9 cm internal diameter, Kovacs Enterprises), as described in detail in Riedel et al. (2006). Ice core samples were collected at two sites representative of high and low snow cover, although results from the two sites were later averaged for the present study. The surface water and ice core samples were brought back to the laboratory onboard the ship for chl *a*, POC, PON and salinity analyses.

Table 1. Sampling periods, dates of deployment and recovery, and duration of the underice deployments of particle interceptor traps in Franklin Bay, western Canadian Arctic, in 2004

Period	Sampling date		Duration
	Deployment	Recovery	(d)
Winter	23 February	03 March	8.7
	03 March	11 March	7.8
	11 March	19 March	7.9
Early spring	19 March	27 March	8.0
	27 March	05 April	8.9
	05 April	13 April	7.9
	13 April	19 April	6.0
	19 April	25 April	6.0
	25 April	01 May	6.0
	01 May	07 May	6.0
	07 May	14 May	7.0
	14 May	20 May	6.0
	20 May	26 May	6.0
Melt	26 May	30 May	4.0
	30 May	14 June	15.2
	14 June	20 June	6.3

1.2.2 Analyses

In the laboratory onboard the ship, the total volume of the traps was measured, pre-screened on a 425 µm mesh to remove larger swimmers, and transferred into dark containers. The samples were gently mixed before subsampling for analyses.

Total chl *a* and total phaeopigments were measured in duplicate on 100-500 ml subsamples filtered on Whatman GF/F 25 mm filters. Starting on 27 March, size-fractionated chl *a* and phaeopigments (>5 µm) were measured on samples filtered on Nuclepore polycarbonate 5 µm membranes. The filters and membranes were extracted in 10 ml of 90 % acetone during 24 h at 4°C in dark conditions and analyzed on a Turner Designs 10AU fluorometer, using 90 % acetone as a blank. Chl *a* and phaeopigments

concentrations were estimated according to Parsons et al. (1984). The fluorometer was calibrated before and after the expedition, using a pure chl *a* extract (from *Anacystis nidulans*; Sigma Chemicals).

TPC, POC and PON were measured in duplicate on 100-1000 ml subsamples which were filtered on pre-combusted (450°C during 24 h) Whatman GF/F 21 mm filters. The filters were dried at 60°C during 24 h, pelletized and stored until later analysis on a Perkin-Elmer Model 2400 CHN Analyzer. POC was obtained by acidifying filters in a dessicator saturated with HCl fumes during 24 h, thereby removing any inorganic carbon, before analysis on the CHN Analyzer. POC was sampled from 5 April onwards. Analysis of non-acidified filters produced values of TPC and PON.

BioSi was measured in duplicate on 100-500 ml subsamples. The subsamples were filtered on 0.6 μm Nuclepore polycarbonate membranes using an all-plastic filtration system, and were dried at 60°C for 24 h. BioSi was measured by extraction in 0.2 M NaOH at 95°C for 45 min. Extracted subsamples were then analyzed using a colorimetric reaction involving the formation of a silicomolybdate complex, which was spectrophotometrically determined at 810 nm (Varian Inc. CARY 100 BIO) (adapted from Ragueneau & Tréguer 1994 and Conley 1998).

The same methods as described above were used to determine chl *a*, POC and PON concentrations from surface water samples and melted ice cores. Surface water salinity was

determined using a Guildline Model 8400B Autosal salinometer. Before filtration, the bottom sea ice samples were processed as described in Riedel et al. (2006).

1.2.3 Calculations and statistical analyses

Sinking fluxes were calculated using the following equation:

$$\text{Sinking flux (mg m}^{-2}\text{ d}^{-1}\text{)} = (C_{trap} * V_{trap}) / (A_{trap} * T_{dep}) \quad (1)$$

where C_{trap} is the concentration of the measured variable in the particle interceptor trap (mg m^{-3}), V_{trap} is the volume of the particle interceptor trap sample (m^3), A_{trap} is the particle interceptor trap surface area (m^2) and T_{dep} is the deployment time (d).

The daily loss rate of suspended material due to sinking export at 1 m was estimated using the following equation:

$$\text{Daily loss rate (\% d}^{-1}\text{)} = \text{Sinking flux} / C_{int} * 100 \quad (2)$$

where sinking flux at 1 m is from equation (1) and C_{int} is the integrated concentration of the variable considered (mg m^{-2}) in the bottom sea ice and water column above the particle interceptor trap depth. Because of the missing chl *a* sinking flux at 1 m on 20 June, the chl *a* daily loss rate on that day was estimated using the chl *a* sinking flux measured at 15 m.

The seasonal time-series of sinking flux data was tested for significant differences between selected reference periods using Kruskal-Wallis tests (Sokal & Rohlf 1981), and

between depths using Friedman's method for Randomized Blocks (Sokal & Rohlf 1981). Linear regression analyses between variables are simple linear regressions (Model I) and reduced major axis (model II) regressions (Sokal & Rohlf 1981); the latter takes into account measurement errors for both dependent and independent variables. Regression slopes were compared using analysis of covariance (Sokal & Rohlf 1981).

1.3 Results

The sampling period covered three distinctive time periods, which have been defined as winter, early spring and melt period, as will be referred to in the next sections (Table 1). The winter period extended from 23 February to 19 March and was characterized by continuous sea ice growth from 1.4 to 1.6 m (Fig. 2a) and little changes in ice algal biomass (average of 0.20 ± 0.34 mg chl *a* m^{-2}; Fig. 2c). The early spring period, from 19 March to 26 May, showed continuing sea ice growth with ice thickness increasing from 1.6 to 2.0 m and an increase in ice algal biomass from 0.55 to 22.3 mg chl *a* m^{-2}. During the melt period, from 26 May to 20 June, a decrease in sea ice thickness from 2.0 to 1.6 m and a decrease in surface salinity from 31.2 to 5.4 were observed (Fig. 2a, b), along with a decrease in the ice algal biomass from 22.3 to 1.4 mg chl *a* m^{-2} (Fig. 2c).

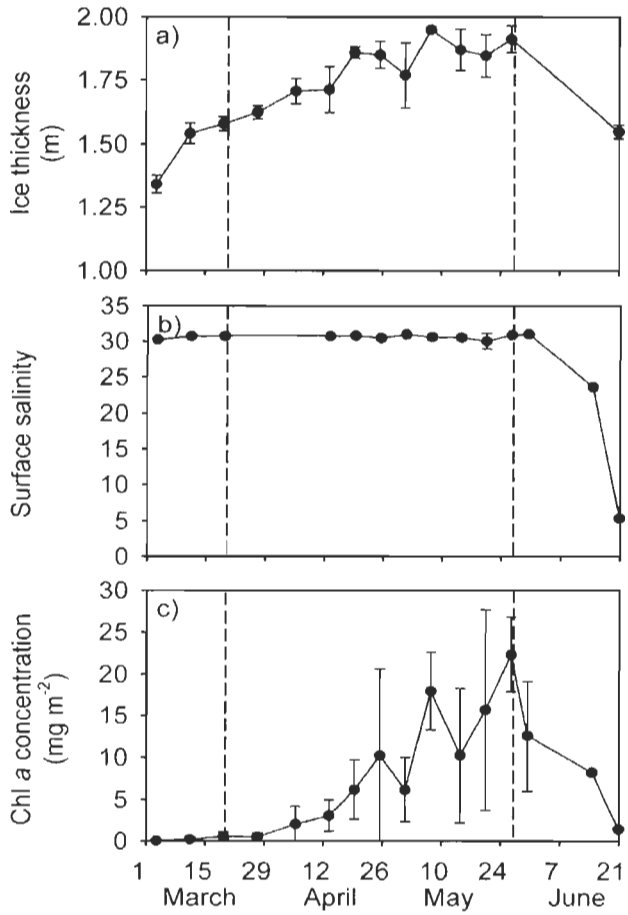

Fig. 2. Seasonal changes in (a) sea ice thickness, (b) surface salinity and (c) sea ice chlorophyll *a* (chl *a*) concentrations, from 23 February to 20 June 2004. In (a) and (c), values were averaged from sites with high and low snow cover during deployment periods of particle interceptor traps. Error bars represent standard deviations. Vertical dashed lines represent reference periods as described in Table 1

Sinking fluxes measured under the sea ice showed a general seasonal increase during the sampling period (Fig. 3a-d, Table 2). Chl *a* and BioSi sinking fluxes both showed a significant increase from winter to early spring and to the melt period (Kruskal-Wallis, $p < 0.05$ and $p < 0.05$, respectively; Fig. 3a, b, Table 2). During winter, chl *a* and BioSi sinking fluxes remained low (median values of 0.01 and ≤ 0.80 mg m^{-2} d^{-1} at all depths, respectively), while a steady increase was observed during early spring reaching 0.23 and

5.8 mg m^{-2} d^{-1} at 1 m on 26 May, respectively. During the following melt period, chl *a* sinking fluxes increased 7 to 9-fold, reaching 2.0 and 0.97 mg m^{-2} d^{-1} at 15 and 25 m, respectively (unfortunately data are not available at 1 m on 20 June). BioSi sinking fluxes increased 7 to 13-fold at all depths during the melt period, reaching 37.9, 90.4 and 72.0 mg m^{-2} d^{-1} at 1, 15 and 25 m, respectively, on 20 June. Throughout the study chl *a* sinking fluxes decreased significantly with depth, on average, by 46.2 ± 18.5 % from 1 to 25 m (Friedman's method, $p < 0.001$), while BioSi sinking fluxes remained stable with depth (Friedman's method, $p > 0.05$; Table 2). Sinking fluxes of phaeopigments increased significantly with depth throughout the study (Friedman's method, $p < 0.05$; Table 2).

TPC and POC showed parallel seasonal sinking flux patterns throughout the study (Fig. 3c, d, Table 2), which differed from chl *a* and BioSi. Missing POC data points from 23 February to 27 March were extrapolated from the strong linear correlation between the measured sinking fluxes of TPC and POC (Fig. 4), using the measured TPC sinking flux values. Sinking fluxes of TPC and POC remained rather stable during the winter (median values of 27.0 and 24.6 mg m^{-2} d^{-1} at 1 m, respectively) and early spring (median values of 24.4 and 21.0 mg m^{-2} d^{-1} at 1 m, respectively) periods. During the melt period, TPC sinking fluxes increased 9 to 18-fold (maximum values of 539.9, 312.8 and 185.5 mg m^{-2} d^{-1} at 1, 15 and 25 m, respectively, on 20 June) and POC increased 7 to 21-fold (maximum values of 521.7, 214.5 and 188.6 mg m^{-2} d^{-1} at 1, 15 and 25 m, respectively, on 20 June). TPC and POC sinking fluxes did not show any significant change with depth during the study period (Friedman's method, $p > 0.05$ and $p > 0.05$, respectively; Table 2). Throughout our study,

POC was the main component of the TPC sinking fluxes making up ca. 91 % of the sinking TPC (Fig. 4).

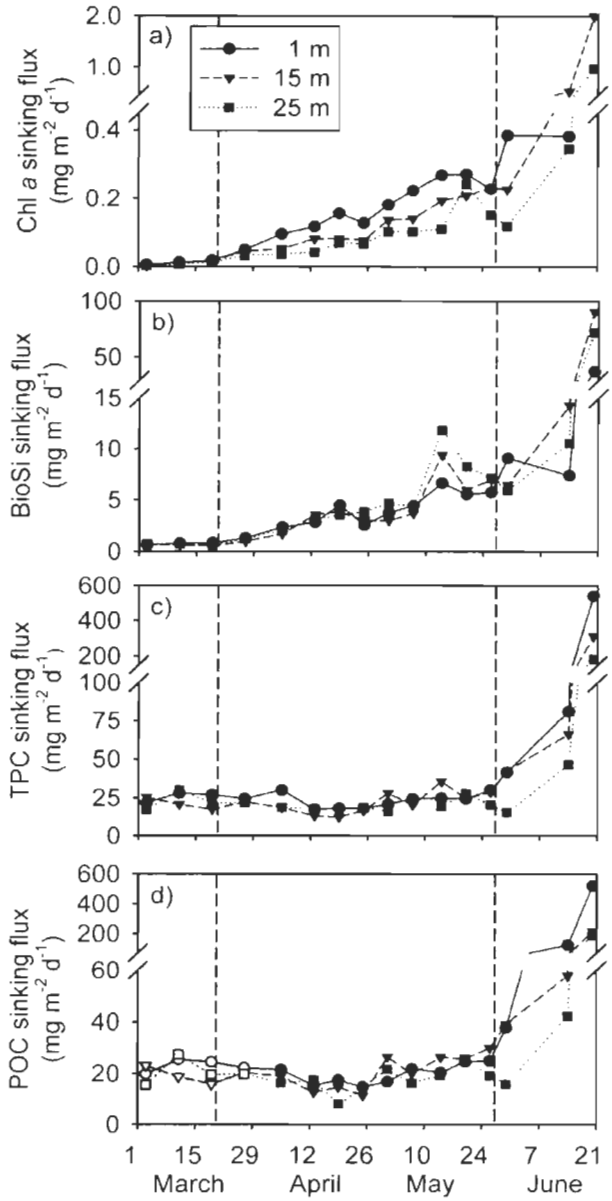

Fig. 3. Seasonal changes in sinking fluxes of (a) chlorophyll *a* (chl *a*), (b) biogenic silica (BioSi), (c) total particulate carbon (TPC) and (d) particulate organic carbon (POC) at 1, 15 and 25 m under the sea ice, from 23 February to 20 June 2004. Data points represent particle interceptor trap recovery dates. The open data points in (d) are POC values estimated from the linear relationship between POC and TPC. Vertical dashed lines represent reference periods as described in Table 1

Table 2. Summary of sinking fluxes and composition ratios of the sinking material in particle interceptor traps at 1, 15 and 25 m during three sampling periods. POC sinking fluxes from 23 February to 27 March were estimated from the linear regression between POC and TPC sinking fluxes (Fig. 4). Chl *a* and phaeopigment sinking fluxes at 1 m on 20 June are missing. Median and range of values are given. Number of deployments for each period (n) is shown

Period	Depth (m)	Chl *a* (mg m^{-2} d^{-1})	Phaeopigments (mg m^{-2} d^{-1})	BioSi (mg m^{-2} d^{-1})	TPC (mg m^{-2} d^{-1})	POC (mg m^{-2} d^{-1})	POC:chl *a* (g:g)	POC:BioSi (mol:mol)	PON:BioSi (mol:mol)	POC:PON (mol:mol)	Chl *a*:total pigments (%)
Winter	1	0.01	0.002	0.79	27.0	24.6	2113	72.8	14.0	4.5	88.5
23 Feb–19 Mar		0.01-0.02	0.001-0.002	0.64-0.85	21.8-28.1	19.8-25.6	1380-3474	68.6-76.1	12.5-14.6	4.2-5.0	78.0-95.2
(n = 3)											
	15	0.01	0.002	0.64	20.7	18.8	1678	69.8	13.8	4.3	91.1
		0-0.02	0.002-0.002	0.56-0.70	17.4-25.4	15.9-23.1	1035-8425	66.4-78.1	13.6-16.3	3.5-4.9	64.9-91.5
	25	0.01	0.003	0.73	21.6	19.7	4766	73.8	15.2	4.2	60.4
		0-0.01	0.001-0.005	0.63-0.75	17.1-30.2	15.6-27.4	1651-7045	49.2-73.8	10.0-15.9	4.0-5.0	55.9-81.4
Early spring	1	0.17	0.004	4.1	24.4	21.0	110.9	11.0	2.5	4.2	98.1
19 Mar–26 May		0.05-0.27	0-0.05	1.3-6.6	17.5-30.3	14.7-25.0	75.8-459.6	7.2-40.2	1.1-8.0	3.1-7.9	70.5-100
(n = 10)											
	15	0.11	0.02	3.6	21.3	20.1	151.0	10.1	2.1	4.6	85.7
		0.04-0.23	0-0.09	1.0-9.4	12.2-35.7	11.2-29.9	124.3-468.9	6.6-48.6	1.2-10.3	3.2-7.5	46.5-100
	25	0.09	0.03	4.1	19.0	19.2	194.8	9.7	2.0	5.6	76.0
		0.03-0.24	0-0.13	1.2-11.8	16.0-27.8	16.1-25.7	106.1-628.1	3.8-38.4	0.46-8.0	4.1-9.7	41.7-94.9
Melt	1	0.39	0	9.1	81.0	123.5	209.8	32.1	3.4	9.8	100
26 May–20 Jun		0.38-0.39	0-0	7.4-37.9	41.6-539.9	37.8-521.7	97.9-321.6	9.7-39.0	0.74-4.8	5.7-11.2	100-100
(n = 3)											
	15	0.53	0.02	14.3	66.2	57.8	109.2	9.4	0.77	10.5	96.6
		0.23-2.0	0.008-0.39	6.4-90.4	42.4-312.8	39.3-214.5	107.5-173.4	5.5-14.2	0.59-1.1	8.0-11.3	83.6-98.5
	25	0.35	0.02	10.6	46.6	42.3	134.9	6.2	0.59	11.0	84.7
		0.12-0.97	0.01-0.58	5.9-72.0	15.3-185.5	15.8-188.6	121.7-194.5	6.1-9.3	0.43-0.73	9.1-12.3	62.6-97.1

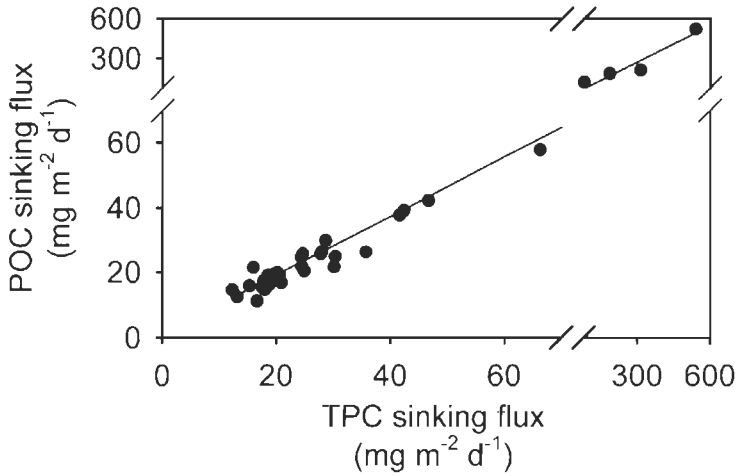

Fig. 4. Linear regression of POC sinking flux *versus* TPC sinking flux at all depths, from particle interceptor trap deployments under the sea ice, from 5 April to 20 June 2004. Solid lines represent the simple linear regression (model I): $y = 0.91x + 1.0$; $r^2 = 0.97$; $p < 0.001$

The contribution of chl *a* from large algae (>5 μm) to the total chl *a* sinking flux increased during early spring from initial values of 57.4, 62.3 and 66.5 % at 1, 15 and 25 m, respectively, on 27 March to median values of 87.7, 91.2 and 89.0 %, respectively, after 13 April (Fig. 5a). The percent contribution of chl *a* from large algae (>5 μm) did not change significantly with depth during the entire sampling period (Friedman's method, $p > 0.05$). The percent chl *a* in total pigments showed some variability, but no significant seasonal trends (Kruskal-Wallis, $p > 0.05$), with median values of 97.6, 91.3 and 76.0 % at 1, 15 and 25 m, respectively, throughout the entire sampling period (Fig. 5b). The percent contribution of chl *a* to total pigments sinking fluxes decreased significantly with depth throughout the study (Friedman's method, $p < 0.001$; Table 2).

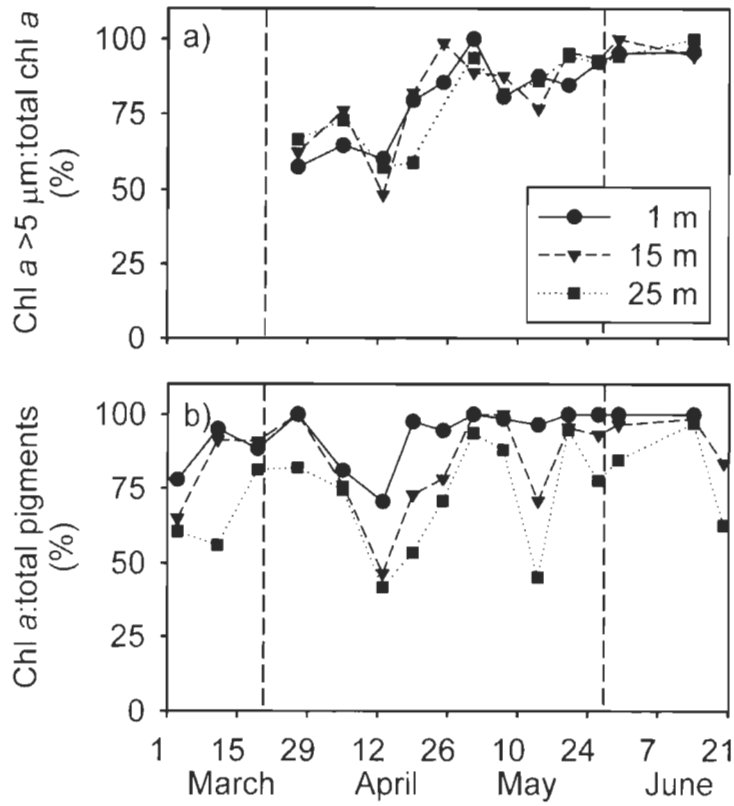

Fig. 5. Seasonal changes in (a) percent contribution of large cells (>5 µm) to the total chlorophyll *a* (chl *a*) sinking flux and (b) percent chl *a* in total pigments (chl *a* + phaeopigments) in particle interceptor traps at 1, 15 and 25 m under the sea ice, from 23 February to 20 June 2004. Data points represent particle interceptor trap recovery dates. Vertical dashed lines represent reference periods as described in Table 1

Parallel seasonal patterns were observed in the POC:chl *a*, POC:BioSi and PON:BioSi ratios of the sinking material throughout the study (Fig. 6a-c, Table 2). High ratios during the winter period (median values 2113 g:g, 72.8 and 14.0 mol:mol at 1 m, respectively) were followed by a decrease during the initial part of the early spring period (median values 110.9 g:g, 11.0 and 2.5 mol:mol at 1 m during early spring, respectively). The POC:chl *a* and POC:BioSi ratios remained rather stable after 13 April, while the

PON:BioSi ratio showed a moderate decrease. All three ratios increased at 1 m from 14 June and onwards. A significant increase in the POC:chl *a* ratio was observed with depth throughout the study (Friedman's method, $p < 0.01$), while the POC:BioSi ratio showed no change and the PON:BioSi ratio showed a decrease with depth (Friedman's method, $p > 0.05$ and $p < 0.05$, respectively; Table 2).

The POC:PON molar ratios of the sinking material remained rather stable prior to the melt period (median values of 4.5 and 4.2 at 1 m during the winter and early spring periods, respectively; Fig. 6d, Table 2). During the melt period, the POC:PON molar ratio at 25 m continuously increased to 12.3 on 20 June, while the ratios at 1 and 15 m peaked at ca. 11.2 on 30 May and then decreased to 6 – 8 on 20 June. The POC:PON ratio at 25 m was generally higher during early spring, although no significant change was observed with depth throughout the study (Friedman's method, $p > 0.05$; Table 2).

Linear regressions between chl *a* and BioSi sinking fluxes showed strong relationships at each sampling depth, with significantly increasing regression slopes with depth (analysis of covariance, $p < 0.01$; Fig. 7a). A significant linear relationship ($r^2 = 0.51$, $p < 0.01$) was observed between the sinking flux of chl *a* at 1 m and the chl *a* biomass in the bottom ice (Fig. 7b). However, a stronger correlation ($r^2 = 0.77$, $p < 0.001$) was found when excluding the two maximum sea ice chl *a* biomass values observed on 7 May and 26 May (> 16 mg chl *a* m^{-2}).

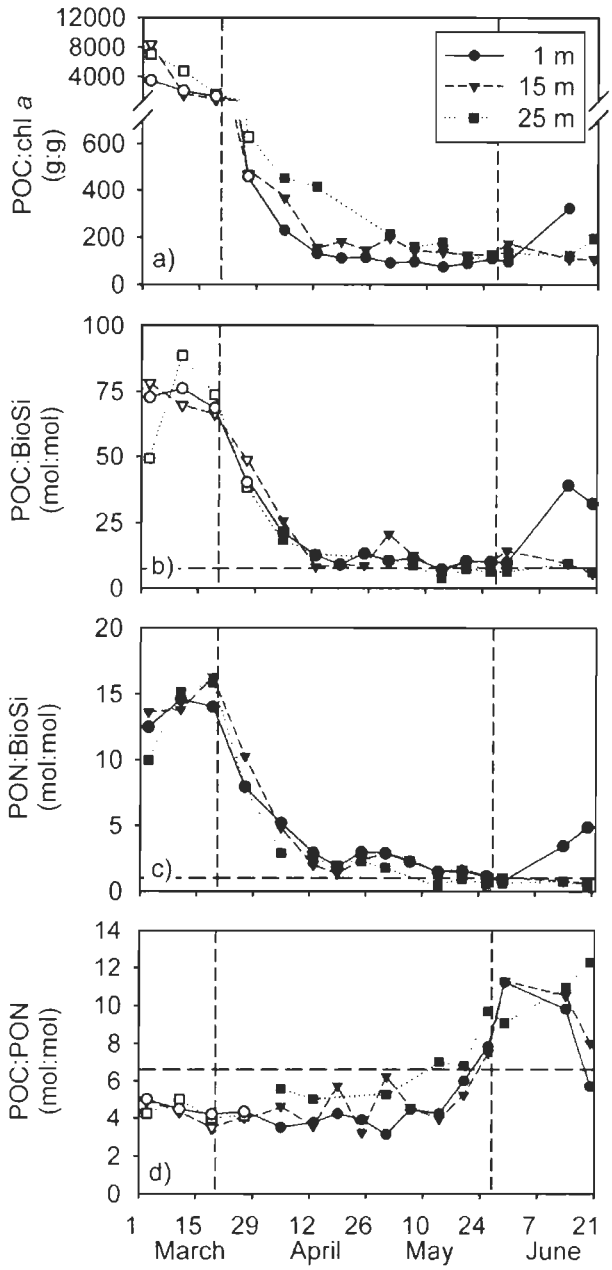

Fig. 6. Seasonal changes in the ratios of (a) particulate organic carbon (POC) to chlorophyll *a* (chl *a*), (b) POC to biogenic silica (BioSi), (c) particulate organic nitrogen (PON) to BioSi and (d) POC to PON in particle interceptor traps at 1, 15 and 25 m under the sea ice, from 23 February to 20 June 2004. Data points represent particle interceptor trap recovery dates. The open data points in (a), (b) and (d) are POC values estimated from the linear relationship between POC and TPC. Vertical dashed lines represent reference periods as described in Table 1. In (b), (c) and (d), horizontal dashed lines represent the ratios of 7.1, 1.1 and 6.6 of Redfield et al. (1963)

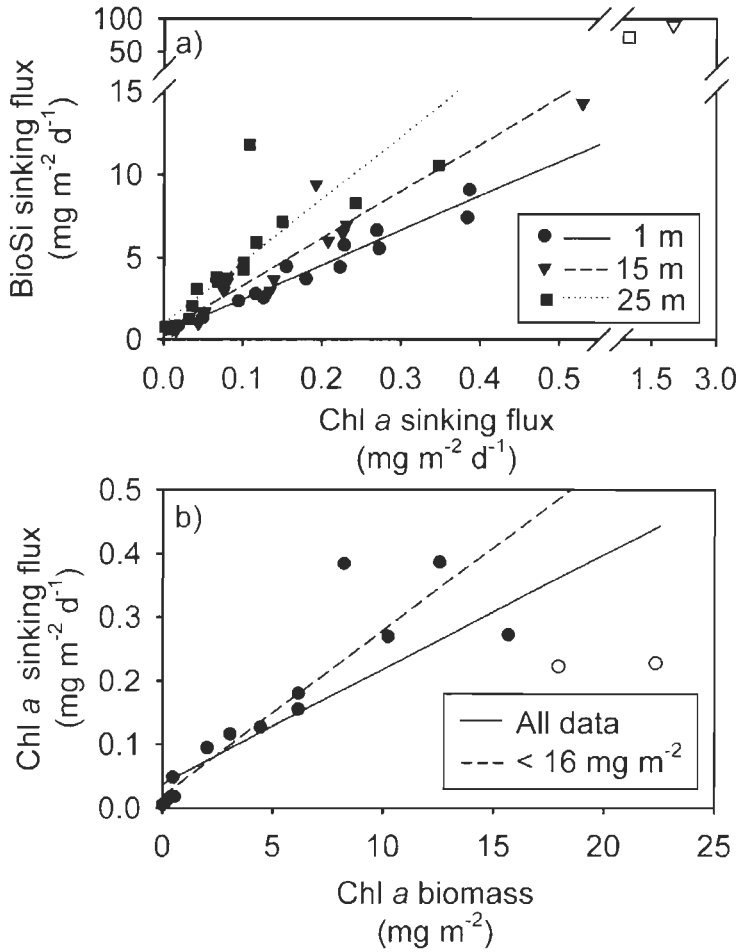

Fig. 7. Linear regressions (a) of biogenic silica (BioSi) sinking flux *versus* chlorophyll *a* (chl *a*) sinking flux at 1, 15 and 25 m, from particle interceptor trap deployments under the sea ice, from 23 February to 20 June 2004, and (b) of chl *a* sinking flux at 1 m *versus* chl *a* concentration in the sea ice bottom from 23 February to 14 June 2004 (sinking flux data not available on 20 June). In (a), lines represent reduced major axis (model II) regressions using BioSi flux data < 15 mg $m^{-2}d^{-1}$ (open symbols not included in regression lines) at: 1 m: $x_2 = 41.54x_1 + 0.81$; $r^2 = 0.96$; $p < 0.001$, 15 m: $x_2 = 56.56x_1 + 1.00$; $r^2 = 0.91$; $p < 0.001$ and 25 m: $x_2 = 62.16x_1 + 2.16$; $r^2 = 0.93$; $p < 0.001$. In (b), the solid line represents reduced major axis (model II) regression for all data points: $x_2 = 0.018x_1 + 0.038$; $r^2 = 0.51$; $p < 0.01$ and the dashed line represents reduced major axis (model II) regression for ice algal biomasses < 16 mg chl *a* m^{-2}: $x_2 = 0.026x_1 + 0.019$; $r^2 = 0.77$; $p < 0.001$. Open circles represent data points > 16 mg chl *a* m^{-2}

Daily sinking losses of chl *a*, POC and PON from the sea ice and interfacial layer (top 1 m of the water column) showed parallel seasonal patterns throughout the study (Fig. 8). The daily loss rates of chl *a*, POC and PON decreased during winter and early spring, from maximum rates of 5.3, 25.4 and 35.0 % d^{-1} to minimum rates of 1.0, 2.0 and 4.2 % d^{-1}, respectively. A subsequent increase was observed during the melt period, reaching daily loss rates of 4.2, 14.3 and 13.6 % d^{-1} for chl *a*, POC and PON, respectively.

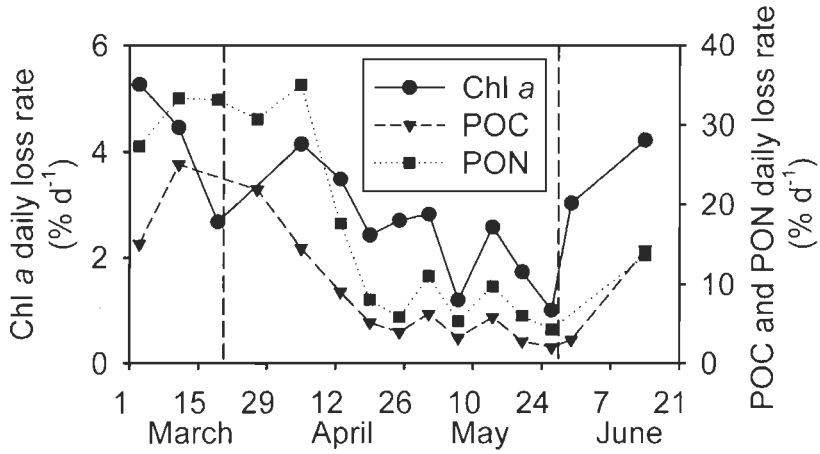

Fig. 8. Seasonal changes in the daily sinking loss rate of chlorophyll *a* (chl *a*), and particulate organic carbon and nitrogen (POC and PON) at 1 m under the sea ice, from 23 February to 20 June 2004. Data points represent particle interceptor trap recovery dates. Vertical dashed lines represent reference periods as described in Table 1

1.4 Discussion

1.4.1 Seasonal variations in underice sinking fluxes

This study started during winter (23 February), at a time when bottom ice algal biomass was still very low (Fig. 2c). Little algal material was collected by the underice

particle interceptor traps before early spring, as shown by the low chl *a* (< 0.02 mg chl *a* m^{-2} d^{-1}) and BioSi sinking fluxes (< 1 mg m^{-2} d^{-1}). To our knowledge, only one other study estimated the sinking export of organic material near Franklin Bay during winter, using long-term sediment traps deployed at 145 m (O'Brien et al. 2006, their station SS-1; Fig. 1). These authors reported low chl *a* (< 0.003 mg chl *a* m^{-2} d^{-1}) and BioSi (< 10 mg BioSi m^{-2} d^{-1}) sinking fluxes from December to March.

The fairly constant POC fluxes (median values of 21.0 and 24.6 mg m^{-2} d^{-1} at 1 m; Fig. 3d, Table 2) until the onset of spring melt indicate negligible seasonal change in the sinking export of POC. Although O'Brien et al. (2006) observed strong seasonality in POC sinking fluxes on the Mackenzie Shelf, they reported POC sinking fluxes < 10 mg C m^{-2} d^{-1} at 145 m under the sea ice near Franklin Bay (their station SS-1; Fig. 1), during April 1987 and from November 1987 to March 1988. Forest et al. (2007) reported comparable POC sinking fluxes at 200 m, from October 2003 to May 2004, on the Mackenzie Shelf slope (< 15 mg C m^{-2} d^{-1} at their station CA-04 and CA-07; Fig. 1), with episodic events of POC advection from the shelf onto the shelf-slope during winter and spring. Despite differences in sampling depths between our and these studies, these observations show that underice sinking export of POC does take place on the Mackenzie Shelf during the winter.

Several studies looking at temporal changes in underice sinking fluxes of organic material have shown increasing sinking fluxes in response to the release of material from the sea ice during spring melt (Carey 1987, Tremblay et al. 1989, Michel et al. 1996,

Fortier et al. 2002). Melnikov (1998) suggested that ice algae are released from the ice during winter through brine drainage during ice growth, in the western Weddell Sea. Furthermore, Carey (1987) suggested that the carbon sinking flux measured near the bottom in the vicinity of Narwhal Island (southwestern Beaufort Sea), from mid-April to end-May, primarily originated from the productive ice communities prior to ice melt. During the present study, ice thickness continuously increased until the onset of spring ice melt, indicating that any release of organic material from the ice during that period would be linked to brine drainage rather than melt processes. An early coupling between ice communities and the underlying water column, prior to spring ice melt, could be of seasonal importance for pelagic herbivores, as suggested by Melnikov (1998), as well as for the benthic community as suggested by Renaud et al. (2007b).

The increasing pelagic grazing activity of copepods observed by Seuthe et al. (2007) during the winter-spring transition in Franklin Bay, although linked to pelagic primary production, may have been supplemented with sinking ice algal material. Indeed, microscopic observations of fecal pellets in sediment traps showed that they contained frustules of pennate diatoms (L. Seuthe unpubl. data), the most abundant algal group in the bottom surface of the ice in April-May (M. Różańska pers. comm.). During our study, bottom ice algal concentrations were, on average, more than 2 orders of magnitude higher than phytoplankton concentrations at 1 m, indicating that any phytoplankton contribution to sinking algae would be minimal.

Assuming that the POC sinking flux measured during the winter period in the present study would have been the same throughout the preceding winter months, we can estimate that ca. 3.5 g C m^{-2} would have been exported through sinking from November to the end of March. This POC sinking flux estimate for the winter period is almost one order of magnitude higher than that reported by O'Brien et al. (2006) near Franklin Bay for November to March (< 0.5 g C m^{-2} at 145 m at their station SS-1), and compares with their annual POC sinking flux estimate (ca. 4 g C m^{-2}). The discrepancy between our results and those obtained from by O'Brien et al. (2006) is likely explained by transformation and loss processes affecting the organic material during its descent to deep waters. This aspect will be discussed in more details in the next section. In addition, the different methods and interannual and spatial differences between the two studies probably also contributed to the observed discrepancy.

The fairly constant POC sinking fluxes prior to spring melt compared to the observed changes in chl *a* and BioSi fluxes suggests a non-algal origin of the sinking POC during winter. This indeed is supported by the high POC:chl *a* ratios and the POC:BioSi and PON:BioSi molar ratios which were considerably higher than Redfield ratios (7.1 and 1.1, respectively; Redfield et al. 1963), during the winter period (Fig. 6a-c). The POC sinking fluxes during the winter period did not appear to be related to the sinking of senescent algae or herbivorous fecal material, as evidenced by negligible sinking fluxes of phaeopigments ($\leq$ 0.002 mg m^{-2} d^{-1}; Table 2) and low POC:PON molar ratios compared to those reported for copepod fecal pellets (33.2; Daly et al. 1999). Qualitative microscopic analysis of the

sinking material collected during winter revealed large amounts of gelatinous material to which detritus were attached, possibly transparent exopolymeric particles (TEP). TEP produced by diatoms have been show to have high C:N molar ratios (26; Engel & Passow 2001). This, in combination with the low abundance of sea ice diatoms during winter does not support that the TEP in the sinking material would have originated from diatoms. Bhaskar et al. (2005) report low C:N molar ratios (2.4) in bacterial exopolymeric substances (EPS). The transparent Coomassie Stained Particles (CSP), first described by Long & Azam (1996), can be produced by marine bacterioplankton and likely have a high nitrogen content due to their protein composition (Radić et al. 2006). Bacteria also have low C:N ratios (3.2; Lee & Fuhrman 1987). We thus surmise that bacteria-mediated sinking fluxes contributed significantly to the export of organic material during winter.

The initial increase in underice chl *a* and BioSi sinking fluxes coincided with the increasing bottom ice chl *a* biomass, suggesting a coupling between sinking fluxes under the sea ice and ice algal biomass. Indeed, a significant relationship between sinking fluxes and ice algal biomass was observed during the present study (Fig. 7b). This relationship was found to be stronger at lower ice algal biomass concentrations. The higher and more variable data points in the regression plot represent measurements obtained towards the onset of spring melt, indicating a stronger relationship between sinking fluxes and ice algal biomass during winter and in early spring.

The POC:chl *a* ratios during early spring (median value of 110.9 g:g; Table 2) were higher than the ratio typically considered for healthy algal cells (40 g:g; Lorenzen 1968), but were within the range reported for ice algae (ca. 15 – 180 g:g; Gosselin et al. 1990). When using the POC:chl *a* ratio for the bottom ice algae during our study (44 g:g; A. Riedel pers. comm.), then the estimated sinking export of POC explained by algal cells would, on average, be 7.5 mg C m^{-2} d^{-1} or 37.8 % of the observed POC sinking flux during early spring. This indicates that a significant part of the POC sinking flux was explained by algal cells during early spring. Diatoms appeared to become a seasonally increasing fraction of the algal sinking flux, as supported by the increase in the contribution of chl *a* >5 μm to the total chl *a* sinking flux, the increasing BioSi sinking flux and the decreasing POC:BioSi and PON:BioSi ratios during early spring. Indeed, increasing sinking fluxes of algal cells, dominated by the pennate diatoms *Nitzschia frigida* and *Navicula* spp., were observed from March to May (from 3.2 to 118.0 x 10^6 cells m^{-2} d^{-1} at 1 m; A. Tatarak pers. comm.). These two species were also dominant in the ice assemblage (M. Różańska pers. comm.).

Analyses of vertical sections of ice cores showed that, on average, 95 % of the total chl *a* biomass in complete ice cores was found in the bottom 4 cm (A. Riedel pers. comm.). Therefore, the initial melting of the bottom section of the sea ice would presumably result in a higher release of organic material as compared to later melt further up in the vertical ice profile. During the spring melt period, sinking fluxes of organic material increased significantly in response to the onset of spring ice melt after 26 May. This initial and rapid

increase in sinking fluxes was observed in all the measured variables, suggesting that all ice-bound material in the bottom ice was rapidly released. The coincident increase in the POC:chl *a*, POC:BioSi and PON:BioSi ratios at 1 m suggest that not only ice algal cells, but other organic material previously retained within the sea ice, was released during the melt period. The increase in sinking export of chl *a* observed during the melt period (from 0.23 to 2.0 mg chl *a* m^{-2} d^{-1} at 15 m; data from 1 m not available on 20 June) is comparable to increases reported during spring ice melt in Resolute Passage (from < 0.1 to 2.3 mg chl *a* m^{-2} d^{-1} at 15 m in May and June; Michel et al. 1996) or southeastern Hudson Bay (from < 0.2 to 0.56 mg chl *a* m^{-2} d^{-1} at 30 m; Tremblay et al. 1989). Moreover, the sinking export of ice algal material at 1 m integrated over the spring melt period (19.9 mg chl *a* m^{-2}; data not shown) exceeded the sinking export at 1 m integrated over the winter and early spring periods (11.4 mg chl *a* m^{-2}; data not shown). Hence, the bulk of the sea ice biomass was released during the spring melt, although the earlier sinking export of ice algal material may still be of seasonal importance to the pelagic (Melnikov 1998) and benthic (Renaud et al. 2007b) communities.

1.4.2 Depth-related changes in the composition of the sinking material

The rationale for deploying multiple particle interceptor traps at successive depths under the sea ice was to assess the initial changes in the amount and composition of the sinking flux of particulate material. Throughout the study, almost half of the chl *a* was lost from the sinking particulate material within the upper 25 m, as seen in the decreasing chl *a*

sinking fluxes with depth (Fig. 3a, Table 2). Assuming that there was no loss of material due to advective processes, this loss of chl *a* during sinking would have been caused by grazing and/or degradation. The constant sinking fluxes of BioSi, TPC and POC with depth support that the loss of chl *a* was not due to advective processes, since these variables would presumably have been equally affected by advection. Several studies have shown that the heterotrophic food web may be capable of assimilating a considerable proportion of the ice algal biomass after its release from the ice (Carey 1987, Tremblay et al. 1989, Michel et al. 1996, Fortier et al. 2002). These studies all show variability in the amount and composition of the sinking organic material in Arctic coastal areas, due to differences in the pelagic heterotrophic food web structure (e.g. Fortier et al. 2002). During our study, grazing and subsequent transformation of chl *a* to phaeopigments (Fig. 5b, Table 2) appeared to take place in the surface 25 m. Increasing copepod grazing rates were observed in April and May (Seuthe et al. 2007), adding support to a possible grazing loss of the sinking algal material.

The increasing POC:PON ratio of the sinking material with depth (Fig. 6d, Table 2), although not statistically significant, could also indicate herbivorous grazing. The POC:PON molar ratios were, however, well below the Redfield ratio at all depths until late in the season (26 May; Fig. 6d), and therefore do not provide a clear indication of grazing (e.g. Daly et al. 1999). In addition, copepods are for the most part limited to ingesting large cells (e.g. Frost 1972), such that grazing on the sinking algal material would likely result in a reduction of the large chl *a* size fraction (>5 μm) with depth. During the present study, no

change in the relative contribution of chl *a* size fractions with depth was observed, thus suggesting a minor influence of large grazers on the sinking material. Moreover, the constant POC sinking fluxes with depth do not indicate a significant loss of sinking organic carbon within the upper water column (upper 25 m). An alternate explanation for the increasing POC:PON ratio of the sinking material with depth would be preferential remineralization of PON compared to POC. Active microbial communities associated with the sinking material (see previous section) would certainly favor such a pathway. The high daily loss rate of PON, compared to POC, indicates a higher sinking export of the PON found in the sea ice and surface waters (upper 1 m).

Strong relationships between BioSi and chl *a* (Fig. 7a) and BioSi and total pigments (data not shown) were observed at all depths, with regression slopes increasing significantly with depth. These trends were expected since BioSi is subject to dissolution rather than biological degradation, although bacterial activity has been shown to increase the rate of BioSi dissolution (Bidle & Azam 1999). Diatom frustules are often found undigested in herbivorous copepod fecal pellets after passing through the digestive tract (Turner 2002), as observed during the present study (L. Seuthe unpubl. data). The constant BioSi sinking fluxes with depth therefore reflect that diatom frustules were preserved, either as intact diatom cells or empty frustules, in the material sinking in the upper water column. This sinking export of BioSi from the sea ice and the lack of remineralization in upper water column (upper 25 m) reflect a removal of silicic acid from the euphotic zone. Unless silicic acid is replenished into the euphotic zone, this removal of BioSi may in turn

contribute to a limitation of sea ice or pelagic diatom production, a process previously described during open-water conditions in the North Water Polynya (NOW; Michel et al. 2002).

The spring ice melt (after 26 May) did not only result in increased sinking fluxes of particulate material, but also in changes to the composition of the sinking material. The higher POC:chl *a*, POC:BioSi and PON:BioSi ratios at 1 m compared to other depths (Fig. 6a-c), resulted from a more moderate increase in the chl *a* and BioSi sinking fluxes compared to those of POC and PON at 1 m. The freshening of the surface layer during the melt period (Fig. 2b) could explain the differences in the composition of the material collected at 1 m compared to other depths. Selective retention of particles with different densities, with low-density particles being retained above a pycnocline, could come into play. The high POC:chl *a* and POC:BioSi in the particulate material collected above the pycnocline do not suggest a selective retention of algal cells in the surface layer, as this would lower these ratios. However, algal and/or bacterial produced EPS released from the sea ice during melt could remain suspended above the pycnocline, due to their low density (Azetsu-Scott & Passow 2004), thus explaining higher POC:chl *a* and POC:BioSi ratios of the material collected in the surface layer. Under such a scenario, i.e. with the pycnocline acting as a barrier to the sedimentation of certain particles, vertical changes in sinking fluxes would not directly reflect the transformation of the sinking material with depth but rather differential sinking of particles. A freshening of the surface layer only occurred during the melt period (Fig. 2b) and the thermocline remained for the most part below the

deployment depths (Forest et al. 2007), which suggests that vertical changes in sinking fluxes observed during winter and early spring were linked to depth-related transformation of the sinking material.

1.4.3 Loss of biomass through sinking export

The overall decreasing trend in the daily loss of chl *a* until the spring ice melt (Fig. 8), indicates that the seasonal increase in sea ice chl *a* biomass was not matched equally by the increasing chl *a* sinking export. The parallel seasonal patterns in the sinking loss of chl *a*, POC and PON suggests that these variables were closely linked and likely reflected the sinking export of algal material. Michel et al. (2002) observed comparable daily sinking loss rates of chl *a* (up to 10 % d^{-1}) and POC (5 to 22 % d^{-1}) at 1 m under first-year sea ice in northern Baffin Bay during April and May. During the present study, between 1.0 and 5.3 % of the chl *a* biomass, 2.0 and 25.4 % of the POC biomass and 4.2 and 35.0 % of the PON biomass was exported daily from the sea ice and interfacial layer through sinking. In the course of this 4-month study, an estimated 31.3 mg chl *a* m^{-2}, 7.2 g C m^{-2} (POC) and 1.2 g N m^{-2} (PON) was exported through sinking at 1 m under the first-year sea ice in Franklin Bay. In comparison, the underice sinking export of POC during a 54 d spring study in Resolute Passage was 11 - 12 g C m^{-2} at 15 m, of which most (8 - 11 g C m^{-2}) remained suspended during the period of study (Michel et al. 1996). These POC sinking export values are considerably higher than the estimate reported by O'Brien et al. (2006) from April to May (ca. 0.5 g C m^{-2} at 145 m; their SS-1 station), which may be

related to a high degradation of the organic material during sinking to depth. A benthic study on the Mackenzie Shelf reports an annual benthic carbon demand of ca. 12.1 g C m^{-2} (ca. 231 m water depth; Renaud et al. 2007a), which falls in the same range as our estimate of carbon sinking export.

1.5 Conclusion

This study showed a tight coupling between the sinking export of algal material and the biomass of ice algae, especially during winter and at the beginning of the early spring period. The observed coupling between ice biomass and sinking export suggests that ice algae can provide a potential food source for the pelagic and benthic communities well before the onset of spring melt. The decreasing sinking fluxes of chl *a* with depth (46 % from 1 to 25 m), showed a considerable loss of pigmented biomass from the sinking particulate organic material after its release from the ice. Diatoms comprised a seasonally increasing fraction of the sinking algal material during early spring, as indicated by the increasing fraction of large chl *a* (>5 μm) and BioSi sinking fluxes. In contrast with the seasonally increasing sinking fluxes of chl *a* and BioSi, POC sinking fluxes remained rather stable until the onset of spring melt. A large part of the sinking POC appeared to be non-algae related, as suggested by the high POC:chl *a* ratios. The onset of spring melt resulted in a considerable increase in sinking fluxes of pigmented and non-pigmented material, indicating a non-selective release of particulate organic material from the sea ice. However, our results also suggest retention of some of the released particulate material

within the low salinity surface layer (between 1 and 15 m) formed at the time of ice melt. Our daily loss rate estimates showed that highest sinking losses of biomass occurred during late winter.

CHAPITRE 2

INFLUENCE OF THE MACKENZIE RIVER PLUME ON THE SINKING EXPORT OF PARTICULATE MATERIAL ON THE SHELF

RÉSUMÉ

Nous avons étudié l'influence du fleuve Mackenzie sur l'exportation verticale de la matière particulaire organique et inorganique, sur le plateau du Mackenzie, dans l'Arctique canadien. Des pièges à particules à court terme ont été installés sous la halocline à trois stations réparties dans l'axe transversal du plateau continental, à l'automne 2002, et à trois stations réparties le long de ce plateau, à l'été 2004. Au cours de ces deux périodes d'échantillonnage, le patron spatial de variation des flux verticaux du carbone organique particulaire (POC) et de la chlorophylle *a* (chl *a*) était semblable à celui de la biomasse chlorophyllienne dans le panache du fleuve Mackenzie. Les taux de sédimentation maximum du matériel organique particulaire ont été observés aux stations fortement influencées pas le panache du fleuve (sédimentation maximale du POC à 25 m de 98 mg C m^{-2} d^{-1} et 197 mg C m^{-2} d^{-1} en 2002 et 2004, respectivement). La composition biogéochimique du matériel qui sédimente a varié de façon saisonnière; les cellules phytoplanctoniques et les pelotes fécales contribuaient considérablement au flux vertical en période estivale, alors que les détritus dominaient le flux vertical à l'automne. De plus, l'assemblage phytoplanctonique du matériel qui sédimente a présenté une succession saisonnière, passant d'une dominance de diatomées à l'été à une dominance de flagellés et dinoflagellés à l'automne. La présence de la diatomée d'eau douce *Eunotia* sp. dans l'assemblage phytoplanctonique du matériel qui a sédimenté directement sous le panache du fleuve indique une contribution fluviale à l'exportation verticale du matériel organique sur le plateau. Toutefois, l'augmentation des flux verticaux de chl *a* et de silice biogénique avec la profondeur indique aussi une exportation verticale de phytoplancton présent dans la colonne d'eau, sous le panache du fleuve, au cours de l'été et de l'automne. Le broutage, surtout par les copépodes et, de façon moindre, par les appendiculaires, semble avoir pris place dans une couche bien définie sous le panache du fleuve, particulièrement en période estivale. Ces résultats montrent que le fleuve Mackenzie influence la quantité ainsi que la composition du matériel qui sédimente sur le plateau continental en été et à l'automne. Toutefois le fleuve Mackenzie ne constitue pas la seule source de matériel qui sédimente en profondeur, aux stations sous l'influence de son panache.

ABSTRACT

We examined the influence of the Mackenzie River plume on sinking fluxes of particulate organic and inorganic material on the Mackenzie Shelf, Canadian Arctic. Short-term particle interceptor traps were deployed under the halocline at 3 stations across the shelf during fall 2002 and at 3 stations along the shelf edge during summer 2004. During the two sampling periods, the horizontal pattern in sinking fluxes of particulate organic carbon (POC) and chlorophyll *a* (chl *a*) paralleled that in chl *a* biomass within the plume. Highest sinking fluxes of particulate organic material occurred at stations strongly influenced by the river plume (maximum POC sinking fluxes at 25 m of 98 mg C m^{-2} d^{-1} and 197 mg C m^{-2} d^{-1} in 2002 and 2004, respectively). The biogeochemical composition of the sinking material varied seasonally with phytoplankton and fecal pellets contributing considerably to the sinking flux in summer, while amorphous detritus dominated in the fall. Also, the sinking phytoplankton assemblage showed a seasonal succession from a dominance of diatoms in summer to flagellates and dinoflagellates in the fall. The presence of the freshwater diatom *Eunotia* sp. in the sinking assemblage directly underneath the river plume indicates the contribution of a phytoplankton community carried by the plume to the sinking export of organic material. Yet, increasing chl *a* and biogenic silica (BioSi) sinking fluxes with depth indicated an export of phytoplankton from the water column below the river plume during summer and fall. Grazing activity, mostly by copepods, and to a lesser extent by appendicularians, appeared to occur in a well-defined stratum underneath the river plume, particularly during summer. These results show that the Mackenzie River influences the amount and the composition of the sinking material on the shelf in summer and fall, but does not constitute the only source of material sinking to depth at stations influenced by the river plume.

2.1 Introduction

The Arctic Ocean covers an area of 9534 km^2 and comprises ca. 4 % of the surface area of the world's oceans (Jakobsson 2002). Nonetheless, the Arctic Ocean encompasses ca. 20 % (5025 km^2) of the world's continental shelf areas (Stein & Macdonald 2004). Hence, the shallow continental shelf regions constitute a major part of the Arctic Ocean, making up ca. 53 % of its total surface area (Jakobsson 2002). The Arctic Ocean receives a large seasonal freshwater discharge from rivers (3299 km^3 y^{-1}; Stein & Macdonald 2004), equivalent to ca. 11 % of the global runoff (Shiklomanov 1998), bringing along organic and terrigenous material. Though a large part of the material carried by the rivers sediments in the deltas and estuaries (Carson et al. 1999), river discharge is considered to be the most important source of terrigenous material to the Arctic Ocean (Stein & Macdonald 2004). Riverine freshwater discharge may in some areas form distinctive plumes carrying material onto and beyond the nearshore continental shelf regions (Dittmar & Kattner 2003). The direction and extent of the river plumes are generally controlled by the Coriolis force, wind forcing, currents and tide (e.g. Fong & Geyer 2002).

Particulate inorganic and organic material associated with river plumes may instigate aggregation and subsequent sedimentation, which may increase vertical sinking fluxes in the plume area (Hamm 2002). The heterotrophic food web may utilize part of the particulate organic material discharged by Arctic rivers (e.g. Parsons et al. 1989, O'Brien et al. 2006) but, to a high degree, this material is often preserved in the marine sediments due to its refractory nature (e.g. Dittmar & Kattner 2003). Arctic rivers generally display a

strong seasonality, with the highest freshwater and sediment discharge onto the continental shelf areas during spring ("freshet") and summer (Stein & Macdonald 2004).

Most Arctic shelves experience a seasonal landfast sea ice cover and a rubble ice field can be present at the inner-shelf, often separated from offshore drifting pack ice by a flaw lead (e.g. Carmack & Macdonald 2002). Sea ice affects the seasonal primary production on shelf areas by generally sustaining ice algae production during spring, and restricting pelagic primary production due to light limitation (Sakshaug & Skjoldal 1989).

The phytoplankton production cycle in Arctic coastal areas experiencing seasonal sea ice cover generally shows an initial pelagic "ice-edge bloom" during break-up (Sakshaug & Skjoldal 1989), which may be followed by one or more pelagic summer or fall blooms (e.g. Arrigo & Dijken 2004). Pelagic primary production accounts for the majority of the annual primary production on Arctic continental shelves (Stein & Macdonald 2004); although ice algal production is thought to represent a seasonally important source of organic material for pelagic grazers. Arctic river plumes may sustain a high phytoplankton biomass and production (e.g. Parsons et al. 1988, Springer & McRoy 1993, Garneau et al. 2006), particularly some distance from the river mouth where nutrient concentrations are high and turbidity is low (e.g. Parsons et al. 1988).

Vertical sinking export constitutes the main transport pathway for supplying the benthos with particulate organic material originating from pelagic primary production (e.g.

Wassmann 1998). The particulate organic material may either sink directly as intact phytoplankton cells or be diverted through the pelagic heterotrophic food web. Grazing by herbivorous zooplankton results in the degradation of photosynthetic pigments (e.g. Welschmeyer & Lorenzen 1985) and carbon loss during assimilation (Møller et al. 2003). Subsequent repackaging of egested material into fecal pellets, especially by copepods and appendicularians, may reduce further degradation and increase the sinking velocity of the material (Turner 2002). On Arctic shelves, the quality and quantity of the particulate material exported to the benthos therefore depend on allochthonous input (e.g. riverine discharge), pelagic and ice-associated primary production as well as heterotrophic activity.

The Mackenzie Shelf covers ca. 120 km in width (offshore) and ca. 530 km in length comprising an area of ca. 6.0×10^4 km^2 (Carmack et al. 2004). The shelf receives 249 - 333 km^3 of freshwater annually from the Mackenzie River (Dittmar & Kattner 2003), most of which is discharged from May to September (Macdonald et al. 1998). The highest discharge of freshwater is usually observed from early May to early July, which is also the time of the largest terrigenous sediment discharge (O'Brien et al. 2006). Although the Mackenzie River constitutes the fourth largest Arctic river in regards to freshwater discharge, it represents the largest in terms of sediment discharge, delivering ca. 127 Mt of sediment (Macdonald et al. 1998), or an estimated 1.8 - 2.1 Mt of particulate organic carbon (POC) annually (Dittmar & Kattner 2003). Coastal erosion (ca. 5.6 Mt y^{-1} on the entire shelf; Macdonald et al. 1998) and resuspension (O'Brien et al. 2006) of sediment material may be of seasonal local importance, but the Mackenzie River remains the major

contributor of sediments to the shelf. The Beaufort Sea Gyre is the major offshore surface current, flowing to the west (anti-cyclonic) along the Mackenzie Shelf, while a cyclonic deeper undercurrent has been observed flowing to the northeast nearer the shelf edge (Pickart 2004).

The main objective of this study was to evaluate the influence of the Mackenzie River on the magnitude of the sinking export and on the composition of the sinking material on the shelf. In order to address this objective, we studied spatial and vertical patterns of sedimentation at stations located on two transects, i.e. perpendicular to the coastline across the shelf and parallel to the coastline along the shelf edge. We also evaluated the composition of the sinking material, especially the contribution of fecal pellets and phytoplankton algal cells to the sinking material. The sinking export of particulate material was determined immediately under the surface halocline and at deeper depths, in order to capture the signature of the Mackenzie River on the vertical export of material. It was hypothesized that the presence of the river plume would induce higher sinking fluxes of particulate organic material and would affect the composition of the sinking material.

2.2 Materials and methods

2.2.1 Study area

The sampling stations visited during fall 2002 were positioned along a cross-shelf transect perpendicular to the coastline, from the shallow inner-shelf station (43 m at St. 65)

to the outer-shelf station (77 m at St. 66) and the deeper shelf-slope station (1280 m at St. 49; Fig. 1 and Table 1). When the Mackenzie Shelf was revisited during summer 2004, sampling was conducted at three stations (St. 906, St. 803 and St. 708) located along a transect parallel to the coastline (along-shelf), with fairly constant water depth (ranging from 236 to 280 m). The Mackenzie River plume has been observed to extend up to 400 km offshore during summer (Carmack & Macdonald 2002), and may veer in different directions depending on the Coriolis force, wind direction and currents (O'Brien et al. 2006). During this study, the Mackenzie River plume extended northeastward along the coastline during fall 2002 (Garneau et al. 2006; see section 2.4.1) and northwestward during summer 2004, as per SeaWiFS image (Fig. 2). It is worth noticing that St. 708 was covered by sea ice two days prior to sampling, according to the SeaWiFS image.

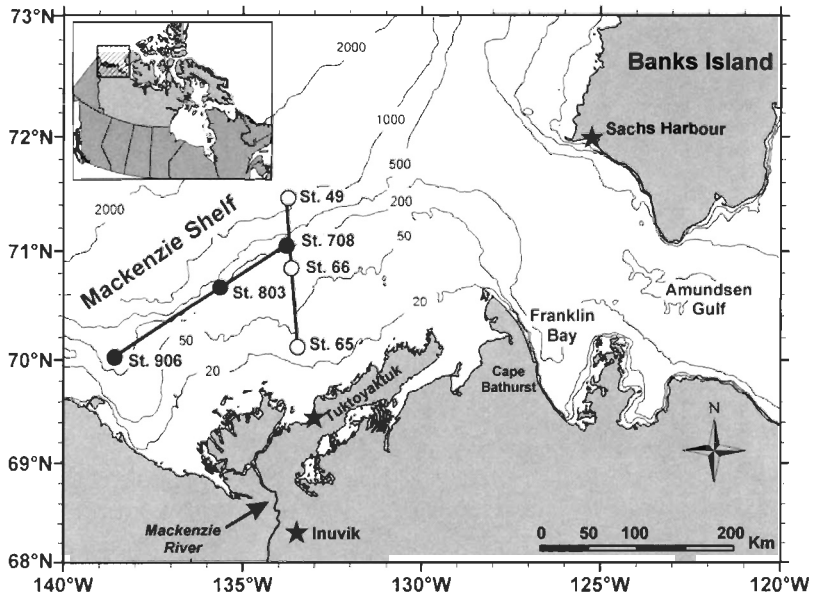

Fig. 1. Location of sampling stations on the Mackenzie Shelf, Arctic Canada. Open circles and close circles represent sampling stations visited during fall 2002 and summer 2004, respectively. Lines show the cross-shelf and along-shelf transects formed by the sampling stations. Contour depths in meters

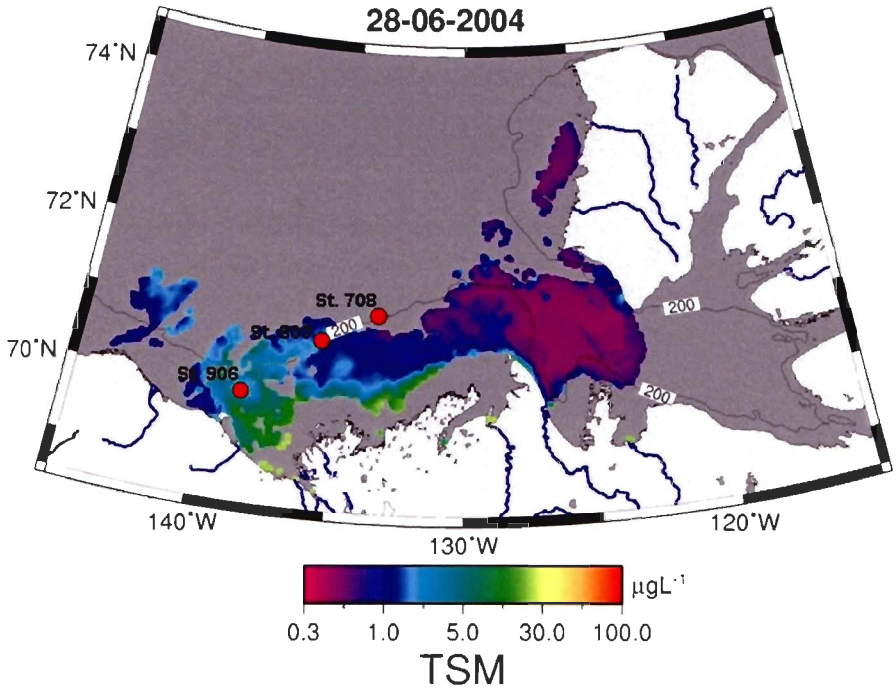

Fig. 2. Sea-viewing Wide Field-of-View Sensor (SeaWiFS) image depicting the distribution of sea ice (grey color) and total suspended material (TSM, color scale) within the open-water area on 28 June 2004 (courtesy of S. Bélanger and P. Larouche). Circles represent sampling stations visited during summer 2004. The 200 m isobath is indicated

2.2.2 Sampling

The sampling program was conducted onboard the Canadian research ice-breakers CCGS *Pierre Radisson* between 28 September and 5 October 2002 and CCGS *Amundsen* between 30 June and 8 July 2004 during the Canadian Arctic Shelf Exchange Study (CASES). At each sampling station, CTD profiles were performed with a SBE-911+ SeaBird profiler equipped with a Seapoint fluorometer. During fall 2002, additional CTD profiles were conducted in ca. 10 km increments along the cross-shelf transect.

Sinking fluxes of particulate material were measured using free-drifting particle interceptor traps deployed at multiple depths ranging from 25 to 150 m, depending on water depth (Table 1 and Fig. 3). Consequently, due to the shallow water depth at the shelf stations (43 and 77 m at St. 65 and St. 66, respectively), no data are available at depths >25 m at St. 65 and only two deployment depths (25 and 50 m) are available at St. 66 (Table 1).

Duplicate particle interceptor traps were deployed at each depth to ensure that enough particulate material was collected for analyses. The free-drifting trap array was equipped with a wave dampening device made of a series of 7 buoys of which 3 were submerged. Particle interceptor traps were constructed of PVC (Polyvinyl Chloride) cylinders closed at one end, with an internal diameter of 10 cm and an aspect ratio (height:diameter) of 7. The free-drifting trap array was fitted with a CAST ARGOS Drifter (Seimac Smart Cat PTT/GPS transmitter) for long-range satellite tracking and a Novatech Designs Ltd. RF-700C1 radio beacon for short-range positioning.

The particle interceptor trap sampling was carried out in accordance with JGOFS protocols (Knap et al. 1996) and recommendations by Gardner (2000). Filtered (0.22 μm) seawater, collected well below the deployment depths, was added to the particle interceptor traps prior to deployment to ensure that the higher density particle-free water remained inside the traps.

Table 1. Characteristics of free-drifting particle interceptor trap deployments during fall 2002 and summer 2004

Station	Deployment date	Duration	Deployment		Recovery		Distance travelled	Average speed	Water depth	Deployment depth
			Latitude	Longitude	Latitude	Longitude				
		(d)	(°N)	(°W)	(°N)	(°W)	(km)	(cm s^{-1})	(m)	(m)
49	28 Sep 2002	1.0	71° 27.60'	133° 43.90'	71° 32.15'	133° 40.43'	8.2	9.5	1280	25, 50, 75, 100, 125, 150
65	1 Oct 2002	1.0	70° 06.75'	133° 28.03'	70° 05.05'	133° 32.33'	4.9	5.7	43	25
66	5 Oct 2002	0.9	70° 50.45'	133° 38.45'	70° 50.20'	133° 32.00'	4.2	5.4	77	25, 50
708	30 Jun 2004	1.3	71° 02.77'	133° 46.31'	71° 03.66'	133° 43.34'	2.3	2.1	236	25, 50, 75, 100, 125, 150
906	3 Jul 2004	1.5	70° 01.10'	138° 34.57'	69° 50.10'	138° 21.96'	21.9	16.9	280	25, 50, 75, 100, 125, 150
803	8 Jul 2004	1.0	70° 39.94'	135° 37.89'	70° 38.60'	135° 54.14'	10.1	11.7	243	25, 50, 75, 100, 125, 150

Upon recovery, the particle interceptor traps were fitted with a clean lid and set aside for sedimentation during 8 h in a cold-room (0°C) onboard the ship. After the sedimentation period the supernatant was gently removed, the remaining trap sample was pre-screened (425 μm) to remove large swimmers, and the volume was measured. Duplicate particle interceptor trap samples from each depth were pooled together in dark containers for subsampling and analyses.

2.2.3 Analyses

The particle interceptor trap samples from different depths were gently mixed before subsampling for various analyses. Subsamples (100 - 250 ml) for fecal pellet and phytoplankton identification and enumeration were taken first to ensure minimal disturbance of the collected material. Fecal pellet samples were preserved with 2 % (v/v) buffered formaldehyde, while phytoplankton samples were preserved with 1 % (v/v) acidic Lugol's solution for later analyses. Fecal pellets were counted and the dimensions of each pellet were measured (length and width), using a Carl Zeiss inverted microscope (100 x magnification). Fecal pellets were classified according to type (cylindrical or elliptical) and their condition (intact or broken). The volume of intact cylindrical fecal pellets was calculated using the equation for a cylinder with half-spherical ends, while the volume of broken cylindrical fecal pellets was calculated as cylinders. The volume of the intact elliptical fecal pellets was calculated using the equation for an ellipsoid. No broken elliptical fecal pellets were observed. Phytoplankton identification and enumeration were

performed on 5 – 100 ml subsamples, using a Leica DM IRB inverted microscope (400 x magnification).

Chlorophyll *a* (chl *a*) and phaeopigments were measured on 50 - 200 ml subsamples filtered onto Whatman GF/F 25 mm filters. The filters were extracted in 90 % acetone for 24 h in cold dark conditions (4°C). After extraction, the samples were analyzed on a Turner Designs 10AU fluorometer, using 90 % acetone as a blank. Pigment concentrations in the samples were calculated according to Parsons et al. (1984).

Total particulate carbon (TPC) and particulate organic carbon (POC) and nitrogen (PON) were measured on 50 - 700 ml subsamples filtered onto pre-combusted (450°C for 24 h) Whatman GF/F 21 mm filters. After filtration, the filters were dried at 60°C for 24 h before being stored in separate Petri dishes for later analysis on a Perkin Elmer Model 2400 CHN Analyzer. POC was measured on filters which had been acidified during 24 h in a dessicator saturated with HCl fumes, thereby removing any inorganic carbon.

Biogenic and lithogenic silica (BioSi and LithoSi) were measured on 50 - 250 ml subsamples filtered onto 0.6 µm Nuclepore polycarbonate membranes, dried at 60°C for 24 h, and stored in cryovials for later analysis. BioSi was extracted in 0.2 M NaOH at 95°C, and sequential extraction was performed at 10, 15, 20, 30, 45, 60 and 90 min. BioSi in the subsamples was measured using a colorimetric reaction involving the formation of a silico-molybdate complex and spectrophotometric determination at 810 nm (Varian Inc.

CARY 100 BIO) (adapted from Conley 1998, Ragueneau & Tréguer 1994). The slope of silicic acid concentrations in sequential subsamples was used to correct for the presence of LithoSi in the samples. LithoSi was subsequently measured on the same membranes using hydrofluoric acid extraction for 48 h and a similar colorimetric reaction procedure as for BioSi (adapted from Conley 1998, Ragueneau & Tréguer 1994).

2.2.4 Calculations and statistical analyses

Sinking fluxes of the measured variables were calculated using the equation of the JGOFS protocol (Knap et al. 1996):

Sinking flux (mg m^{-2} d^{-1}) = (C_{trap} * V_{trap}) / (A_{trap} * T_{dep})

where C_{trap} is the concentration of the measured variable in the particle interceptor trap (mg m^{-3}), V_{trap} is the volume of the particle interceptor trap sample (m^3), A_{trap} is the particle interceptor trap surface area (m^2) and T_{dep} is the deployment time (d).

Fecal pellet volumes were converted into fecal pellet based carbon (FPC), using a volume to carbon conversion factor of 0.057 pg C μm^{-1} for cylindrical fecal pellets (i.e. copepod fecal pellets) and 0.042 pg C μm^{-1} for elliptical fecal pellets (i.e. appendicularian fecal pellets) (González et al. 1994).

Sinking flux data at depths >25 m, during summer 2004 (Table 1), was tested for significant differences between stations using Kruskal-Wallis tests (Sokal & Rohlf 1981). The lack or low number of deployments at depths >25 m, during fall 2002 (Table 1), at the

inner-shelf (n = 0 at St. 65) and outer-shelf stations (n = 1 at St. 66) prevented statistical analyses between stations along the cross-shelf transect.

2.3 Results

CTD profiling along the cross-shelf transect, during fall 2002, showed a continuous halocline at ca. 20 m, which was formed by the low-salinity Mackenzie River plume (Fig. 3a, c). The halocline was strongest at the inner-shelf and outer-shelf stations (St. 65 and St. 66), compared to the shelf-slope station (St. 49). Salinity profiles obtained on the along-shelf transect, during summer 2004, also showed a halocline at ca. 20 m (Fig. 3b, d). The salinity at 25 m was between 29.1 and 30.9 in 2002 and between 30.3 and 30.5 in 2004. *In situ* fluorescence profiling above the halocline (20 m), showed that chl *a* biomass increased towards the center of the river plume, during the two sampling periods (average of 0.3, 0.5 and 0.1 $\mu g\ l^{-1}$ at <20 m at St. 65, St. 66 and St. 49, in fall 2002; 0.7, 0.2 and 0.1 $\mu g\ l^{-1}$ at <20 m at St. 906, St. 803 and St. 708, in summer 2004; data not shown).

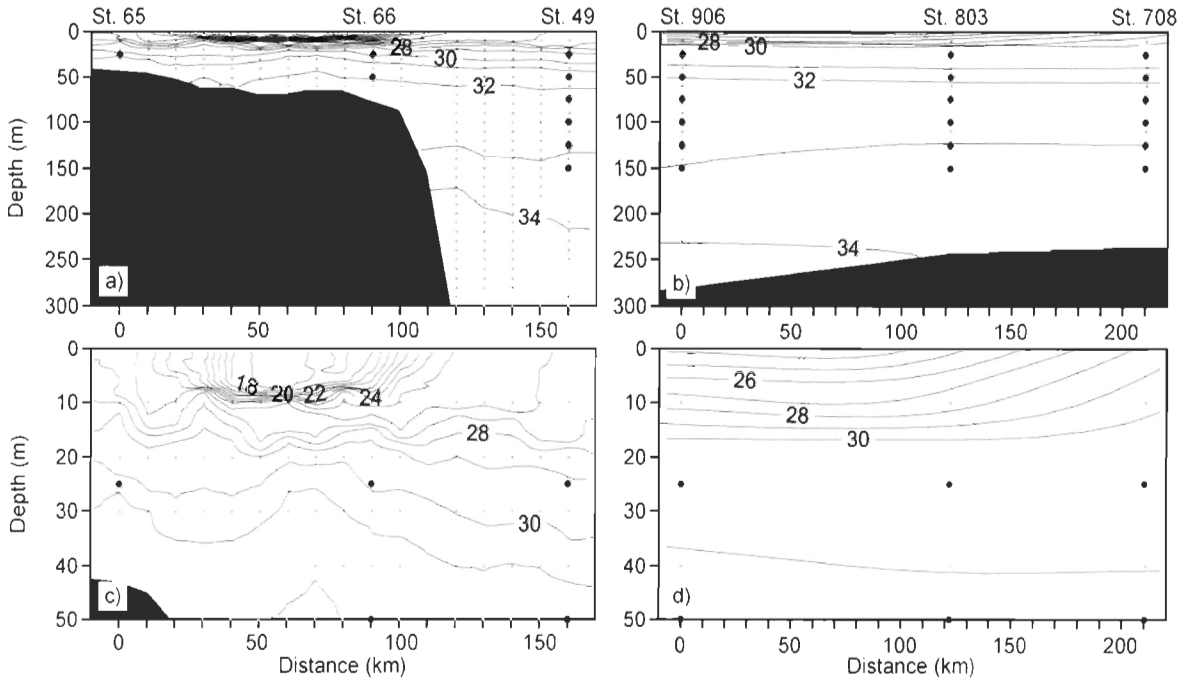

Fig. 3. Salinity profiles (a, c) across the shelf (fall 2002) and (b, d) along the shelf edge (summer 2004); (a, b) down to 300 m and (c, d) down to 50 m. Black circles represent particle interceptor trap deployment depths and grey dots represent CTD profiling depths in 10 m increments

Sampling along the cross-shelf transect, during fall 2002, showed higher chl *a* sinking fluxes at the inner-shelf and outer-shelf stations at 25 m (0.08 and 0.09 mg m^{-2} d^{-1} at St. 65 and St. 66, respectively) and at depths >25 m (0.15 mg m^{-2} d^{-1} at St. 66, data not available from St. 65), compared to the shelf-slope station (0.02 and 0.03 mg m^{-2} d^{-1} at 25 m and >25 m, respectively, at St. 49; Fig. 4a). During summer 2004, the highest chl *a* sinking fluxes were observed at St. 906 at all depths and decreased significantly (Kruskal-Wallis, $p < 0.01$; at depths >25 m) northeastwardly on the along-shelf transect (Fig. 4b). Chl *a* sinking fluxes at depths >25 m were higher than at 25 m at all stations during 2002 and 2004.

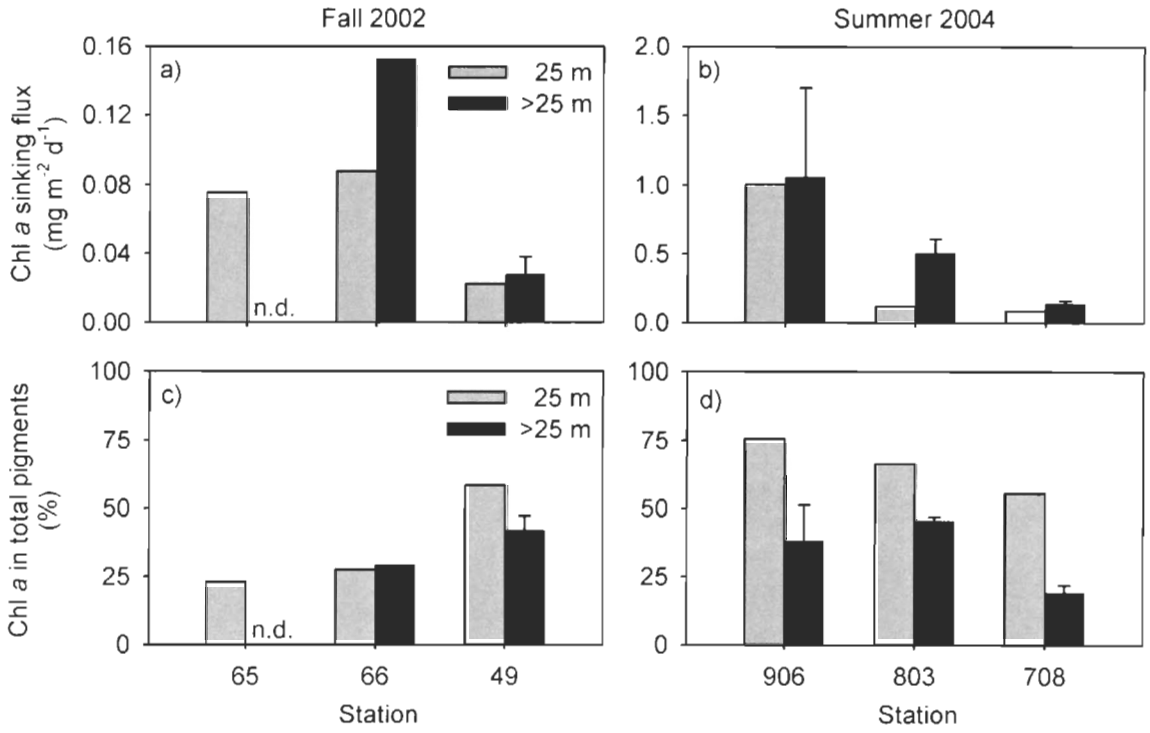

Fig. 4. Spatial variations of (a, b) sinking flux of chlorophyll *a* (chl *a*) and (c, d) percent contribution of chl *a* to total pigment (i.e. chl *a* + phaeopigments) sinking flux at 25 m and >25 m during (a, c) fall 2002 and (b, d) summer 2004. Mean ± standard deviation are shown for depths >25 m. n.d. = no data

The contribution of chl *a* to total pigments in the particulate material collected at 25 m increased from inshore to offshore, during fall 2002 (from 23.0 to 58.2 %; Fig. 4c). Similarly, at depths >25 m the chl *a* contribution to total pigments was higher at the shelf-slope station (41.7 % at St. 49) than at the outer-shelf station (29.2 % at St. 66). On the along-shelf transect, during summer 2004, the contribution of chl *a* to total pigments at 25 m progressively decreased northeastwardly (from 76.4 to 46.1 %; Fig. 4d). At depths >25 m, the percent contribution of chl *a* in total pigments was significantly (Kruskal-Wallis, $p < 0.01$) lower at St. 708 than at St. 906 and St. 803 (Fig. 4d). The chl *a*

contribution to total pigments was lower at depths >25 m than at 25 m at all stations on the along-shelf transect.

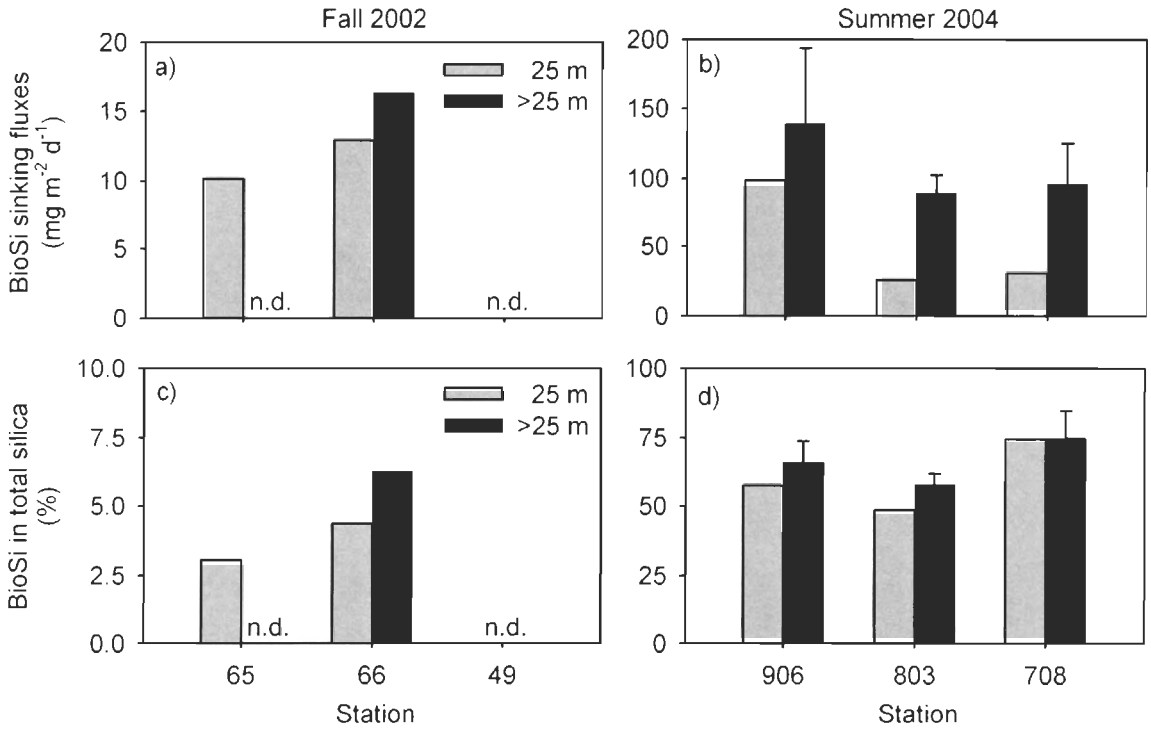

Fig. 5. Spatial variations of (a, b) sinking flux of biogenic silica (BioSi) and (c, d) percent contribution of BioSi to total silica (i.e. BioSi + LithoSi) sinking flux at 25 m and >25 m during (a, c) fall 2002 and (b, d) summer 2004. In (a) and (c), data are not available at St. 49. Mean ± standard deviation are shown for depths >25 m. n.d. = no data

Only two stations were sampled for BioSi and LithoSi in fall 2002. The outer-shelf station (St. 66) showed higher sinking fluxes of BioSi at 25 m, compared to the inner-shelf station (St. 65; Fig. 5a). The only available BioSi sinking fluxes at depths >25 m, during fall 2002, are from the outer-shelf station (St. 66; Fig. 5a). At 25 m, the contribution of BioSi to total silica sinking fluxes was higher at the outer-shelf station (St. 66) than at the inner-shelf station (St. 65; Fig. 5c). During summer 2004, high BioSi sinking fluxes were

measured at St. 906 (98.8 mg m^{-2} d^{-1} and 138.3 mg m^{-2} d^{-1} at 25 and >25 m, respectively; Fig. 5b). However, fluxes at depths >25 m were not significantly different among stations (Kruskal-Wallis, $p = 0.36$; Fig. 5b). BioSi sinking fluxes were higher at depths >25 m than at 25 m, and the difference was most evident at St. 803 and St. 708 (Fig. 5b). The contribution of BioSi to total silica sinking fluxes showed no clear trend along the shelf transect during summer 2004 (Fig. 5d).

POC sinking fluxes at 25 m were highest at the inner-shelf and outer-shelf stations during fall 2002 (75.5 and 97.6 mg m^{-2} d^{-1} at St. 65 and St. 66, respectively; Fig. 6a). Similarly, POC sinking fluxes at depth >25 m were higher at the outer-shelf station (70.2 mg m^{-2} d^{-1} at St. 66), compared to the shelf-slope station (10.1 mg m^{-2} d^{-1} at St. 49). Sinking fluxes of POC at depths >25 m were lower than the fluxes measured at 25 m during fall 2002. During summer 2004, the highest POC sinking flux at 25 m was observed at St. 906 (197.3 mg m^{-2} d^{-1}), whereas St. 803 and St. 708 showed comparable sinking fluxes (37.5 and 51.1 mg m^{-2} d^{-1}, respectively; Fig. 6b). Average POC sinking fluxes at depths >25 m decreased northeastwardly on the along-shelf transect (from 165.1 to 100.1 mg m^{-2} d^{-1}), although this trend was not statistically significant (Kruskal-Wallis, $p = 0.28$). The POC contribution to TPC sinking fluxes was 83.1 and 88.2 % at the inner-shelf (St. 65) and outer-shelf (St. 66) stations during 2002, while TPC values are not available for the shelf-slope station (St. 49; data not shown). During 2004, the POC contribution to TPC sinking fluxes ranged from 65.9 to 83.9 % along the transect (data not shown).

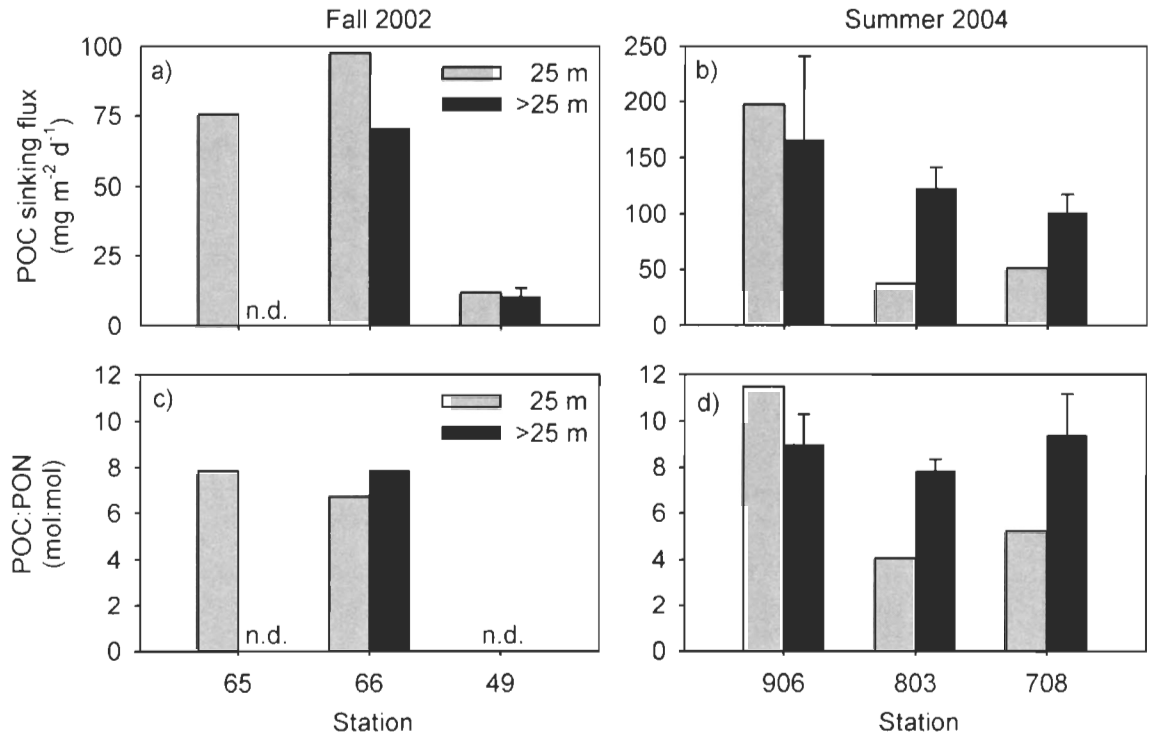

Fig. 6. Spatial variations of (a, b) sinking flux of particulate organic carbon (POC) and (c, d) ratio of POC to particulate organic nitrogen (PON) in the sinking material at 25 m and >25 m during (a, c) fall 2002 and (b, d) summer 2004. In (c), data are not available at St. 49. Mean ± standard deviation are shown for depths >25 m. n.d. = no data

The POC:PON molar ratios of the sinking particulate material collected at 25 m, during fall 2002, were comparable to the Redfield ratio (6.6 mol:mol; Redfield et al. 1963) at the shelf stations (7.9 and 6.7 at St. 65 and St. 66, respectively; Fig. 6c). PON values are not available for the shelf-slope station (St. 49). In contrast, the POC:PON molar ratio measured at 25 m on the along-shelf transect were above the Redfield ratio at St. 906 (11.5) and below the Redfield ratio at St. 803 and St. 708 (4.1 and 5.2 mol:mol, respectively; Fig. 6d). At depths >25 m, comparable (Kruskal-Wallis, $p = 0.30$) POC:PON molar ratios were observed at all stations on the along-shelf transect (ranging from 7.8 to 9.4; Fig. 6d).

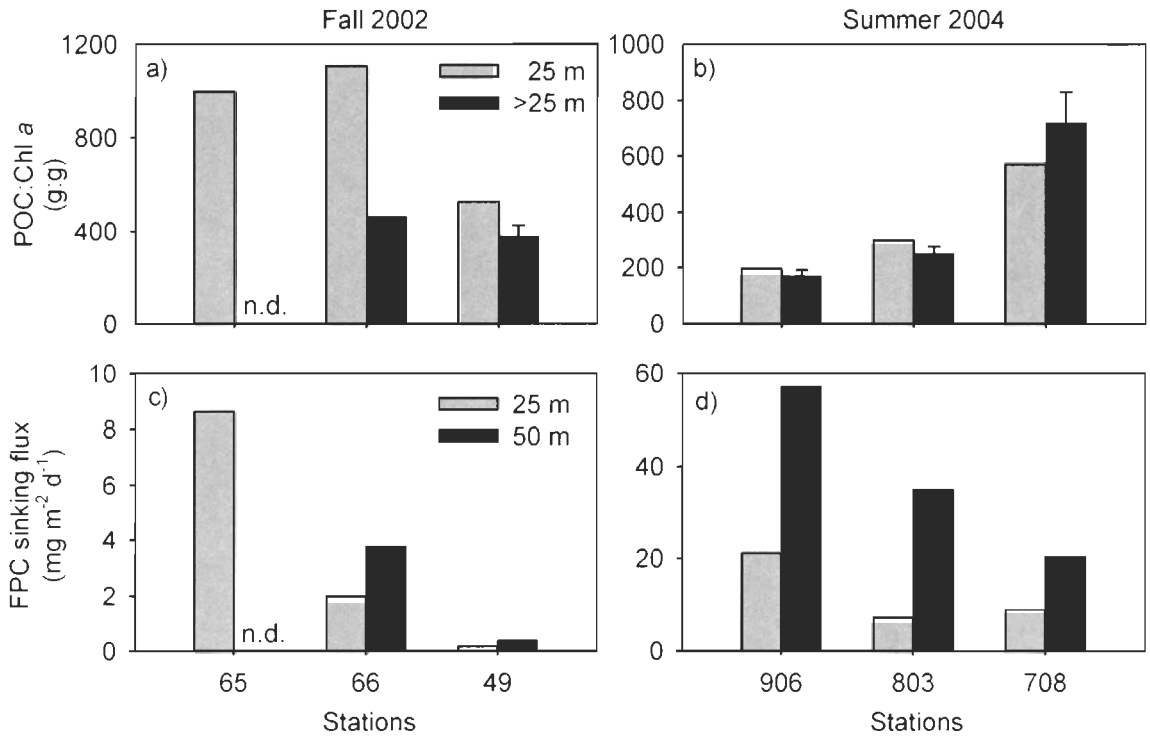

Fig. 7. Spatial variations of (a, b) ratio of particulate organic carbon (POC) to chlorophyll *a* (chl *a*) in the sinking material at 25 m and >25 m and (c, d) sinking flux of carbon-based (FPC) fecal pellets at 25 m and 50 m during (a, c) fall 2002 and (b, d) summer 2004. In (a) and (b), mean ± standard deviation are shown for depths >25 m. n.d. = no data

The POC:chl *a* ratios of the sinking material at stations across the shelf (Fig. 7a) showed trends similar to those of POC (Fig. 6a). At 25 m, POC:chl *a* ratios were highest at the inner and outer-shelf stations (1000 and 1109 g:g at St. 65 and St. 66, respectively; Fig. 7a), whereas at depths >25 m comparable POC:chl *a* ratios were observed at the outer-shelf and shelf-slope stations (460.2 and 375.4 g:g at St. 66 and St. 49, respectively). In contrast, at stations along the shelf, during summer 2004, the trends in the POC:chl *a* ratios were opposite to those in POC (Fig. 6b), as they increased at all depths

northeastwardly along the transect (from 184.0 to 801.2 and from 167.0 to 717.8 g:g at 25 and >25 m, respectively; Fig. 7b).

Sinking fluxes of FPC at 25 m decreased from 8.6 to 0.17 mg m^{-2} d^{-1} along the transect during fall 2002 (Fig. 7c), and from 21.1 mg m^{-2} d^{-1} at St. 906 to 7.4 and 9.1 mg m^{-2} d^{-1} at St. 803 and St. 708, respectively, during summer 2004 (Fig. 7d). FPC sinking fluxes at 50 m were 2 times higher than at 25 m during fall 2002 (ranging from 3.8 to 0.36 mg m^{-2} d^{-1}) and 2-5 times higher during summer 2004 (ranging from 20.5 to 57.0 mg m^{-2} d^{-1}). Cylindrical fecal pellets were the main contributors to FPC at all stations and depths during fall 2002 (ranging from 75.6 to 100.0 %; data not shown) and summer 2004 (ranging from 71.9 to 99.2 %; data not shown).

Sampling along the cross-shelf transect, during fall 2002, showed the highest sinking fluxes of phytoplankton cells at the inner-shelf station (325.7, 7.7 and 27.2 x 10^6 cells m^{-2} d^{-1} at St. 65, St. 66 and St. 49, respectively; Fig. 8a). Flagellates, especially flagellates <5 µm, were the most abundant phytoplankton cells collected along the cross-shelf transect (ranging from 74.4 to 93.7 %), although dinoflagellates, primarily *Gymnodinium* and *Gyrodinium* spp., contributed increasingly to the sinking assemblage across the shelf (from 5.1 to 19.9 %; Table 2). Diatoms comprised a minor fraction of the phytoplankton sinking flux along the cross-shelf transect (ranging from 1.2 to 9.4 %; Table 2). The freshwater diatom, *Eunotia* sp., was found in the material collected at 25 m at the inner-shelf station (St. 65) in fall 2002. During summer 2004, a strong decrease in

phytoplankton cell sinking fluxes was observed northeastwardly on the along-shelf transect (from 569.8 x 10^6 cells m^{-2} d^{-1} at St. 906 to 132.5 x 10^6 cells m^{-2} d^{-1} at St. 708; Fig. 8b). Diatoms, primarily the pennate diatoms *Fragilariopsis cylindrus* and *Navicula vanhoeffenii* and the centric diatom *Chaetoceros* spp., were the main contributors to the sinking cell assemblage, though their combined contribution decreased northeastwardly on the along-shelf transect (from 73.9 to 51.3 %; Table 2). In contrast, flagellates, mainly flagellates <5 μm, contributed increasingly to sinking fluxes of phytoplankton cells northeastwardly along the transect during summer 2004 (from 25.8 to 46.8 %; Table 2).

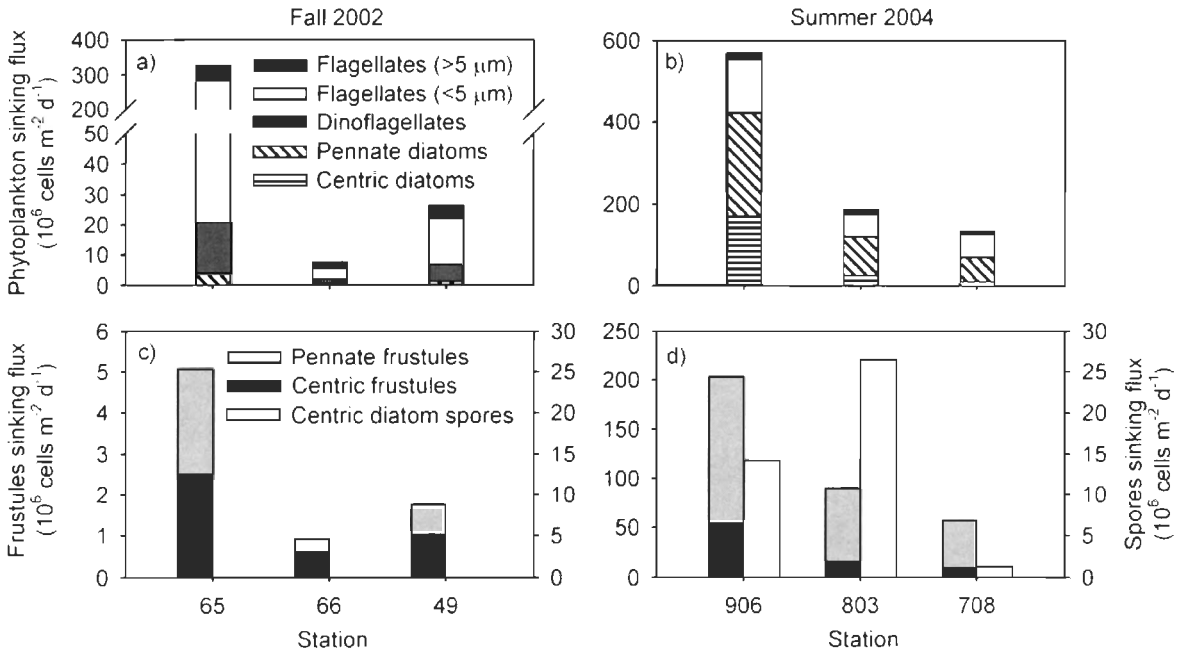

Fig. 8. Spatial variations in the sinking flux of (a, b) phytoplankton cells of various taxonomic groups and (c, d) empty diatom frustules and centric diatom spores during (a, c) fall 2002 and (b, d) summer 2004 at 50 m (25 m at St. 65). In (c), no spores were observed in fall 2002

Table 2. Percent contribution of phytoplankton taxonomic groups and dominant taxa in the sinking material collected at 50 m (25 m at St. 65) during fall 2002 and summer 2004. A dominant taxon is defined as the species or genus representing a minimum of 15 % total phytoplankton abundance at one station

	2002			2004		
Phytoplankton groups/species	St. 65	St. 66	St. 49	St. 906	St. 803	St. 708
Centric diatoms	0.0	7.8	0.8	29.7	13.2	6.7
Chaetoceros spp.	0.0	1.0	0.0	22.8	9.8	2.6
Pennate diatoms	1.2	1.6	3.2	44.1	51.8	44.6
Fragilariopsis cylindrus	0.0	0.3	0.0	17.0	32.0	27.9
Navicula vanhoeffenii	0.0	0.0	0.3	17.8	8.3	15.1
Dinoflagellates	5.1	16.2	19.9	0.3	0.0	1.9
Gymnodinium/Gyrodinium spp.	5.1	15.9	18.4	0.3	0.0	1.9
Flagellates (<5 μm)	80.9	49.7	60.0	23.1	30.1	42.0
Flagellates (>5 μm)	12.8	24.7	16.2	2.7	4.9	4.8

During fall 2002, the highest sinking fluxes of empty diatom frustules were observed at the inner-shelf station (5.1 x 10^6 cells m^{-2} d^{-1} at St. 65), equally comprised of empty centric and pennate diatom frustules (Fig. 8c). At the outer-shelf and shelf-slope stations the sinking fluxes of empty diatom frustules were mainly explained by centric diatoms (0.93 and 1.8 x 10^6 cells m^{-2} d^{-1} at St. 66 and St. 49, respectively; Fig. 8c). No diatom spores were observed in the sinking assemblage during fall 2002 (Fig. 8c). Sampling on the along-shelf transect, during summer 2004, showed decreasing sinking fluxes of empty diatom frustules northeastwardly along the transect (from 203.1 x 10^6 cells m^{-2} d^{-1} at St. 906 to 56.5 x 10^6 cells m^{-2} d^{-1} at St. 708; Fig. 8d). Pennate diatom frustules, such as *Fragilariopsis cylindrus,* were the most abundant of the identified frustules and represented

the majority of the empty diatom frustules (> 73 %), at all stations on the along-shelf transect. Centric diatom spores were present in the collected material at all stations on the along-shelf transect, with a maximum sinking flux observed at St. 803 (Fig. 8d).

2.4 Discussion

Predicted consequences of global warming in Arctic continental shelf regions include increased river runoff as a result of increasing precipitation on land (e.g. Peterson et al. 2002). The Mackenzie River already discharges more suspended material than any other river flowing into the Arctic Ocean (Stein & Macdonald 2004), and previous studies have established the major influence of this river on sediment and carbon fluxes on the adjacent shelf (e.g. Macdonald et al. 1998, O'Brien et al. 2006). This study provides new insights into the influence of the Mackenzie River on the sinking fluxes and composition of particulate material sedimenting on the shelf during the ice-free period.

Although the sampling was carried out in two different years and during different seasons (fall of 2002, summer of 2004), the study was designed such that the transects would intercept at the shelf-slope (near the 200 m isobath; Fig. 1), thus aiming for potential comparisons between transects. While it is not our intent to rule out interannual variability in sinking fluxes of particulate material (see sections 2.4.1 and 2.4.2), results from the two sampling periods will be brought together to discuss seasonal changes in the composition of the material exported vertically on the shelf (see sections 2.4.2 and 2.4.4).

In this study, cylindrical particle interceptor traps with a high aspect ratio (7) were used to assess sinking fluxes in the study area, as trap aspect ratios >3 are recommended (Gardner 1980, Hargrave & Burns 1979, Taguchi et al. 1993, Bale 1998), in particular in dynamic environments (e.g. current velocities up to 20 cm s^{-1}; White 1990). Estimated sinking fluxes of POC, using similar free-drifting particle trap arrays in the North Water Polynya (NOW), were in very good agreement with POC sinking flux estimates using the $^{234}Th/^{238}U$ disequilibrium method (Tremblay et al. 2006b).

2.4.1 Effect of the river plume on the magnitude of sinking fluxes

The river plume observed during fall 2002 likely originated further to the southwest and extended along the coastline into the sampling area, as suggested by Garneau et al. (2006). The sampling transect therefore covered a cross-section of the river plume, with a decreasing influence of the river when progressing offshore along the transect (Fig. 3a, c). Similarly, the along shelf transect sampled during summer 2004 covered a partial cross-section of the northwestwardly extending river plume, with a decreasing influence of the river plume from St. 906 to St. 708 (Fig. 2 and 3b, d). The shallowest particle interceptor trap deployments (25 m) were in close proximity to the halocline along the two transects, with the intent of collecting particulate material exported from the river plume. Indeed, the freshwater pennate diatom *Eunotia* sp. found in the sinking material collected at the inner-shelf station (at 25 m at St. 65), clearly indicated phytoplankton that had been

transported onto the shelf by the river plume and subsequently exported to the underlying water column.

The presence of a phytoplankton community carried by the river plume was supported by the high chl *a* biomass in surface waters, particularly at the stations strongly influenced by the plume (St. 65 and St. 66 during 2002, St. 906 during 2004). The spatial trend observed in fall 2002, with a high river plume chl *a* biomass at the shelf stations, agrees with the spatial trend reported during two parallel studies focussing on surface water samples collected along the cross-shelf transect during the same period. During these studies, higher POC (Wells et al. 2006) and chl *a* (Garneau et al. 2006) concentrations in the surface waters, i.e. above the halocline, were found at the stations strongly influenced by the river plume (St. 65 and St. 66) compared to the shelf-slope station (St. 49). In addition, Wells et al. (2006) established, based on similarity of biochemical variables, that the surface water on the cross-shelf transect corresponded to Mackenzie River water.

The presence of the river plume influenced the magnitude of the sinking flux of particulate organic material during both fall 2002 and summer 2004, as reflected by higher fluxes of chl *a* and POC at 25 m at the stations strongly influenced by the plume (Figs. 4a, b and 6a, b). The chl *a* biomass within the river plume therefore appeared to be coupled with the magnitude of sinking fluxes of particulate organic material to the underlying water column during both sampling periods. River plumes are usually associated with high concentrations of particulate organic material (e.g. Dittmar & Kattner

2003, Dagg et al. 2004), but mixing with surrounding seawater may dilute the biomass along the extent of the river plume (e.g. Dagg et al. 2004). During our sampling, dilution effects on the river plume biomass likely explain the lower suspended chl *a* concentrations (St. 49 during 2002, St. 708 during 2004) and lower sinking fluxes of particulate organic material towards the periphery of the river plume (Figs. 4a, b and 6a, b). In addition, our results show that the direct sinking of algal biomass from the surface layer to deeper waters in nearshore areas is likely to contribute to the removal of biomass from the river plume as it extends offshore.

While there was overall similarity in the spatial trends of particulate organic material sinking fluxes along the two transects (i.e. higher sinking fluxes of POC and chl *a* at stations strongly influenced by the river plume), a seasonal difference in the magnitude of fluxes was observed at the stations strongly influenced by the river plume. A previous study in one of the major channels in the Mackenzie Delta, the East Channel, showed increasing chl *a* concentrations from June to August (from ca. 2 to 5 $\mu g\ l^{-1}$) followed by a decrease in September (to ca. 1 $\mu g\ l^{-1}$; Anema et al. 1990), which agrees with the higher chl *a* biomass observed in the river plume in summer than in the fall during our study. As a corollary, the higher sinking fluxes of particulate organic material from the halocline during summer (at St. 906) compared to fall (St. 65 and St. 66), can be linked to seasonal changes in river plume biomass.

The influence of the Mackenzie River plume on sinking fluxes on the shelf therefore depends on seasonal differences in the concentration of particulate organic material in the discharged river water and how strongly a particular area is influenced by the plume. Moreover, the seasonal magnitude of freshwater discharge may influence the extent of the Mackenzie River plume (Carmack & Macdonald 2002).

2.4.2 Effect of the river plume on the composition of the sinking material

In the next section, we will discuss the influence of the Mackenzie River plume on the biogeochemical composition of the material exported from surface waters. While the presence of the river plume appeared to induce higher sinking fluxes of chl *a* and POC during the two sampling years and seasons, the effect of the plume on the composition of the exported material varied between sampling years. For this reason, the following discussion will address processes influencing the biogeochemical composition of the material for each sampling period separately.

Fall of 2002

During fall 2002, the particulate material exported from surface waters (25 m) at the shelf stations strongly influenced by the river plume showed a high particulate organic content, as POC dominated the TPC sinking export (83.1 and 88.2 % at St. 65 and St. 66, respectively; data not shown). This is in contrast with the very high (> 95 %; Fig. 5c) contribution of LithoSi to the total particulate silica in the sinking material collected underneath the river plume at those stations. This high LithoSi contribution to the exported

material along the cross-shelf transect can be explained by a combination of low BioSi sinking fluxes (< 15 mg m^{-2} d^{-1}; Fig. 5a) and high LithoSi fluxes (320.7 and 282.4 mg m^{-2} d^{-1} at St. 65 and St. 66, respectively; data not shown). The measured BioSi sinking fluxes were lower than fluxes reported during spring and summer in the NOW using similar short-term particle interceptor traps (ca. 50 - 800 mg m^{-2} d^{-1} at 50 m; Michel et al. 2002), while they compared with sinking fluxes reported during fall of 1987 on the Mackenzie Shelf edge using long-term moorings (ca. 5 - 30 mg m^{-2} d^{-1} at 128 and 145 m; O'Brien et al. 2006). The LithoSi contribution to the total silica sinking fluxes measured in the present study compare with those (> 90 %) reported by O'Brien et al. (2006) at the Mackenzie shelf edge in fall of 1987. Low sinking fluxes of intact diatom cells, empty diatom frustules and the lack of highly silicified diatom spores (Hargraves & French 1983) during fall 2002 (Fig. 8a, c) explain the low BioSi fluxes. LithoSi usually originates from terrestrial soils and sediments, and as a consequence may be abundant in river plumes containing a high terrestrial sediment load (e.g. Dagg et al. 2004). To our knowledge, particulate LithoSi has not been documented for the Mackenzie River, however, O'Brien et al. (2006) reported an increased contribution of LithoSi, i.e. decreased contribution of BioSi to total silica, resulting from the influence of the Mackenzie River plume and during episodes of resuspension or coastal erosion. While no indication of resuspended material was apparent at our deployment depths, it is possible that, during the fall, resuspended material was introduced into the river plume closer to the river. The similarity between the POC:PON and POC:chl *a* ratios measured in the material sinking from the river plume during our fall sampling (POC:PON ranging from 6.7 - 7.9 mol:mol, POC:chl *a* ranging

from 527.3 to 1109 g:g; Fig. 6c and 7a) and those reported by Wells et al. (2006) in the river plume (POC:PON ranging from 5.4 to 6.8 mol:mol, POC:chl *a* ranging from 312.5 to 1250 g:g) lends further support to a close coupling between the river plume and the material sinking underneath the halocline.

The river plume had a distinct signature reflected in the biogeochemical composition of the material sinking out of surface waters, with high POC:chl *a* ratios and a low percent contribution (< 30 %; Fig. 4c) of chl *a* to total sinking pigments during fall. Accordingly, estimates of the percent contribution of algal-based carbon to the total POC sinking fluxes, using a POC:chl *a* ratio of 40 g:g (Lorenzen 1968) at the shelf stations give values ≤ 4 %, thus reflecting a minor contribution of algae to the sinking flux of organic material from the river plume in fall. In contrast, at the shelf-slope station (St. 49), the percent contribution of algal-based carbon to total POC sinking fluxes estimated using the same carbon conversion factor, was somewhat higher (7.6 %). These values are conservative estimates, as POC:chl *a* ratios may vary considerably depending on the physiological condition of the phytoplankton cells (e.g. up to 221 g:g in nutrient deficient cells; Stramski et al. 2002). In addition, zooplankton fecal pellets contributed only a small fraction of the POC sinking flux from surface waters (25 m) at the shelf stations (11.4 and 2.3 % at St. 65 and St. 66; data not shown). Therefore, neither algal-based material nor fecal pellets were major contributors to the POC sinking out of surface plume waters during fall.

Garneau et al. (2006) showed the importance of particle-attached prokaryotes in surface waters along the cross-shelf transect in fall 2002. Microscopic observations of our samples showed abundance of amorphous detritus which, together with bacteria, likely comprised a large part of the POC exported from the river plume. Interestingly, the POC:PON ratio of the material sinking out of the river plume did not significantly depart from the Redfield ratio (6.6 mol:mol; Redfield et al. 1963) although various constituents other than algae contributed to the exported material. Marine bacterioplankton generally have a low POC:PON ratio (e.g. down to 3.8 mol:mol; Vrede et al. 2002), which would have contributed to lowering the POC:PON ratio in the collected material, while fecal pellets, with their high POC:PON ratios (e.g. up to 33.2; Daly et al. 1999), would have increased the ratio.

Copepods were the main grazers along the cross-shelf transect in fall, and they may have been grazing on material within the river plume, as indicated by the fecal pellets collected directly underneath the plume (at 25 m; Fig. 7c). Mesozooplankton communities have been reported to develop within river plumes (e.g. Dagg et al. 2004), whereas zooplankton underneath the plume can make diurnal migrations to graze on the abundant organic material in the plume (e.g. Pagona et al. 1993). Whether the fecal pellet exported from the surface layer reflected the grazing activity of a river plume community or zooplankton migrating daily to the river plume can not be inferred from our results. Yet, the fecal pellet flux directly underneath the river plume, and the higher chl *a* concentrations and FPC fluxes at the shelf stations (St. 65 and St. 66), lend support to the hypothesis that

the particulate organic material within the river plume provided a food source for grazers during fall.

Summer of 2004

Similarly as during fall 2002, the particulate material collected underneath the river plume in summer 2004 was dominated by organic material, as shown by the high organic carbon contribution to total carbon (POC ranging from 65.9 to 83.9 % of TPC; data not shown). However, in summer 2004, BioSi dominated the total silica sinking export (average of 60.2 %; Fig. 5d). The dominance of diatoms (51.3 - 73.9 %; Table 2), the abundance of empty diatom frustules and the presence of resting spores in the sinking assemblages would all contribute to explain the high BioSi sinking fluxes. Estimates of algal-based carbon using the same POC:chl *a* conversion factor as above, point to a percent contribution from algal cells to the total POC sinking export from surface waters ranging from 20.5 to 7.0 % in a northeastwardly direction (at 25 m at St. 906 and St. 708, respectively). As during fall, these are conservative estimates as considerably higher POC:chl *a* ratios have been observed for phytoplankton cells. These results, together with the decreasing POC:chl *a* ratios towards the river plume (ca. 200 g:g at St. 906), clearly indicate that the signature from the chl *a* biomass within the plume was recorded in the sinking material at 25 m and at greater depth (e.g. Fig. 7b).

The declining trend in FPC sinking fluxes away from the river influence, at 25 m and 50 m (Fig. 7d), points to higher grazing activity in the plume area. At the river plume

station (St. 906), the percent POC explained by fecal pellets was 10.7 % at 25 m, while fecal pellets contributed 19.6 and 17.8 % at 25 m at St. 803 and St. 708, respectively (data not shown). Overall, it is estimated that fecal pellets and algal cells contributed 31.1 % of the total POC sinking export at 25 m at the river plume station (St. 906), and 33.0 and 24.8 % at St. 803 and St. 708, respectively. Amorphous detritus therefore appear to have been an important component of the particulate organic material exported during summer, considering that our estimate does not include the contribution of diatom resting spores. In addition, amorphous detritus appeared to contribute an increasing fraction of the POC sinking fluxes towards the periphery of the river plume (at St. 708).

Interestingly, the drastic decrease in POC sinking fluxes from the surface water (at 25 m) between the river plume station (St. 906) and the other stations (St. 803 and St. 708; Fig. 6b) was paralleled by a decrease in the POC:PON ratio along the transect (Fig. 6d). The high POC:PON ratio at the river plume station (11.5 mol:mol at St. 906; Fig. 2) agrees with the high ratios reported from the river water in the fall (ca. 13.0 - 16.5 mol:mol; Wells et al. 2006). In contrast, the low POC:PON ratios at St. 803 and St. 708 (4.1 and 5.2 mol:mol, respectively; Fig. 6d), which were well below the Redfield ratio (6.6 mol:mol; Redfield et al. 1963), may have been due to particle-attached bacteria in the sinking material, as suggested for the fall period (see previous section).

Altogether, these results show a seasonal succession in the biogeochemical composition of the particulate material exported from Mackenzie River plume, from a

significant contribution of phytoplankton and fecal pellets during summer to material dominated by amorphous detritus during fall. In addition, the influence of the river plume on the biogeochemical composition of the exported material is largely concentrated to areas strongly influenced by the plume, as the plume signature decreases progressively towards its periphery.

2.4.3 Pelagic export and transformation of sinking material

The presence of the river plume also influenced the magnitude of the sinking fluxes of organic material at depths below the halocline, as reflected by highest sinking fluxes of chl *a* and POC at the stations strongly influenced by the plume during fall 2002 (St. 65 and St. 66) and summer 2004 (St. 906) (Figs. 4a, b and 6a, b). The Mackenzie River plume has previously been reported to induce high sinking fluxes of particulate organic material at depth (213 m) on the shelf in the summer of 1987, using long-term moorings (near our St. 906; O'Brien et al. 2006).

The higher chl *a* sinking fluxes at depths >25 m than at 25 m during the two sampling periods (Fig. 4a, b) are interpreted in terms of downward export of phytoplankton below the river plume as, without the introduction of new material, sinking fluxes of organic material are expected to decrease with depth (e.g. Sarmiento & Gruber 2006). Similarly, increasing BioSi fluxes with depth (Fig. 5a, b) indicate that diatom-based material, i.e. intact algal cells or feces containing diatoms, contributed to this sinking export of phytoplankton below the river plume.

Zooplankton was grazing on particulate organic material below the river plume in summer and fall, as reflected by the higher FPC sinking fluxes at 50 m, than at 25 m, in fall and summer (Fig. 7c, d). Still, the contribution of fecal pellets from zooplankton located below the river plume was higher during summer, compared to in fall, as seen by the more pronounced increase in FPC sinking fluxes from 25 m to 50 m in summer. Copepods were the main grazers in summer and fall, as FPC sinking fluxes were predominantly comprised of cylindrical fecal pellets. This grazing on the sinking particulate organic material below the river plume was also reflected in the increasing proportion of phaeopigments with depth occurring at most stations (Fig. 4c, d) and the decreasing POC sinking fluxes with depth during fall (Fig. 6a). This shift took place within a well-defined depth stratum at each station (from 25 to 50 m at St. 49, St. 803 and St. 708, and from 25 to 100 m at St. 906; data not shown), indicating production of fecal pellets in these depth strata. The grazing activity below the river plume (from 25 to 50 m) could also explain the increasing POC:PON ratios with depth (except for St. 906; Fig. 6c, d), as herbivorous fecal pellets have a high POC:PON ratio (e.g. Daly et al. 1999).

The FPC contribution to POC sinking fluxes at 50 m at St. 708 on 30 June 2004 (24.4 %; data not shown), corresponds with results (ca. 20 %) reported during July 2004 in a parallel study using long-term sediment trap moorings at 200 m at a nearby station on the upper-slope of the Mackenzie Shelf (Forest et al. 2007). FPC sinking fluxes during summer (20.5 - 55.9 mg C m^{-2} d^{-1}; Fig. 7d) were comparable to fluxes reported during June and July in the NOW (ca. 25 - 75 mg C m^{-2} d^{-1}; Caron et al. 2004), but considerably higher than

fluxes reported at the deeper nearby station in July 2004 (ca. 2 mg m^{-2} d^{-1}; Forest et al. 2007). In contrast, during fall 2002 the measured FPC fluxes (0.17 - 8.6 mg C m^{-2} d^{-1} at 25 m and 50 m; Fig. 7c) were comparable to those reported by Forest et al. (2007) in October 2003 (ca. 2 mg m^{-2} d^{-1}, similar to their July 2004 value), but were considerably lower than the values reported in August and September in the NOW (ca. 100 mg C m^{-2} d^{-1}; Caron et al. 2004). The high fecal pellet sinking fluxes in the NOW relates to a high primary production and a high transfer rate of primary-produced material through the herbivorous food web in this area during spring and summer (Mei et al. 2003).

The size range of cylindrical fecal pellets collected during summer and fall (width ranging from ca. 20 - 100 µm; data not shown) indicates the presence of small copepods as well as of large *Calanus* spp. (Riser et al. 2002). This corresponds with the species composition observed by Forest et al. (2007) on the Mackenzie Shelf, where *Oithona similes*, *Microcalanus pygmaeus* and *Cyclopina* sp. showed the highest abundance, whereas the larger *Calanus hyperboreus* and *C. glacialis* comprised the highest biomass during October 2003 and June 2004.

Although appendicularian feces contributed much less to FPC fluxes on the shelf than copepods (0.83 - 28.1 and 0 - 24.4 % during summer and fall, respectively; Fig. 7c, d), their presence in the sinking biomass reflects a utilization of particles smaller than those effectively grazed by copepods (Urban et al. 1992). Our results thus reflect two distinct pathways of export of organic material to pelagic grazers, i.e. large cells being grazed by

copepods and small (<5 μm) cells, which were particularly abundant in the material collected during fall (Table 2), being transferred to appendicularians.

The observed FPC sinking fluxes (at 50 m) represent a higher POC ingestion by grazers, as only a small fraction of the POC removed from suspension by the grazers is reintroduced into the water column as FPC (ca. 15 % of POC for *Calanus* spp.; Møller et al. 2003). These authors, found high DOC production, due to sloppy-feeding (49 % of POC removed from suspension) and leakage from fecal pellets (6 % of POC removed from suspension) using ^{14}C-labeled phytoplankton as tracers, which may have been underestimated in other studies. Using the value from Møller et al. (2003), it is estimated that 136.5 - 372.4 mg m^{-2} d^{-1} of algal-based POC was removed from suspension by grazers in summer and 3.0 - 57.5 mg m^{-2} d^{-1} in the fall. These grazing estimates are equivalent to 5.4 - 86.0 % and 0.8 - 7.0 % of the integrated algal-based POC biomass above 50 m (25 m at St. 65) in summer and fall, respectively, based on *in situ* fluorescence and a POC:chl *a* ratio of 40 g:g for algae (Lorenzen 1968). Although these grazing estimates are subject to change if using a different percent removal from suspension by grazing and/or different POC:chl *a* values, the relative values clearly indicate higher grazing pressure in summer than in fall. The dominance of smaller phytoplankton cells (<5 μm) in the fall and/or the fact that large arctic copepods of the genus *Calanus* descend to deeper waters late in the season in preparation for their diapause (Hirche 1998), would explain the lower grazing activity in fall. In contrast, smaller copepods may remain active during the entire or part of

the winter period, and have been reported to graze on the early ice algae production during the winter-spring transition (e.g. Runge & Ingram 1988).

2.4.4 Species composition of the sinking assemblage

The comparable sinking fluxes of particulate organic material from the surface waters, i.e. chl *a*, BioSi and POC fluxes at 25 m (Figs. 4a, b; 5a, b and 6a, b), towards the periphery of the river plume during fall 2002 (St. 49) and summer 2004 (St. 803 and St. 708), together with the community succession observed in the trap material, lend support to discuss the datasets in terms of seasonal trends.

In addition to the seasonally higher sinking fluxes of particulate organic material at the station strongly influenced by the river plume in summer (St. 906) than in fall (St. 65 and St. 66; see section 2.4.1), there was also a transition from a higher contribution of algal-based material in summer towards a higher contribution of amorphous detritus and degraded material in the fall. Microscopic analyses of the collected particulate material reflected comparable ranges of phytoplankton cell sinking fluxes in fall 2002 (ranging from 7 to 326 x 10^6 cells m^{-2} d^{-1}; Fig. 8a) and summer 2004 (ranging from 133 to 569 x 10^6 cells m^{-2} d^{-1}; Fig. 8b). The low phytoplankton cell sinking flux at the outer-shelf station (St. 66) where the river plume influence was strong, in the fall, may reflect an underestimation of cell numbers due to the high degree of aggregation of the collected material. The sinking fluxes of phytoplankton cell numbers observed during our study are comparable to values reported during open-water conditions in Frobisher Bay

(280 x 10^6 cells m^{-2} d^{-1}; Hsiao 1987), on the shelf of northern Spitsbergen (ca. 42.7 x 10^6 cells m^{-2} d^{-1}; Andreassen et al. 1996) and following the early phytoplankton bloom in the NOW (ca. 500 x 10^6 cells m^{-2} d^{-1}; Caron et al. 2004).

The mismatch between comparable phytoplankton cell sinking fluxes, by numbers, and different chl *a* fluxes during summer and fall was likely explained by the seasonal change in phytoplankton cell composition in the collected material. The larger diatom cells which dominated the sinking assemblage during summer, would have a higher chl *a* content per cell than the small flagellates which dominated in the fall (Table 2), thus leading to higher chl *a* sinking fluxes in summer (Fig. 4b). The seasonal succession observed in the sinking cell assemblage, from a dominance of diatom cells during summer to a dominance of flagellates and dinoflagellates during fall (Fig. 8a, b and Table 2), resembles the seasonal progression commonly found in Arctic coastal waters (e.g. Rat'kova et al. 1998). As diatoms become nutrient limited during summer, the smaller flagellates and dinoflagellates take over, in part due to their higher nutrient uptake efficiency, i.e. ability to take up nutrients at low nutrient concentrations (e.g. Aksnes & Egge 1991), and their lack of requirement for silicic acid, which may become limiting at the end of diatom blooms (e.g. Dale et al. 1999). The presence of diatom resting spores in the sinking particulate material during summer (Fig. 8d), suggests that the diatom community may have been nutrient limited, as the production of resting spores has been linked to nutrient limitation (Hargraves & French 1983). Overall, despite the influence of the river plume on phytoplankton sinking export, the seasonal change in the cell

composition of the sinking assemblage during summer and fall indicates a species succession comparable to other Arctic coastal regions (e.g. Rat'kova et al. 1998).

2.5 Conclusion

The presence of the Mackenzie River plume increased the sinking fluxes of chl *a* and POC in the underlying water column, reflecting a spatial link between the plume biomass and the magnitude of downward sinking fluxes of organic material. In addition, seasonal changes in the magnitude of sinking fluxes of organic material were linked to the presence of the river plume, as high summer biomass in the river plume biomass induced higher sinking fluxes than in fall. Seasonal changes in the biogeochemical composition of the material exported from the river plume were also observed, as phytoplankton and fecal pellets contributed significantly to the sinking material during summer while amorphous detritus dominated during fall. The presence of the river plume clearly influenced the composition of the sinking assemblage as the freshwater diatom *Eunotia* sp. was observed in the material sinking out of the surface water during fall. Yet, in spite of the influence of the river plume, the sinking phytoplankton assemblage appeared to follow a seasonal succession similar to that observed in other Arctic coastal regions, with a dominance of diatoms in summer and of flagellates and dinoflagellates in the fall. Accordingly, our results showed increasing chl *a* and BioSi sinking fluxes with depth, which indicate that phytoplankton cells produced under the halocline in both seasons supplemented the export of material from the river plume. Grazing activity, mainly by copepods, had a significant

impact on the biogeochemical composition of the sinking material, in particular during summer. Overall, these results provide valuable information on the effects of a river plume on the magnitude and biogeochemical composition of sinking fluxes on an Arctic shelf. This study emphasizes that various processes, including the presence of river plumes together with production and grazing in the water column, determine the sinking export of organic material on Arctic shelves.

CHAPITRE 3

SINKING EXPORT OF PARTICULATE ORGANIC MATERIAL FROM THE EUPHOTIC ZONE IN THE EASTERN BEAUFORT SEA

RÉSUMÉ

Cette étude présente une couverture extensive de la sédimentation de la matière organique particulaire sous la zone euphotique, dans le secteur est de la mer de Beaufort. Des pièges à particules dérivants à court terme ont été déployés, généralement à 50 m, au cours de l'automne 2002 et 2003, et à l'été 2004. Les différentes régions de la zone d'échantillonnage, i.e. la polynie du Cap Bathurst ainsi que le plateau et le talus continental du Mackenzie, ont présenté des taux de sédimentation de la chlorophylle *a* (chl *a*) et du carbone organique particulaire (POC) comparables à l'automne, alors que des différences régionales ont été observées en période estivale. Les deux régions ont montré un patron général de décroissance saisonnière dans les taux de sédimentation. Les taux maximum de sédimentation de la chl *a* et du POC au cours de cette étude ont été observés au cours de l'été (3.6 et 258.4 mg m^{-2} d^{-1}, respectivement). Une forte rétention de la biomasse suspendue a été observée au cours de cette étude, i.e. de faibles taux de perte de la chl *a* et du POC (ca. 1 % d^{-1} en moyenne) ont été mesurés. Toutefois, la sédimentation du POC comptait en moyenne pour la moitié de la production primaire particulaire, tout au long de cette étude. Le zooplancton, surtout les copépodes, a joué un rôle important dans la sédimentation de la matière organique particulaire, et ce particulièrement dans la polynie du Cap Bathurst. Un groupement basé sur la composition de l'assemblage des protistes du matériel qui sédimente a révélé une succession saisonnière, celle-ci prévalant sur les différences spatiales et interannuelles entre les stations échantillonnées dans le secteur est de la mer de Beaufort. Les flagellés étaient dominants, alors que la contribution des diatomées, dominées par *Fragilariopsis cylindrus*, a diminué au cours de la saison. La présence des diatomées de glace *Nitzschia frigida* et *Navicula vanhoeffenii* dans le matériel qui a sédimenté au cours de l'été, a indiqué un apport de matériel organique provenant de la glace de mer. Les résultats de pièges à particules déployés à une station de glace de rive au cours de la période englacée et en période d'eau libre, ont révélé l'importance de considérer l'exportation sous glace (jusqu'à 115.4 mg C m^{-2} d^{-1} pour le POC) dans les estimations de sédimentation sur le plateau continental arctique.

ABSTRACT

This study presents an extensive spatial and seasonal coverage of the sinking export of particulate organic material below the euphotic zone in the eastern Beaufort Sea. Free-drifting short-term particle interceptor traps were deployed, generally at 50 m, during fall 2002 and 2003 and summer 2004. The different regions of the sampling area, i.e. the Cape Bathurst Polynya and the Mackenzie shelf and slope, showed comparable ranges in the sinking export of chlorophyll *a* (chl *a*) and particulate organic carbon (POC) in fall, while regional differences were observed in summer. The two regions showed a general decreasing trend in sinking fluxes towards fall. The highest chl *a* and POC sinking fluxes during this study were therefore recorded during summer (3.6 and 258.4 mg m^{-2} d^{-1}, respectively). A high retention of suspended biomass was observed throughout this study, i.e. low daily loss rates of suspended chl *a* and POC (both averaging ca. 1 % d^{-1}) were observed. Still, the POC sinking export accounted for, on average, half of the particulate primary production throughout this study. Zooplankton, primarily copepods, played an important role in the sinking export of particulate organic material, particularly in the Cape Bathurst Polynya. A cluster-based analysis of the sinking protist cell assemblage revealed a seasonal succession that prevailed over spatial and interannual differences between the stations sampled in the eastern Beaufort Sea. Flagellates dominated throughout the study area, while diatoms, dominated by *Fragilariopsis cylindrus*, showed a decreasing contribution to the sinking protist cell assemblage towards fall. The presence of the sea ice related pennate diatoms *Nitzschia frigida* and *Navicula vanhoeffenii* in the material collected during summer reflected an input of organic material from the sea ice. Results from particle interceptor traps deployed at a landfast sea ice station during ice-covered and ice-free conditions showed the importance of taking into account underice sinking fluxes (up to 115.4 mg C m^{-2} d^{-1} for POC) for sinking export estimates on Arctic shelves.

3.1 Introduction

The extent and thickness of the sea ice cover have changed in the Northern Hemisphere during the last three decades; these changes are thought to be a consequence of the ongoing global warming trend (IPCC 2007). The extent of multi-year sea ice, primarily found in the central Arctic Ocean, has been decreasing by ca. 7 % per decade since 1978 (IPCC 2007), as multi-year sea ice is being replaced by seasonal first-year sea ice in many areas (e.g. Belchansky et al. 2005). Moreover, the number and size of sea ice flaw leads and polynyas in the Arctic Ocean is expected to increase if the climate change trend continues (ACIA 2005). Consequently, the duration and extent of seasonally ice-free areas is expected to increase in the Arctic Ocean, in particular in the coastal regions (ACIA 2005, IPCC 2007).

Changes in sea ice dynamics may have impacts on marine productivity and ecosystem structure, especially on Arctic continental shelves (e.g. Grebmeier et al. 2006) which comprise a large part of the Arctic Ocean (i.e. 53 % of the total surface area; Jakobsson 2002). An increase in the duration and extent of ice-free areas is likely to improve conditions for phytoplankton production in the Arctic Ocean, due to increased light availability in the upper water column (ACIA 2005). Phytoplankton production already contributes ca. 75 to >97 % of the total annual primary production (i.e. ice algal and phytoplankton production) on Arctic shelves (Subba Rao & Platt 1984, Legendre et al. 1992, Gosselin et al. 1997).

Spring phytoplankton production on Arctic shelves, which is often dominated by diatoms, is generally associated with the moving ice edge during spring melt, as the upper water column is stabilized via the halocline formed by released melt water (e.g. Sakshaug & Skjoldal 1989, Carmack et al. 2006). Ice edge blooms or spring blooms in polynyas are often terminated by nutrient limitation within the surface mixed layer (e.g. Sakshaug & Skjoldal 1989, Carmack et al. 2006, Tremblay et al. 2006a). Nutrient limitation often induces a succession in phytoplankton species, from diatoms to flagellates and dinoflagellates (e.g. Rat'kova et al. 1998, Dale et al. 1999, Hill et al. 2005). Flagellates and dinoflagellates generally have higher uptake efficiency for nitrate and phosphate than diatoms (e.g. Dale et al. 1999). In addition, they are not dependent on the availability of silicic acid which may limit diatom production during summer (e.g. Dale et al. 1999). A phytoplankton bloom can occur during fall in Arctic areas, as wind mixing can reintroduce nutrients into the surface mixed layer (e.g. Klein et al. 2002, Arrigo & Dijken 2004, Carmack et al. 2006).

Primary-produced organic material may be vertically exported to the benthos as intact algal cells, or it may be diverted through the pelagic heterotrophic food web (e.g. Turner 2002, Wassmann et al. 2006). Sinking of intact algal cells generally conveys organic material of a high quality to the benthos, while algal material diverted through the heterotrophic food web results in a reduced sinking export of organic material of usually lesser quality (e.g. Turner 2002). Herbivorous grazers, particularly copepods, may at times effectively graze on suspended algal material in some Arctic areas (e.g. Michel et al. 1996,

Fortier et al. 2002, Forest et al. 2007). Fecal pellets from herbivorous grazers may therefore at times represent an important component of the vertically exported organic material (e.g. up to ca. 60 % of POC sinking fluxes; Juul-Pedersen et al. 2006). A potential increase in the annual primary production in the Arctic Ocean associated with climate changes (ACIA 2005), accompanied by changes in the pelagic heterotrophic food web (Grebmeier et al. 2006), will likely result in changes to the pelagic-benthic coupling on the Arctic continental shelves.

This study investigates spatial and temporal variability in the sinking export of organic material from the euphotic zone in the eastern Beaufort Sea. The objectives of this study were to (1) asses spatial variations in the magnitude of sinking export of organic material from the euphotic zone in the eastern Beaufort Sea, (2) characterize any patterns in the composition of the sinking material within the sampling area, especially with respect to protist cell assemblages, and (3) make a comparison between the magnitudes of sinking export of particulate organic material during sea ice covered and subsequent ice-free conditions at a landfast sea ice station. A first hypothesis was that the eastern Beaufort Sea would display spatial and seasonal differences, from spring to fall, in the magnitude of sinking of particulate organic material. It was also hypothesized that higher sinking fluxes of organic material would be observed during ice-free conditions, than during landfast ice cover, as phytoplankton may be exported from the euphotic zone.

3.2 Materials and methods

3.2.1 Study area

This study was conducted during a multi-year sampling program of the Canadian Arctic Shelf Exchange Study (CASES) in the eastern Beaufort Sea, during fall 2002 and 2003 and summer 2004 (Table 1 and Fig. 1). The sector of the Beaufort Sea studied here covers two distinctive regions, i.e. the Mackenzie shelf and slope and the Cape Bathurst Polynya. The Mackenzie shelf extends ca. 120 km offshore and ca. 530 km along the Tuktoyaktuk peninsula until the Cape Bathurst peninsula (ca. 6.0 x 10^4 km^2; Carmack et al. 2004; Fig. 1). Landfast first-year sea ice generally covers the inshore part of the Mackenzie shelf (until the ca. 20 m isobath) from December to May/June (Carmack & Macdonald 2002). A flaw lead system which separates the landfast sea ice from offshore drifting pack-ice generally develops into the recurring Cape Bathurst Polynya protruding into the Amundsen Gulf (Barber & Hanesiak 2004). The polynya generally starts forming during May, and the sea ice continues to retreat during summer leading to largely ice-free conditions in the Amundsen Gulf by August (Barber & Hanesiak 2004). A five year satellite study of the area showed two distinctive phytoplankton blooms generally occurring each year within the polynya, with some interannual variability in the timing and intensity of these blooms (Arrigo & Dijken 2004). An initial spring bloom is typically observed in May, while an often more intense fall bloom takes place in September. The Mackenzie shelf is strongly influenced by the Mackenzie River, which has the highest sediment discharge of the rivers entering the Arctic Ocean (Macdonald et al. 1998). The Mackenzie

River has been shown to have a strong influence on sinking fluxes of particulate material in the plume area (Macdonald et al. 1998, O'Brien et al. 2006, see Chapter 2).

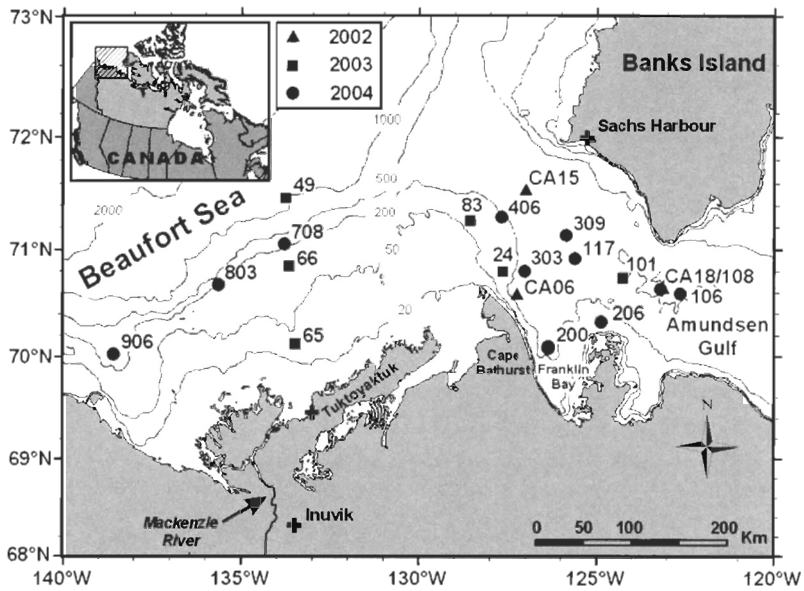

Fig. 1. Location of the sampling stations in eastern Beaufort Sea, in fall 2002 and 2003 and summer 2004. Depth contours in meters

3.2.2 Sampling

Sampling was carried out from the icebreakers CCGS *Pierre Radisson* (in 2002) and CCGS *Amundsen* (in 2003 and 2004). Sinking fluxes of particulate material were measured using short-term (1.03 ± 0.34 d, n = 21; Table 1) free-drifting deployments of particle interceptor traps. Particle interceptor traps were deployed at 50 m, except at the shallow stations 65 and 83, and at station 106 where traps were deployed at 25 m and 75 m, respectively. The free-drifting trap deployments were all below the euphotic zone which is defined in the present study as the depth receiving 1 % of surface irradiance. At the open water stations, the depth of the euphotic zone ranged from 11 to 60 m, with an average of 35 m (S. Brugel pers. comm.).

Table 1. Characteristics of free-drifting particle interceptor trap deployments during 2002, 2003 and 2004

Region	Station	Deployment date	Duration	Deployment		Recovery		Average speed	Distance travelled	Water depth
				Latitude	Longitude	Latitude	Longitude			
			(d)	(°N)	(°W)	(°N)	(°W)	(cm s^{-1})	(km)	(m)
Cape Bathurst Polynya	24	23 Sep 2002	1.2	70° 47.50'	127° 37.20'	70° 44.00'	127° 45.00'	7.7	8.0	165
Mackenzie slope	49	28 Sep 2002	1.0	71° 27.60'	133° 43.90'	71° 32.15'	133° 40.43'	9.5	8.2	1280
Mackenzie shelf	65	1 Oct 2002	1.0	70° 06.75'	133° 28.03'	70° 05.05'	133° 32.33'	5.7	4.9	43
Mackenzie shelf	66	5 Oct 2002	0.9	70° 50.45'	133° 38.45'	70° 50.20'	133° 32.00'	5.4	4.2	77
Cape Bathurst Polynya	83	6 Oct 2002	1.1	71° 15.80'	128° 31.70'	71° 12.24'	128° 11.95'	14.1	13.4	72
Cape Bathurst Polynya	101	9 Oct 2002	0.8	70° 44.10'	124° 14.30'	70° 42.10'	124° 14.30'	5.3	3.7	535
Cape Bathurst Polynya	CA15	9 Oct 2003	0.6	71° 32.77'	126° 59.53'	71° 32.02'	126° 49.09'	12.1	6.3	409
Cape Bathurst Polynya	CA06	11 Oct 2003	0.5	70° 35.45'	127° 13.94'	70° 38.09'	127° 09.90'	12.6	5.5	258
Cape Bathurst Polynya	CA18	13 Oct 2003	0.3	70° 38.61'	123° 07.46'	70° 37.04'	123° 09.94'	12.7	3.3	570
Cape Bathurst Polynya	108	6 Jun 2004	1.6	70° 37.90'	123° 10.30'	70° 25.40'	123° 25.60'	18.0	24.9	483
Cape Bathurst Polynya	117	9 Jun 2004	1.5	70° 54.70'	125° 34.80'	70° 54.80'	125° 43.40'	4.0	5.2	400
Cape Bathurst Polynya	406	15 Jun 2004	1.2	71° 17.30'	127° 40.00'	71° 25.10'	127° 43.70'	14.0	14.5	170
Cape Bathurst Polynya	303	18 Jun 2004	1.3	70° 47.50'	127° 00.00'	70° 44.00'	126° 58.80'	5.8	6.5	255
Mackenzie shelf	708	30 Jun 2004	1.3	71° 02.77'	133° 46.31'	71° 03.66'	133° 43.34'	2.1	2.3	236
Mackenzie shelf	906	3 Jul 2004	1.5	70° 01.10'	138° 34.57'	69° 50.10'	138° 21.96'	16.9	21.9	280
Mackenzie shelf	803	8 Jul 2004	1.0	70° 39.94'	135° 37.89'	70° 38.60'	135° 54.14'	11.7	10.1	243
Franklin Bay	200 (1)	16 Jul 2004	1.0	70° 02.53'	126° 18.20'	69° 57.50'	126° 12.72'	11.4	9.9	235
Cape Bathurst Polynya	309	18 Jul 2004	1.1	71° 07.40'	125° 50.66'	71° 07.25'	126° 13.90'	14.6	13.9	395
Cape Bathurst Polynya	206	1 Aug 2004	0.6	70° 19.30'	124° 50.43'	70° 18.99'	124° 52.24'	2.4	1.3	94
Franklin Bay	200 (2)	6 Aug 2004	1.1	70° 02.30'	126° 13.20'	70° 00.90'	126° 09.50'	3.7	3.5	231
Cape Bathurst Polynya	106	9 Aug 2004	1.0	70° 35.00'	122° 37.80'	70° 34.80'	122° 38.10'	0.5	0.4	521

Duplicate particle interceptor traps were deployed at the sampling depth. A wave dampening device comprised of a series of 7 floaters, of which 3 were submerged, was arranged on the free-drifting trap arrays. The submerged floaters increased water resistance of the array thereby reducing the vertical movement of the particle interceptor traps attached to the drifting line. The particle interceptor traps were made of PVC (polyvinyl chloride) cylinders closed at one end, with an internal diameter of 10 cm and an aspect ratio (height:diameter) of 7. A CAST ARGOS drifter buoy (Seimac Smart Cat PTT/GPS transmitter) and a Novatech Designs Ltd. RF-700C1 radio beacon were used to track the position of the free-drifting trap arrays.

Sampling by particle interceptor traps was carried out in accordance with JGOFS protocols (Knap et al. 1996) and recommendations by Gardner (2000). The particle interceptor traps were filled with filtered (0.22 μm) seawater collected at depths >200 m prior to deployment, to ensure that the higher density particle-free water remained inside the traps. Upon recovery, the free-drifting particle interceptor traps were fitted with a clean lid and set aside for sedimentation during 8 h in a cold-room (0°C) onboard the ship. The supernatant was gently removed after the sedimentation period and the remaining sample was pre-screened (425 μm) to remove large swimmers. Duplicate particle interceptor trap samples were pooled together, their volume measured, and the samples were stored in dark containers for analyses.

Particle interceptor traps were also deployed at a landfast first-year sea ice station in Franklin Bay (station 200; Fig. 1) on 16 consecutive occasions from 23 February to 20 June 2004. The trap array was fixed to the sea ice with traps deployed at 25 m under the sea ice during, on average, 7.8 ± 0.8 days (n = 6) from 23 February to 13 April and 6.2 ± 0.4 days (n = 8) from 13 April to 20 June, except for two deployments of 4.0 and 15.2 days on 26 May and 30 May, respectively. Upon recovery, the entire volume of the underice particle interceptor traps were pre-screened (425 μm) to remove large swimmers and measured, and was stored in black containers for analyses (see Chapter 2 for further details).

Sampling of the suspended material was carried out at each station with a rosette sampler equipped with 12 L bottles (OceanTest Equipment) deployed at 3-8 depths within the upper 50 m.

3.2.3 Analyses

Trap samples were gently mixed prior to subsampling. To ensure minimal disturbance of the collected material, samples for microscopic examination were taken first. Subsamples for fecal pellet (100-250 ml) and protist (100-250 ml) analyses were preserved with 2 % (v/v) buffered formaldehyde and 1 % (v/v) acidic Lugol's solution, respectively. Enumeration and measurement (length and width) of fecal pellet dimensions were later conducted using a Carl Zeiss inverted microscope (100 x magnification). Fecal pellets were classified according to type (i.e. cylindrical or elliptical) and condition (i.e. intact or

broken). The volume of intact and broken cylindrical fecal pellets was calculated using the equation for a cylinder with half-spherical ends and for a cylinder, respectively. The volume of intact elliptical fecal pellets was calculated using the equation for an ellipsoid; no broken elliptical fecal pellets were observed during the present study. Fecal pellet based carbon (FPC) was estimated using a volume to carbon conversion factor of 0.057 pg C μm^{-1} for cylindrical fecal pellets (i.e. copepod fecal pellets) and 0.042 pg C μm^{-1} for elliptical fecal pellets (i.e. appendicularian fecal pellets) (González et al. 1994). Identification and enumeration of phytoplankton and other protists were conducted using a Leica DM IRB inverted microscope (400 x magnification), according to the method of Lund et al. (1958). For each sample, a minimum of 300 cells were counted.

Chlorophyll *a* (chl *a*) and phaeopigments were measured on subsamples (50-200 ml) filtered onto Whatman GF/F 25 mm glass fiber filters. Pigments were extracted in 90 % acetone for 24 h in cold dark conditions (4°C). Samples were then analyzed on a Turner Designs 10AU fluorometer, using 90 % acetone as a blank. The pigment concentration in the samples was calculated in accordance with Parsons et al. (1984).

Total particulate carbon (TPC) and particulate organic carbon (POC) were measured on subsamples (50-900 ml) filtered onto precombusted (450°C for 24 h) Whatman GF/F 21 mm filters. The filters were dried at 60°C for 24 h and stored in separate Petri dishes. Filters for POC determination were acidified during 24 h in a dessicator saturated with HCl fumes, thereby removing any inorganic carbon. Analyses were conducted on a Perkin-

Elmer Model 2400 CHN Analyzer. POC analysis could not be conducted at several stations in the Cape Bathurst Polynya during the study because of insufficient collection of material in the short-term particle interceptor traps (stations CA15 and CA18 during fall 2003; stations 108, 117 and 303 during summer 2004). Missing POC data at these stations were extrapolated from the measured TPC sinking fluxes, using the strong linear regression between sinking fluxes of POC and TPC at other stations ($y = 0.84x + 1.69$; $r^2 = 0.87$; $p < 0.001$). Unfortunately TPC and POC data are missing from station 406.

The water samples for suspended material were analysed for chl *a* and POC, although different sample volumes were used (S. Brugel pers. comm.).

During the trap deployment period, particulate phytoplankton production was measured at 5 optical depths (100, 50, 25, 10 and 1 % of surface irradiance) with the ^{14}C uptake method in accordance with JGOFS protocols (Knap et al. 1996) (S. Brugel pers. comm.). After 24 h on-deck *in-situ* simulated incubation, samples were filtered onto Whatman GF/F filters. The filters were placed in borosilicate scintillation vials and acidified overnight with 0.5 N HCl, in order to remove ^{14}C that was not incorporated (Lean & Burnison 1979). Scintillation cocktail was then added to the vials. The vials were stored in the dark for 24 h before being counted on a Packard Tri-Carb 2900 TR Liquid Scintillation Analyzer. Particulate primary production corrected for dark uptake was calculated according to Knap et al. (1996).

3.2.4 Calculations and statistical analyses

The sinking flux of the measured variables was calculated using the following equation:

$$\text{Sinking flux (mg m}^{-2}\text{ d}^{-1}) = (C_{trap} * V_{trap}) / (A_{trap} * T_{dep}) \quad (1)$$

where C_{trap} (mg m^{-3}) is the concentration of the measured variable in the particle interceptor trap, V_{trap} (m^3) is the volume of the particle interceptor trap sample, A_{trap} (m^2) is the particle interceptor trap surface area and T_{dep} (d) is the deployment time.

The daily loss rate of suspended chl *a* and POC biomass in a given depth stratum due to sinking export was estimated using the following equation:

$$\text{Daily loss rate (\% d}^{-1}) = \text{Sinking flux} / C_{int} * 100 \quad (2)$$

where sinking flux is from equation (1), at 50 m generally and C_{int} is integrated biomass of chl *a* and POC in the upper 50 m generally, estimated using chl *a* and POC concentrations measured at 3-8 depths in the 0 to 50 m stratum. The export-ratio was calculated as the ratio of the POC sinking flux at a given depth (at 50 m, except for stations 65, 83 and 106) to the particulate phytoplankton production integrated over the euphotic zone depth. This ratio is dimensionless.

A group-average linkage cluster analysis was performed to determine similarities in the sinking protist cell assemblage (including empty diatom frustules and diatom spores) between stations, based on a Bray-Curtis similarity matrix computed on the logarithmic transformed (Log (x + 1)) sinking cell numbers (Field et al. 1982, Legendre & Legendre

1998). The difference between groups of sampling stations, at an arbitrarily level of similarity selected to obtain four groups, was tested using Analysis of Similarities (one-way ANOSIM; Legendre & Legendre 1998). The Global R value obtained provided an absolute measure of how separated the groups were on a scale of 0 (indistinguishable) to 1 (all similarities within groups are greater than similarities between groups) (Clarke & Gorley 2001). The cluster analysis and ANOSIM were performed using the PRIMER software package (Clarke & Gorley 2001).

Differences between two or more average values of sinking fluxes in groups, of varying sample sizes, were analysed using a one-way ANOVA (Sokal & Rohlf 1981).

3.3 Results

Figure 2 shows the chl *a* and POC sinking fluxes measured in the two sampling regions, i.e. the Cape Bathurst Polynya and the Mackenzie shelf and slope, in the eastern Beaufort Sea, during fall 2002 and 2003 and summer 2004. The sinking fluxes of chl *a* and POC were comparable in both regions during fall 2002 and 2003 (Fig. 2a-d and Table 2). The sinking fluxes of both chl *a* and POC were higher during summer 2004 (Fig. 2e, f and Table 2) than during fall 2002 and 2003 (Fig. 2a-d and Table 2). In addition, the sinking fluxes of POC in summer 2004 were generally higher on the Mackenzie shelf and slope than in the Cape Bathurst Polynya region (Fig. 2e, f and Table 2). The highest chl *a* and POC sinking fluxes recorded throughout this study were respectively measured at

station 303 in the Cape Bathurst Polynya and at station 906 on the Mackenzie shelf during summer 2004.

Cluster analysis of the sinking assemblage of autotrophic and heterotrophic protists (including empty diatom frustules and resting spores), at each sampling station, showed significant (one-way ANOSIM, similarity level = 43 %, Global $R = 0.76$, $p < 0.001$) similarity between the stations sampled in the eastern Beaufort Sea (Fig. 3). Based on the species composition of the sinking assemblage, four groups of stations were obtained. One group comprised stations visited during June 2004 (Group I: stations 108, 117, 406 and 303), while the stations sampled from July to August 2004 formed another distinctive group (Group II: stations 708, 906, 803, 309, 106 and 206). The stations sampled in September and October 2002 and 2003 formed another group (Group III: stations CA15, CA18, CA06, 83, 24, 101, 49 and 66), except for station 65 (October 2002) which constituted a separate group (Group IV).

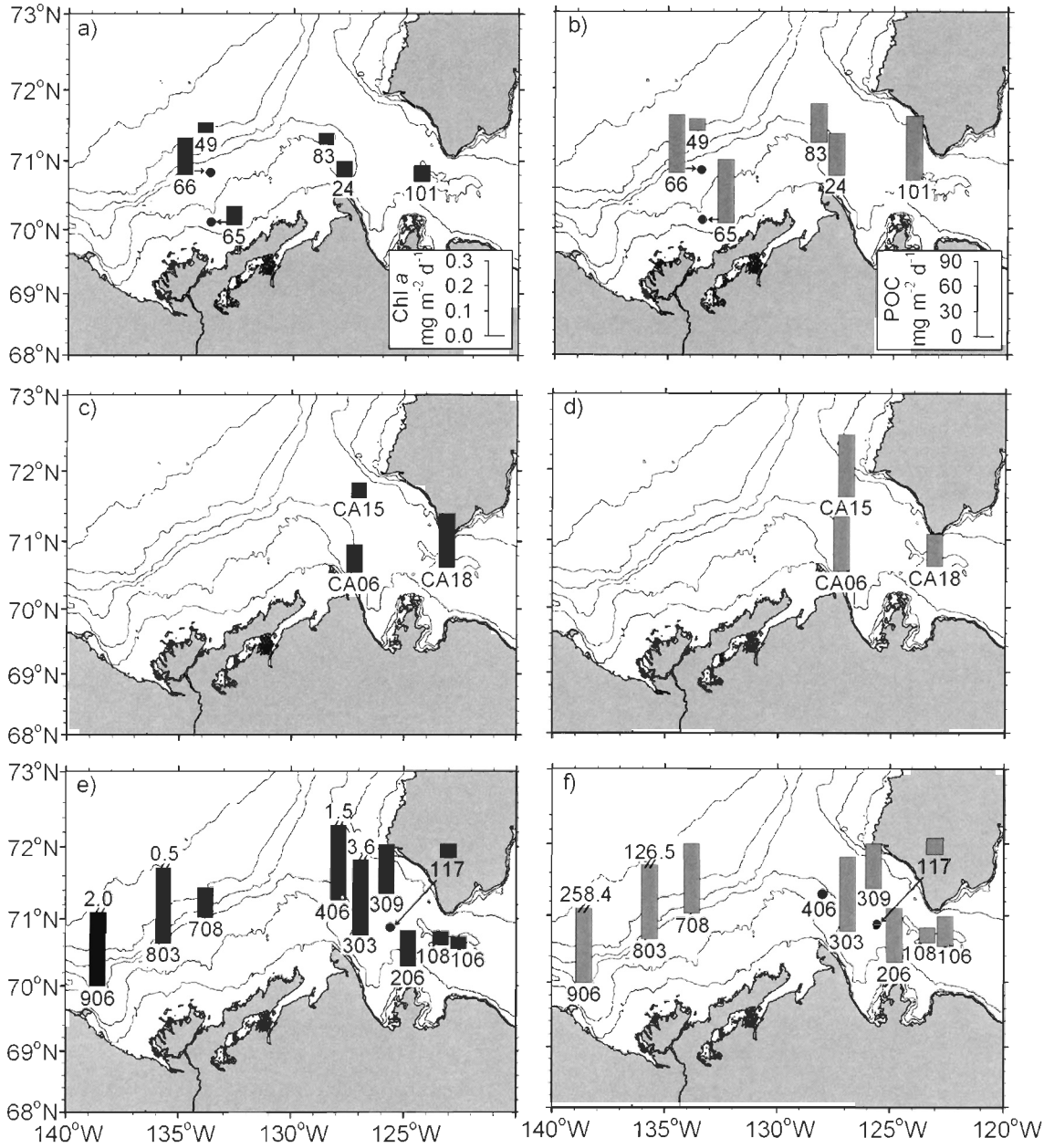

Fig. 2. Spatial variations in sinking fluxes of chlorophyll *a* (chl *a*) and particulate organic carbon (POC) during (a, b) fall 2002, (c, d) fall 2003, and (e, f) summer 2004 at 50 m (25 m at stations 83 and 65 and 75 m at station 106). In (e, f), sinking fluxes exceeding the scale shown in the legends are presented above bars

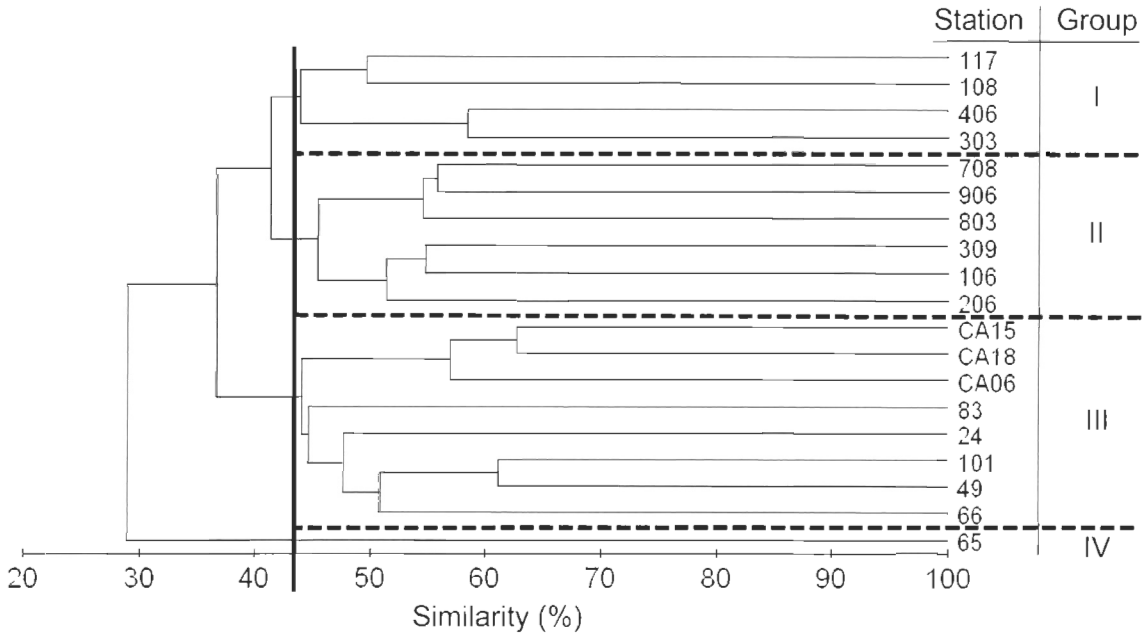

Fig. 3. Dendrogram showing four groups of stations obtained from group-average clustering of all sampling stations, in eastern Beaufort Sea, based on the sinking fluxes of protistan cells at 50 m (25 m at stations 83 and 65 and 75 m at station 106). Groups were formed at a similarity level of 43 % (Global R = 0.76, $p < 0.001$)

Figure 4 presents the species composition of the sinking protists (including autotrophs and heterotrophs), dominant diatom species and empty diatom frustules and diatom spores assemblage within the four seasonal groups of stations obtained from the cluster analysis. Flagellates were the dominant group of protists in the sinking cell assemblage in June and July/August (52.2 and 50.6 % of cell numbers, respectively), and were even more abundant in September/October (69.1 % of cell numbers; Fig. 4a). Pennate diatoms comprised 30.3 and 34.0 % of protists cells, by numbers, in June and July/August, respectively. The maximum contribution of centric diatoms to the sinking protist cell assemblage was observed in July/August, at which time they made up 12.6 % of cell numbers. Dinoflagellates, ciliates and unidentified protists comprised 12.1 % of cell

numbers in June, while their contributions were negligible in July/August and September/October (comprising 2.4 and 2.5 % of cell numbers, respectively). The diatom species composition showed a seasonally decreasing pennate diatom contribution (from 77.0 to 49.9 % of diatom cell numbers from June to July/August), except at station 65 (100 % of diatom cell numbers; Fig. 4b). The freshwater pennate diatom *Eunotia* sp. was the only identified diatom species in the material exported from the euphotic zone at station 65. The pennate diatom *Fragilariopsis cylindrus* was the dominant diatom species in June and July/August (36.0 and 50.7 % of diatom cell numbers), although other pennate diatoms contributed significantly in June (28.7 % of diatom cell numbers). The pennate diatoms *Nitzschia frigida* and *Navicula vanhoeffenii* were present in the sinking diatom assemblage in June and July/August (together contributing 12.3 and 15.1 % of diatom cell numbers), while their contribution was negligible in September/October. Centric diatoms, such as *Chaetoceros* spp., showed a seasonally increasing contribution (from 23.1 to 50.1 % of diatom cell numbers from June to September/October), except at station 65. Average sinking fluxes of empty centric and pennate diatom frustules showed a seasonal decrease from June (30.2 and 258.4 x 10^6 cells m^{-2} d^{-1}, respectively) to September/October (7.0 and 3.9 x 10^6 cells m^{-2} d^{-1}, respectively; Fig. 4c). Centric diatom spores were only present in July/August and September/October, and showed seasonally decreasing average sinking fluxes during these months (8.8 and 2.4 x 10^6 cells m^{-2} d^{-1}, respectively).

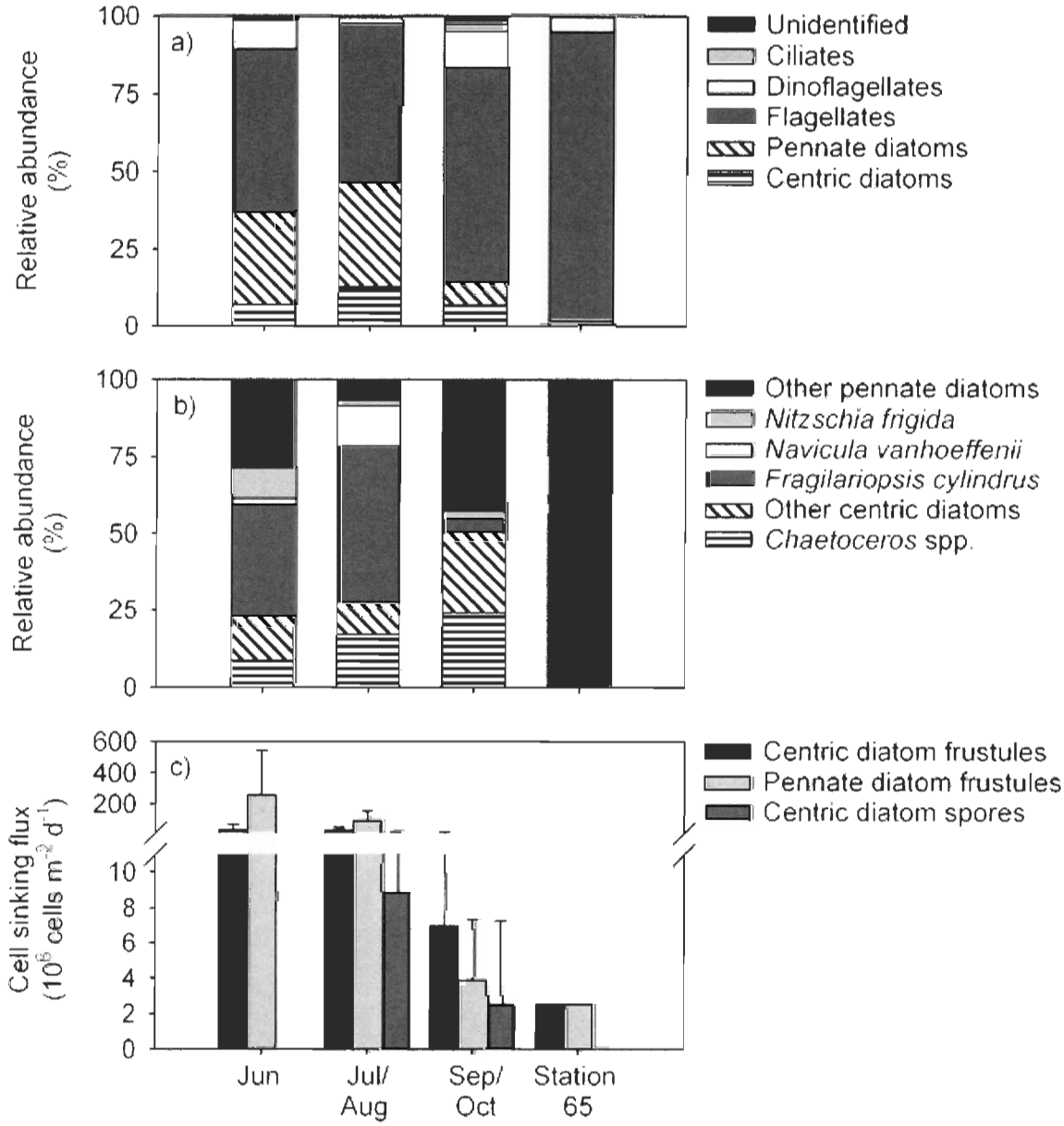

Fig. 4. Average relative abundances of (a) autotrophic and heterotrophic protists, (b) dominant diatom taxa, and (c) average sinking fluxes of empty diatom frustules and centric diatom spores at 50 m (25 m at stations 83 and 65 and 75 m at station 106), for the four groups of stations with similar taxonomic composition in eastern Beaufort Sea. The grouping of stations is based on the cluster analysis (see Fig. 3). In (c), bars represent standard deviations within each group

Figure 5 presents monthly-averaged sinking fluxes of organic material, from March to August, at 25 m at the landfast sea ice station in Franklin Bay (station 200). Monthly-averaged sinking fluxes of chl *a* increased significantly from March to June (one-way ANOVA, $p < 0.01$) and consistently decreased thereafter (Fig. 5a). Sinking fluxes of POC under the sea ice did not vary significantly from March to May, but increased rapidly in June (Fig. 5b). During the ice-free period (July and August), POC sinking fluxes remained high in July and decreased in August.

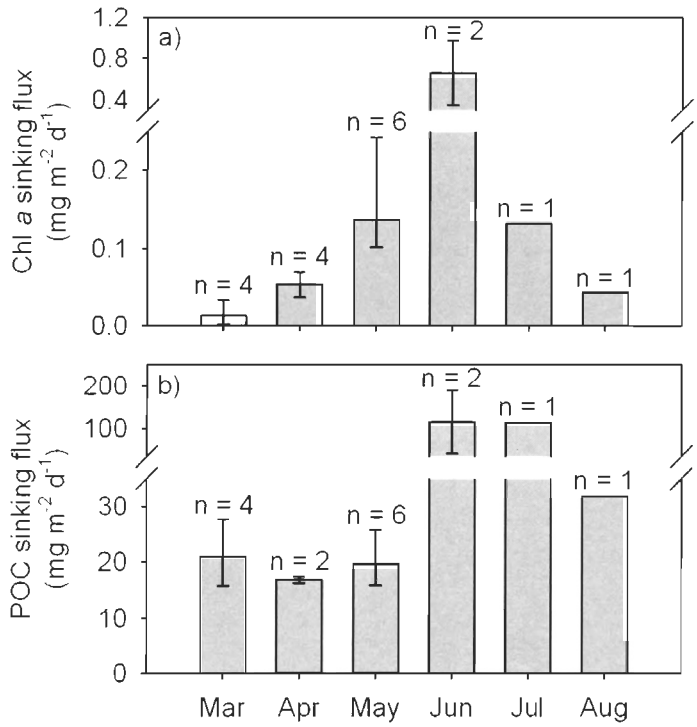

Fig. 5. Seasonal variations in sinking fluxes of (a) chlorophyll *a* (chl *a*) and (b) particulate organic carbon (POC) at 25 m during underice sampling (i.e. March to June) and at 50 m during open water sampling (i.e. July and August) at a landfast sea ice station, in Franklin Bay (station 200). Monthly-averaged values are presented when applicable, with bars showing minimum and maximum values. n represents number of sampling points during each period

Table 2 summarizes the sinking fluxes and daily loss rates of chl *a* and POC together with the export-ratios, for each region, and according to the seasonal grouping obtained from the cluster analysis. For comparative purposes, this Table also reports observations at the landfast first-year ice station in Franklin Bay during the open water period. Seasonally decreasing trends in the average chl *a* sinking fluxes were observed in each region, although these trends were not statistically significant. Average sinking fluxes of POC did not show any clear seasonal trend in the Cape Bathurst Polynya, while a decreasing trend was observed on the Mackenzie shelf and slope. In Franklin Bay, sinking fluxes of chl *a* and POC decreased from July to August. A seasonally decreasing trend was also observed in the daily loss rate of chl *a* in the Cape Bathurst Polynya and in the daily loss rate of chl *a* and POC on the Mackenzie shelf and slope, although neither of these trends were statistically significant. The average daily loss rates of POC in the Cape Bathurst Polynya showed a significant (one-way ANOVA, $p < 0.001$) increase from June to July/August. Franklin Bay showed a seasonal decrease in the daily loss rates of suspended chl *a* and POC from July to August. The average export-ratios increased significantly (one-way ANOVA, $p < 0.01$) throughout the open water period (i.e. from June to September/October) in the Cape Bathurst Polynya, while the export-ratio decreased from July to August in Franklin Bay. Primary production was unfortunately not measured on the Mackenzie shelf and slope.

Table 2. Sinking fluxes and daily loss rates of chlorophyll *a* (chl *a*), particulate organic carbon (POC), and export-ratio at 50 m (25 m at stations 83 and 65 and 75 m at station 106) during open water periods, in eastern Beaufort Sea. The seasonal grouping of stations in the Cape Bathurst Polynya and on the Mackenzie shelf and slope is based on the cluster analysis (see Fig. 3). Averages and ranges of values are presented when applicable. N/A: not available

			Sinking flux		Daily loss rate		Export-ratio
			Chl *a*	POC	Chl *a*	POC	Particulate phytoplankton production
Region	Period	Group	(mg m^{-2} d^{-1})	(mg m^{-2} d^{-1})	(% d^{-1})	(% d^{-1})	(%)
Cape Bathurst Polynya	June 2004	I	1.3 0.06-3.6	42.8 18.2-89.3	1.2 0.53-2.5	0.40 0.36-0.45	14.5 5.2-21.1
	July/August 2004	II	0.13 0.05-0.20	52.4 36.0-67.0	0.78 0.31-1.2	1.3 1.2-1.3	51.6 40.1-57.8
	September/October 2002 and 2003	III	0.10 0.05-0.22	58.9 37.8-77.5	0.43 0.29-0.65	0.72 0.37-1.3	65.4 41.3-79.7
Mackenzie shelf and slope	July/August 2004	II	0.86 0.12-2.0	156.3 84.1-258.4	2.8 1.5-3.6	2.9 2.7-3.1	N/A
	September/October 2002 and 2003	III	0.10 0.04-0.15	42.5 14.8-70.2	0.54 0.22-0.86	0.96 0.65-1.0	N/A
	Station 65 in fall 2002	IV	0.08	75.5	2.0	1.8	N/A
Franklin Bay	July 2004		0.13	113.5	0.78	2.7	97.2
	August 2004		0.04	31.9	0.26	0.86	28.8
All regions	Average		0.44 0.04-3.6	70.7 14.8-258.4	1.1 0.26-3.6	1.3 0.22-3.1	50.1 5.2-97.2

Table 3 presents a summary of sinking fluxes of FPC and their contribution to total POC sinking fluxes according to the same grouping of stations as that of Table 2. Cylindrical fecal pellets were the main contributors to total FPC sinking fluxes in the eastern Beaufort Sea throughout the study (averaging 91.4 % of total FPC at all stations). Average sinking fluxes of cylindrical FPC and total FPC showed seasonally decreasing trends in the Cape Bathurst Polynya and on the Mackenzie shelf and slope, although these trends were not statistical significant. Similarly, the average contribution of FPC to total POC sinking fluxes showed seasonally decreasing trends in the two regions. In Franklin Bay, the sinking fluxes of cylindrical FPC and total FPC, as well as the contribution of FPC to total POC sinking fluxes, also decreased from July to August.

Table 3. Sinking fluxes of fecal pellet based carbon (FPC) and contribution of FPC to total particulate organic carbon (POC) sinking flux at 50 m (25 m at stations 83 and 65 and 75 m at station 106) during open water periods, in eastern Beaufort Sea. The seasonal grouping of stations in the Cape Bathurst Polynya and on the Mackenzie shelf and slope is based on the cluster analysis (see Fig. 3). Averages and ranges of values are presented when applicable

			Sinking flux			
Region	Period	Group	Cylindrical FPC ($mg\ m^{-2}\ d^{-1}$)	Elliptical FPC ($mg\ m^{-2}\ d^{-1}$)	Total FPC ($mg\ m^{-2}\ d^{-1}$)	FPC contribution to POC sinking flux (%)
Cape Bathurst Polynya	June 2004	I	35.4 2.0-84.4	0.24 0-0.58	35.6 2.4-84.4	33.7 13.0-54.5
	July/August 2004	II	14.9 3.6-28.2	0.16 0-0.47	15.0 3.6-28.2	27.3 10.1-52.1
	September/October 2002 and 2003	III	3.3 1.9-5.0	0.55 0.12-1.3	3.9 2.8-6.1	6.8 4.3-8.4
Mackenzie shelf and slope	July/August 2004	II	11.4 7.0-20.1	1.1 0.1-2.1	12.5 7.4-21.1	8.3 5.8-10.8
	September/October 2002 and 2003	III	1.8 0.27-8.0	0.29 0.09-0.57	2.1 0.36-8.6	3.9 2.4-11.4
	Station 65 in fall 2002	IV	8.0	0.57	8.6	11.4
Franklin Bay	July 2004		84.0	2.0	86.0	75.7
	August 2004		7.9	0.07	8.0	25.1
All regions	Average		16.4 0.27-84.4	0.54 0-2.1	16.9 0.36-86.0	18.4 2.4-75.7

3.4 Discussion

3.4.1 Sinking export in the eastern Beaufort Sea

This multi-year study provides extensive spatial coverage of the sinking export of chl *a* and POC below the euphotic zone in the eastern Beaufort Sea. This sampling program covered most of the ice-free season in this area, which generally begins with initial sea ice break-up in late-April and lasts until freeze-up commences in late-October (e.g. Carmack & Macdonald 2002, Barber & Hanesiak 2004). The two first sampling periods, i.e. September/October of 2002 and 2003, indicated that rather stable conditions of sinking export of particulate organic material prevailed in the fall, during this study, as comparable chl *a* and POC sinking fluxes were observed in the eastern Beaufort Sea (Fig. 2 and Table 2). These similarities also tend to support interannual comparisons within the present dataset. The subsequent sampling period, in summer 2004, showed that the highest sinking fluxes of chl *a* and POC occur early during the ice-free period, i.e. June and July/August, in the eastern Beaufort Sea. It has previously been shown that two key features, i.e. the Cape Bathurst Polynya and the Mackenzie River, which characterize this part of the Beaufort Sea (e.g. Carmack & Macdonald 2002), may induce high sinking fluxes of particulate organic material during spring and summer in this area (O'Brien et al. 2006, see Chapter 2). The same has been reported for other Arctic regions, where high sinking fluxes of particulate organic material have been linked to spring phytoplankton production in polynyas (e.g. North Water Polynya (NOW); Amiel et al. 2002, Michel et al. 2002, Caron et al. 2004) and increased river discharge during freshet in spring and summer (Dittmar & Kattner 2003,

Stein & Macdonald 2004 and references therein, Carmack & Wassmann 2006). The highest POC sinking export recorded in the eastern Beaufort Sea (station 906; Fig. 2f), during this study, was linked to a high sinking export of particulate organic material from the Mackenzie River plume in summer (2004), as described in details in a companion study (see Chapter 2).

The POC sinking export values observed throughout our multi-year sampling in eastern Beaufort Sea (ranging from 18.2 to 258.4 mg C m^{-2} d^{-1}; Table 2) were persistently higher than previously reported values from the same shelf slope area (< 20 mg C m^{-2} d^{-1} at 200 m; Forest et al. 2007) and, for the most part, exceeded values previously reported across the same shelf area (< 80 mg C m^{-2} d^{-1} at 118 to 213 m; O'Brien et al. 2006). Both of these studies used long-term sediment trap moorings deployed well below the euphotic zone, and their lower values, compared to the present study, may have been due to a loss of sinking POC with depth (i.e. vertical flux attenuation) and/or methodological differences (i.e. short-term *versus* long-term deployments). However, a study of the benthic carbon demand in the eastern Beaufort Sea suggested a tight pelagic-benthic coupling and an annual benthic carbon demand of ca. 12.1 g C m^{-2} on the shelf (Renaud et al. 2007a); this estimate exceeds the annual carbon sinking export values from the other two studies on the shelf (ca. 1.7 to 5.8 g C m^{-2}; O'Brien et al. 2006) and shelf slope (ca. 1 g C m^{-2}; Forest et al. 2007). From a pan-Arctic perspective, the Beaufort Sea shelf showed a lower POC sinking export than reported below the euphotic zone on the extensively studied shelf of the central Barents Sea in spring and summer (range: ca. 250 to 850 mg C m^{-2} d^{-1}, between 40 and

60 m; Wassmann 1989, Wassmann et al. 1990, Olli et al. 2002). Yet, the sinking export values in the present study are between values reported from a short-term sediment trap study during summer on the Chukchi Sea shelf (depths averages: 129 and 442 mg C m^{-2} d^{-1}, between 30 and 100 m; Lalande et al. 2007), and are generally higher than those reported from the Kara Sea shelf and slope in fall (range: 0.5 to 185 mg C m^{-2} d^{-1}, between 9 and 360 m; Wassmann et al. 2004), using sediment traps deployed for periods of 1 to 10 days.

3.4.2 Seasonal and regional sinking export

A general decrease in the sinking export of chl *a* was observed in the eastern Beaufort Sea towards fall, i.e. from June to September/October (Table 2), indicating a seasonal decrease in the export of phytoplankton material from euphotic zone. This seasonal decrease occurred mainly during spring in the Cape Bathurst Polynya, as average chl *a* sinking fluxes decreased by one order of magnitude from June to July/August. The seasonally decreasing chl *a* sinking fluxes also reflected a declining contribution of algal cells to POC sinking fluxes (from 121.5 to 6.8 % in June and September/October; data not shown), using a POC:chl *a* ratio of 40 g:g from healthy algal cells (Lorenzen 1968) and the average chl *a* and POC sinking fluxes in this region (Table 2). This agrees with the termination of a phytoplankton bloom during July in this region, as suggested by Simpson et al. (ms), based on decreasing integrated surface nitrate concentrations and phytoplankton biomass. The significantly lower export-ratio in June, compared to the following months (Table 2), is consistent with the biomass build-up during a phytoplankton bloom. Unfortunately no sampling was carried out on the Mackenzie shelf and slope in June, so

that we can not conclude on the seasonal trend of the chl *a* sinking export at that time. However, the seasonal decrease in chl *a* sinking fluxes in this region, from July/August to September/October, was linked to a lower sinking export induced by decreased input by the river plume in fall compared summer (see Chapter 2). This seasonal decreasing sinking export of algal material also represented a halving of the algal contribution to sinking POC from July/August (22.0 %; data not shown) to September/October (9.4 %; data not shown), estimated using the same POC:chl *a* ratio as above and the regional average chl *a* and POC sinking fluxes (Table 2). Thus, the overall seasonal decrease in sinking export of chl *a* and POC in the Cape Bathurst polynya and the Mackenzie shelf appears to have been largely driven by different regional processes, i.e. the termination of the phytoplankton bloom and the decreasing input from the river.

The seasonal decrease in chl *a* sinking fluxes was also paralleled by an increasing retention of phytoplankton material within the euphotic zone, as evidenced from the seasonal decrease in daily loss rates of chl *a* through sinking (Table 2). Yet, the retention of phytoplankton material within the euphotic zone was generally high throughout this study, as the daily loss rates of chl *a* remained low at all stations (< 4.0 % d^{-1}; Table 2). High retention within the euphotic zone was also observed for POC (daily loss rates < 3.5 d^{-1}; Table 2). These daily loss rates of POC were generally below those reported in Disko Bay, Greenland in spring (from ca. 18 to 3 % d^{-1}at 15 and 100 m; Juul-Pedersen et al. 2006), while they compare with values reported in the marginal ice zone in the Barents Sea during summer (< 4 % d^{-1} at 50 m; Olli et al. 2002). Still, the POC sinking export accounted for a

high proportion of the phytoplankton production, in the Cape Bathurst Polynya, in summer and fall (> 50 %; Table 2). These results indicate that a negligible fraction of the biomass accumulated in the euphotic zone was sinking to the benthos, but that little additional biomass accumulation was taking place as more than half of the phytoplankton production was exported through sinking. A high transfer of organic material to the pelagic food web reduces the sinking export, due to assimilation and remineralization, thus resulting in low daily loss rates of organic material, as observed in this region. The high fecal pellet sinking export in summer supports the strong influence of mesozooplankton on the suspended biomass. Grazing or destruction of fecal pellets by mesozooplankton (i.e. coprophagy and coprorhexy, respectively) may have further elevated the retention and remineralization of organic material in the pelagos, as reported from the Barents Sea (e.g. Olli et al. 2002, Riser et al. 2007).

Concomitant with the seasonal decrease in the sinking export of phytoplankton material (chl *a*), in the eastern Beaufort Sea, zooplankton mediated sinking export, i.e. total FPC sinking flux, also decreased (Table 3). A seasonal decrease in the fecal pellet contribution to total POC sinking fluxes was also observed towards fall (i.e. from July/August to September/October), suggesting a lower grazing activity later in the season. The generally higher FPC contribution to total POC sinking fluxes in the Cape Bathurst Polynya, compared to the Mackenzie shelf and slope (Table 3), suggests a higher zooplankton grazing activity in this region. However, the landfast sea ice station in Franklin Bay showed the highest fecal pellet contribution to total POC sinking fluxes observed

during this study (ca. 76 %; Table 3), indicating a high transfer of organic material to pelagic grazers. The zooplankton mediated sinking export was primarily due to copepods throughout this study, as cylindrical fecal pellets dominated the total FPC sinking fluxes (contributing on average ca. 90 %; Table 3). Several Arctic copepod species have been shown to descend to depth to overwinter during summer and fall (e.g. Madsen et al. 2001), which may explain the seasonal trend in fecal pellet sinking fluxes. The maximum values of the fecal pellet contribution to total POC observed throughout this study, particularly in the Cape Bathurst Polynya (54.5 %) and in Franklin Bay (75.7 %; Table 3), were comparable with or exceeded some of the highest values reported from other Arctic areas (up to ca. 60 %; Riebesell et al. 1995, Riser et al. 2002, Sampei et al. 2004, Juul-Pedersen et al. 2006). Overall, these findings indicate a strong regional and seasonal transfer of sinking organic material through the large pelagic grazers, primarily copepods; though organic material is mainly exported from the euphotic zone as amorphous detritus in the eastern Beaufort Sea. This investigation also shows that while the eastern Beaufort Sea has a high retention of the suspended biomass, i.e. low daily loss rates of organic material, the sinking export of organic material accounts for a high fraction of the primary production in summer and fall (i.e. high export ratio).

3.4.3 Species composition of the sinking material

The cluster-based analysis of the composition of the protist cell assemblage sinking out of the euphotic zone revealed clear seasonal patterns which prevailed throughout the eastern Beaufort Sea (Fig. 3). The sinking protist (i.e. autotrophic and heterotrophic)

assemblage from the euphotic zone was characterized by a dominance of flagellates and a seasonally decreasing diatom contribution from spring to fall (Fig. 4a). Flagellates often dominate during post-bloom conditions in Arctic waters, as diatom cells become nutrient limited (e.g. Rat'kova et al. 1998, Dale et al. 1999, Hill et al. 2005). The pennate diatom *Fragilariopsis cylindrus*, which was the dominant diatom species in June and July/August throughout the sampling area (Fig. 4b), is often associated with sea ice, although it has been found to be abundant and productive in cold marine waters as well (von Quillfeldt 2004). In the NOW polynya, high sinking fluxes of *F. cylindrus* cells were linked to the spring phytoplankton bloom in June (Caron et al. 2004). *F. cylindrus* was also present in the water column during this study (M. Poulin pers. comm.). While the origin of the sinking *F. cylindrus* cells can not be confirmed, it is likely that their presence reflects a sinking export of pelagic microalgae. In our study area, a parallel study on ice algal composition found *Nitzschia frigida* and *Navicula vanhoeffenii* to be the dominant microalgal species in bottom landfast first-year sea ice in Franklin Bay, while *F. cylindrus* were not abundant (M. Różańska pers. comm.). An input of algae from the sea ice is thus inferred from the presence of the pennate diatoms *N. frigida* and *N. vanhoeffenii* in June and July/August, and their minor contribution to the sinking assemblage in September/October (Fig. 4b). These pennate diatoms are considered typically ice algae species (e.g. Sakshaug 2004, Michel et al. 2006).

The increasing contribution of *Chaetoceros* spp. and other centric diatoms to the diatom sinking assemblage, in September/October, is consistent with the seasonal

phytoplankton species succession reported in Frobisher Bay (Hsiao 1992) and in the sinking diatom assemblage in the NOW polynya (Caron et al. 2004). The fact that centric diatom spores were only observed in July/August and September/October (Fig. 4c) agrees with nitrate depletion during summer and fall, as suggested by Simpson et al. (ms). The production of diatom resting spores has been linked to nutrient limitation (e.g. Hargraves & French 1983). Interestingly, empty diatom frustules were an abundant part of the material exported from the euphotic zone throughout this study (Fig. 4c), contributing on average ca. 3 times as much as intact diatom cells, by numbers (data not shown). A significant degradation of diatom cells thus appeared to have occurred within the euphotic zone, possibly relating to zooplankton grazing activity. Altogether, the cluster-based analysis revealed a general seasonal phytoplankton species succession similar to that of other high-latitude coastal waters (e.g. Dale et al. 1999). The analysis also revealed the strong influence of the Mackenzie River, as already discussed in Chapter 2, since station 65 formed a distinctive group comprising the freshwater pennate diatom *Eunotia* sp.

3.4.4 A landfast sea ice perspective

In contrast with the adjacent Cape Bathurst Polynya, Franklin Bay is characterized by a prolonged landfast first-year sea ice cover. The time-series obtained at this location, from March to August, illustrates the importance of landfast spring melt for the sinking export of chl *a* and POC (Fig. 5). The underice sinking export of chl *a* and POC, during landfast spring melt (averaging 0.66 and 115.4 mg m^{-2} d^{-1} in June, respectively; Fig. 5), was

comparable to the highest open water sinking fluxes recorded in the eastern Beaufort Sea, during this study (Table 2).

The sinking fluxes of chl *a* and POC observed during open water sampling in Franklin Bay, in July and August, were comparable with the ranges of values observed in the Cape Bathurst Polynya at the same time (i.e. July/August; Table 2). The similarities between these two areas suggest that there are large scale consistencies in the sinking export of particulate organic material during ice-free conditions in the Amundsen Gulf (i.e. Cape Bathurst Polynya and Franklin Bay), which also agrees with the widespread seasonal pattern in sinking assemblage observed.

The transition from ice-covered (i.e. from March to June) to open waters (i.e. in July and August) in Franklin Bay (Fig. 5 and Table 2, 3) reveals a seasonal shift in sinking export processes. The high chl *a* and POC sinking export in June, during landfast spring melt, was attributed to the release of ice-associated biomass into the underlying water column, as described in Chapter 1. A parallel study found that the sinking of ice algae during landfast spring melt may represent an important cue for the seasonal increase in benthic activity and oxygen demand in Franklin Bay (Renaud et al. 2007b). In contrast, the material collected during open water sampling in July reflected a POC sinking export largely relating to copepod grazing activity, as FPC comprised the majority of the sinking POC (Table 3). It therefore appears that copepods played a key role in the remarkably high export of phytoplankton primary production in July (export-ratio of ca. 97 %; Table 2),

diverting most of the primary-produced organic material through the pelagic heterotrophic food web. Copepod grazing activity and sinking export of phytoplankton primary production, as reflected by FPC sinking fluxes and the export-ratio (Tables 2 and 3), decreased substantially from July to August. Overall, the high sinking export of released ice material during landfast spring melt therefore appeared to have been followed soon after by a peak in copepod grazing activity.

3.5 Conclusion

The extensive spatial and seasonal study of the sinking export of particulate organic material from the euphotic zone, showed comparable chl *a* and POC sinking fluxes throughout the eastern Beaufort Sea in fall. In summer, higher sinking fluxes of POC were observed on the Mackenzie shelf and slope than in the Cape Bathurst Polynya. Overall, a seasonal decrease was observed in the sinking export of chl *a* and POC, from spring to fall. Daily loss rates of chl *a* and POC were low throughout this study (< 4 % d^{-1}), while the Cape Bathurst Polynya showed a high export-ratio of particulate phytoplankton production during summer (ca. 50 %). Zooplankton played an important, but seasonally decreasing, role in the sinking export of particulate organic material, particularly in the Cape Bathurst Polynya. The cluster-based analysis of the sinking protist cell assemblage revealed seasonal groups that prevailed over spatial and interannual differences amongst sampling stations. A seasonal succession of microalgal species in the sinking assemblage was observed throughout the sampling area. A considerable diatom contribution, dominated by the

pennate diatom *F. cylindrus*, in summer was followed by a dominance of flagellated cells towards fall. Still, input from sea ice at the stations visited in summer, was related to the ice diatoms *N. frigida* and *N. vanhoeffenii* which were present in the collected material in June and July. The high chl *a* and POC sinking fluxes measured during landfast spring melt illustrate the importance of including the spring melt period when studying seasonal sinking export in Arctic regions.

CONCLUSION GÉNÉRALE

This study shows patterns of sinking export in the upper water column in different environments of the Canadian Beaufort Sea. The seasonal patterns in sinking export described under landfast sea ice are likely applicable to other Arctic regions experiencing landfast sea ice and relevant to areas of first-year sea ice in general. The strong seasonal patterns in the sinking export of particulate material in the Canadian Beaufort Sea and the insights into the influence of the Mackenzie River plume are believed to be relevant to other Arctic shelves.

In chapter 1, our results showed that the sinking export of organic material was low under landfast first-year sea ice during winter. This research provides new information on shallow sinking export of particulate material during winter, a long period extending from freeze-up typically around October/November (e.g. Carmack et al. 2006) to March on Arctic shelves, and which remains unstudied using shallow short-term particle interceptor traps. These results also showed a strong coupling between the sinking export of algal material underneath landfast sea ice and ice algal biomass was observed during the ice algal productive period in spring, thus substantiating the hypothesis of ice-water coupling taking place prior to spring ice melt, as proposed in other studies (Carey 1987, Melnikov 1998).

These results challenge the view that there is very little export of ice material prior to ice melt. The evidence of an early coupling between ice algal biomass and sinking export of algal material therefore urges future studies of shallow sinking export to include the ice algal growth period.

This research also showed an abrupt increase in sinking export of organic material during spring ice melt, as reported during previous studies of under-ice sinking export (Tremblay et al. 1989, Michel et al. 1996, 2002, Fortier et al. 2002). The onset of spring melt also reflected a release of material with a different biochemical composition, than prior to ice melt. This annual event, i.e. ice melt, is thought to represent an important trigger for increased benthic activity during early spring in the Canadian Beaufort Sea (e.g. Renaud et al. 2007b). Furthermore, the abrupt release and sinking export of organic material, during spring ice melt, exceeded the sinking export of organic material during subsequent ice-free condition, as described in Chapter 3. This study therefore connects shallow sinking export of organic material across the transition from first-year sea ice cover to ice-free conditions, a transition which may be temporally and spatially displaced on Arctic shelves by future climate related changes (e.g. ACIA 2005).

While sinking export of algal material, i.e. chlorophyll *a* (chl *a*), biogenic silica (BioSi) and algal cells, showed a seasonal increase during the developing ice algal bloom, sinking export of particulate organic carbon (POC) remained rather stable prior to the onset of spring ice melt. A significant non-algal component sustained the stable POC sinking

export. This research also showed that almost half (46 %) of the sinking chl *a* was lost in the first 25 meters, due in part to the degradation of chl *a* to phaeopigments predominantly by herbivorous copepods. These results evidence a significant transformation of the sinking pigmented material in the upper most part of the water column under landfast sea ice.

Chapter 2 showed the strong influence of the Mackenzie River plume on the sinking export of particulate material on the shelf and slope. Two sampling transects provided a synoptic view of separate sections of the river plume during summer and fall. Seasonal and spatial differences in the sinking export of chl *a* and POC were linked to the chl *a* biomass carried by the river plume, such that the highest sinking export occurred in summer and at stations most influenced by the river plume. In addition to the effect of the river plume, our results showed that phytoplankton and zooplankton located underneath the plume contributed to the sinking export of organic material at depth.

This research also showed a strong seasonality in the composition of the sinking material in the area of the river plume. Algal based material and fecal pellets contributed much in summer, while amorphous detritus dominated in fall. The sinking phytoplankton assemblage followed a seasonal species succession, from a dominance of diatoms in summer to mainly flagellates and dinoflagellates in fall, similar to the succession observed in most high-latitude waters.

The regional freshwater influence on some Arctic shelves in spring and summer, due to terrestrial riverine runoff, may increase due to climate related changes (e.g. ACIA 2005, IPCC 2007). While the riverine processes affecting sinking export of particulate material is well understood, regional information on the riverine influence on Arctic shelves is incomplete (e.g. Dittmar & Kattner 2003). This research provides not only regional information on the influence of Mackenzie River plume on the sinking export of particulate material, but also shows sinking export from the river plume and the water column below. These components are inevitably integrated in deeper studies of sinking export. As described in Chapter 2, seasonal differences appear not only in the influence of the Mackenzie River plume on sinking export of particulate material, but also in the contribution from the pelagic food web below the river plume, which may apply to other Arctic shelves influenced by river plumes.

The extensive dataset presented in chapter 3 showed comparable sinking fluxes of chl *a* and POC below the euphotic zone throughout the Canadian Beaufort Sea in fall. The seasonally high riverine influence on the sinking export of organic material in summer, as shown in chapter 2, induced higher POC sinking fluxes on the Mackenzie shelf and slope than in the Cape Bathurst Polynya at that time. An overall seasonal decrease in sinking fluxes of chl *a* and POC below the euphotic zone, from spring to fall, persisted throughout the Canadian Beaufort Sea.

Regardless of spatial and interannual variability between sampling stations, a strong seasonal signature in the species composition of the sinking protist assemblage emerged for the study area. These results showed that the phytoplankton species succession generally observed in the high-latitude waters, from a high diatom contribution in summer towards mainly flagellates in fall, prevailed in the sinking material throughout the Canadian Beaufort Sea.

The large scale perspective of sinking export of particulate organic material presented in Chapter 3 connects the different environments in Canadian Beaufort Sea, i.e. the Mackenzie River plume and the Cape Bathurst Polynya. This chapter shows that while these environments may have a strong regional and seasonal impact, large scale consistencies may prevail in both the sinking export of particulate organic material and the composition of the exported material. Prevailing consistencies may aid in the linkage between regional sinking export studies in the Arctic, if similar consistencies can be found on other Arctic shelves.

For future studies, a general aim should be to achieve a better understanding of the sinking export and transformation of the sinking material within the mesopelagic zone, as stressed in a recent review by Boyd & Trull (2007). In continuation with the present findings of a coupling between ice algal biomass and sinking export of algal material prior to ice melt, an investigation of the processes driving the ice-water export of algal material, e.g. brine drainage, would be valuable. Also, future studies oriented towards determining an

early sinking export of organic material from first-year sea ice are needed to corroborate and assess this in other Arctic regions. The observed increase in the proportion of seasonal first-year sea ice in the Arctic Ocean, due to climate related changes, compels to more widespread studies of the sinking export prior to and during ice melt, as well as during the sea ice break-up. In addition, further regional studies of the riverine influence on sinking export of particulate material on Arctic shelves are needed (e.g. Dittmar & Kattner 2003), and may become more important with the predicted increases in terrestrial riverine runoff due to climate related changes (e.g. ACIA 2005).

RÉFÉRENCES

ACIA (2005) Arctic climate impact assessment. Cambridge University Press, Cambridge

Aksnes DL, Egge JK (1991) A theoretical model for nutrient uptake in phytoplankton. Mar Ecol Prog Ser 70:65-72

Amiel D, Cochran JK, Hirschberg DJ (2002) $^{234}Th/^{238}U$ disequilibrium as an indicator for the seasonal export flux of particulate organic carbon in the North Water. Deep-Sea Res II 49:5191–5209

Andreassen IJ, Wassmann P (1998) Vertical flux of phytoplankton and particulate biogenic matter in the marginal ice zone of the Barents Sea in May 1993. Mar Ecol Prog Ser 170:1-14

Andreassen IJ, Nöthig E-M, Wassmann P (1996) Vertical particle flux on the shelf off northern Spitsbergen, Norway. Mar Ecol Prog Ser 137:215-228

Anema C, Hecky RE, Fee EJ, Nernberg D, Guildford SJ (1990) Water chemistry of some lakes and channels in the Mackenzie Delta and on the Tuktoyaktuk Peninsula, N.W.T., 1985. Can Data Rep Fish Aquat Sci 726

Arrigo KR, Dijken GLV (2004) Annual cycles of sea ice and phytoplankton in Cape Bathurst polynya, southeastern Beaufort Sea, Canadian Arctic. Geophys Res Lett 31, L08304, doi:10.1029/2003GL018978

Astthorsson OS, Gislason A (2003) Seasonal variations in abundance, development and vertical distribution of *Calanus finmarchicus*, *C. hyperboreus* and *C. glacialis* in the East Icelandic Current. J Plankton Res 25:843-854

Azetsu-Scott K, Passow U (2004) Ascending marine particles: Significance of transparent exopolymer particles (TEP) in the upper ocean. Limnol Oceanogr 49:741-748

Bale AJ (1998) Sediment trap performance in tidal waters: comparison of cylindrical and conical collectors. Cont Shelf Res 18:1401-1418

Barber DG, Hanesiak JM (2004) Meteorological forcing of sea ice concentration in the southern Beaufort Sea over the period 1979 to 2000. J Geophys Res 109, C0614, doi:10.1029/2003JC0022027

Bélanger S, Xie H, Krotkov N, Larouche P, Vincent WF, Babin M (2006) Photomineralization of terrigenous dissolved organic matter in Arctic coastal waters from 1979 to 2003: Interannual variability and implications of climate change. Global Biogeochem Cycles, 20, GB4005, doi:10.1029/2006GB002708

Belchansky GI, Douglas DC, Eremeev VA, Platonov NG (2005) Variations in the Arctic's multiyear sea ice cover: a neural network analysis of SMMR-SSM/I data, 1979-2004. Geophys Res Lett 32, L09605, doi:10.1029/2005GL022395

Bhaskar PV, Grossart H-P, Bhosle NB, Simon M (2005) Production of macroaggregates from dissolved exopolymeric substances (EPS) of bacterial and diatom origin. FEMS Microbiol Ecol 53:255-264

Bidle KD, Azam F (1999) Accelerated dissolution of diatom silica by marine bacterial assemblages. Nature 397:508-512

Booth BC, Smith WO Jr (1997) Autotrophic flagellates and diatoms in the Northeast Water Polynya, Greenland: summer 1993. J Mar Syst 10:241-261

Boyd PW, Trull TW (2007) Understanding the export of biogenic particles in oceanic waters: Is there consensus? Prog Oceanogr 72:276-312

Buesseler KO, Lamborg CH, Boyd PW, Lam PJ, Trull TW, Bidigare RR, Bishop JK, Casciotti KL, Dehairs F, Elskens M, Honda M, Karl DM, Siegel DA, Silver MW, Steinberg DK, Valdes J, Mooy BV, Wilson S (2007) Revisiting carbon flux through the ocean's twilight zone. Science 316:567-570

Bursa A (1963) Phytoplankton in coastal waters of the Arctic Ocean at Point Barrow, Alaska. Arctic 16:239-262

Carey AG (1987) Particle flux beneath fast ice in the shallow southwestern Beaufort Sea, Arctic Ocean. Mar Ecol Prog Ser 40:247-257

Carmack EC, Chapman DC (2003) Wind-driven shelf/basin exchange on an Arctic shelf: the joint roles of ice cover extent and shelf-break bathymetry. Geophys Res Lett 30, 1778, doi:10.1029/2003GL01752

Carmack EC, Macdonald RW (2002) Oceanography of the Canadian Shelf of the Beaufort Sea: A setting for marine life. Arctic 55:29-45

Carmack E, Wassmann P (2006) Food webs and physical–biological coupling on pan-Arctic shelves: Unifying concepts and comprehensive perspectives. Prog Oceanogr 71:446-477

Carmack EC, Macdonald RW, Jasper S (2004) Phytoplankton productivity on the Canadian Shelf of the Beaufort Sea. Mar Ecol Prog Ser 277:37-50

Carmack E, Barber D, Christensen J, Macdonald R, Rudels B, Sakshaug E (2006) Climate variability and physical forcing of the food webs and the carbon budget on panarctic shelves. Prog Oceanogr 71:145-181

Caron G, Michel C, Gosselin M (2004) Seasonal contributions of phytoplankton and fecal pellets to the organic carbon sinking flux in the North Water (northern Baffin Bay). Mar Ecol Prog Ser 283:1-13

Carson MA, Conly FM, Jasper JN (1999) Riverine sediment balance of the Mackenzie Delta, Northwest Territories, Canada. Hydrol Process 13:2499-2518

Clarke KR, Gorley RN (2001) PRIMER v5 User manual/tutorial. PRIMER-E, Plymouth

Comiso JC (2002) A rapidly declining perennial sea ice cover in the Arctic. Geophys Res Lett 29, 1956, doi:10.1029/2002GL015650

Conley DJ (1998) An interlaboratory comparison for the measurement of biogenic silica in sediments. Mar Chem 63:39-48

Conover RJ (1966) Assimilation of organic matter by zooplankton. Limnol Oceanogr 11:338-345

Conover RJ, Siferd TD (1993) Dark-season survival strategies of coastal zone zooplankton in the Canadian Arctic. Arctic 46:303-311

Dagg M, Benner R, Lohrenz S, Lawrence D (2004) Transformation of dissolved and particulate materials on continental shelves influenced by large rivers: plume processes. Cont Shelf Res 24:833-858

Dale T, Rey F, Heimdal BR (1999) Seasonal development of phytoplankton at a high latitude oceanic site. Sarsia 84:419-435

Daly KL, Wallace DWR, Smith WO, Skoog A, Lara R, Gosselin M, Falck E, Yager PL (1999) Non-Redfield carbon and nitrogen cycling in the Arctic: effects of ecosystem structure and dynamics. J Geophys Res 104:3185-3199

Dawson JK (1978) Vertical distribution of *Calanus hyperboreus* in the central Arctic Ocean. Limnol Oceanogr 23:950-957

Dickson R, Rudels B, Dye S, Karcher M, Meincke J, Yashayaev I (2007) Current estimates of freshwater flux through Arctic and subarctic seas. Prog Oceanogr 73:210-230

Dittmar T, Kattner G (2003) The biogeochemistry of the river and shelf ecosystem of the Arctic Ocean: a review. Mar Chem 83:103-120

Engel A (2003) Distribution of transparent exopolymer particles (TEP) in the northeast Atlantic Ocean and their potential significance for aggregation processes. Deep-Sea Res I 51:83-92

Engel A, Passow U (2001) Carbon and nitrogen content of transparent exopolymer particles (TEP) in relation to their Alcian Blue adsorption. Mar Ecol Prog Ser 219:1-10

Field JG, Clarke KR, Warwick RM (1982) A practical strategy for analysing multispecies distribution patterns. Mar Ecol Prog Ser 8:37-52

Fong DA, Geyer WR (2002) The alongshore transport of freshwater in a surface-trapped river plume. J Phys Oceanogr 32:957-972

Forest A, Sampei M, Hattori H, Makabe R, Sasaki H, Fukuchi M, Wassmann P, Fortier L (2007) Particulate organic carbon fluxes on the slope of the Mackenzie Shelf (Beaufort Sea): Physical and biological forcing of shelf-basin exchanges. J Mar Sys 68:39-54

Fortier M, Fortier L, Michel C, Legendre L (2002) Climatic and biological forcing of the vertical flux of biogenic particles under seasonal Arctic sea ice. Mar Ecol Prog Ser 225:1-16

Frost BW (1972) Effects of size and concentrations of food particles on the feeding behavior of the marine planktonic copepod *Calanus pacificus*. Limnol Oceanogr 17:805-815

Gardner WD (1980) Field assessment of sediment traps. J Mar Res 38:41-52

Gardner WD (2000) Sediment trap sampling in surface waters: issues and recommendations. In: Hanson RB, Ducklow HW, Field JG (eds) The changing ocean carbon cycle: a midterm synthesis of the Joint Global Ocean Flux Study. Cambridge University Press, Cambridge, p 240-281

Garneau M-È, Vincent WF, Alonso-Sáez L, Gratton Y, Lovejoy C (2006) Prokaryotic community structure and heterotrophic production in a river-influenced coastal arctic ecosystem. Aquat Microb Ecol 42:27-40

Garrison DL, Close AR, Reimnitz E (1989) Algae concentrated by frazil ice: evidence from laboratory experiments and field measurements. Antarct Sci 1:313-316

González HE, González SR, Brummer G-JA (1994) Short-term sedimentation pattern of zooplankton, faeces and microplankton at a permanent station in the Bjørnafjorden (Norway) during April-May 1992. Mar Ecol Prog Ser 105:31-45

Gordeev VV, Rachold V (2004) River input. In: Stein R, Macdonald RW (eds) The organic carbon cycle in the Arctic Ocean. Springer, Berlin, p 33-41

Gosselin M, Legendre L, Therriault JC, Demers S, Rochet M (1986) Physical control of the horizontal patchiness of sea-ice microalgae. Mar Ecol Prog Ser 29:289-298

Gosselin M, Legendre L, Therriault J-C, Demers S (1990) Light and nutrient limitation of sea-ice microalgae (Hudson Bay, Canadian Arctic). J Phycol 26:220-232

Gosselin M, Levasseur M, Wheeler PA, Horner RA, Booth BC (1997) New measurements of phytoplankton and ice algae production in the Arctic Ocean. Deep-Sea Res II 44:1623-1644

Gradinger R (1999) Vertical fine structure of the biomass and composition of algal communities in Arctic pack ice. Mar Biol 133:745-754

Gradinger R, Ikävalko J (1998) Organism incorporation into newly forming Arctic sea in the Greenland Sea. J Plankton Res 20:871-886

Grebmeier JM, Cooper LW, Feder HM, Sirenko BI (2006) Ecosystem dynamics of the Pacific-influenced Northern Bering and Chukchi Seas in the Amerasian Arctic. Prog Oceanogr 71:331-361

Grossart H-P, Simon M (2007) Interactions of planktonic algae and bacteria: effects on algal growth and organic matter dynamics. Aquat Microb Ecol 47:163-176

Grossart H-P, Kiørboe T, Tang KW, Allgaier M, Yam EM, Ploug H (2006) Interactions between marine snow and heterotrophic bacteria: aggregate formation and microbial dynamics. Aquat Microb Ecol 42:19-26

Hamm CE (2002) Interactive aggregation and sedimentation of diatoms and clay-sized lithogenic material. Limnol Oceanogr 47:1790-1795

Hargrave BT, Burns NM (1979) Assessment of sediment trap collection efficiency. Limnol Oceanogr 24:1124-1136

Hargraves PE, French FW (1983) Diatom resting spores: Significance and strategies. In: Fryxell, G.A. (ed) Survival strategies of the algae. Cambridge University Press, New York, p 49-68

Hattori H, Saito H (1997) Diel changes in vertical distribution and feeding activity of copepods in ice-covered Resolute Passage, Canadian Arctic, in spring 1992. J Mar Syst 11:205-219

Head EJH, Harris LR, Campbell RW (2000) Investigations on the ecology of *Calanus* spp. in the Labrador Sea. I. Relationship between the phytoplankton bloom and reproduction and development of *Calanus finmarchicus* in spring. Mar Ecol Prog Ser 193:53-73

Heiskanen A-S, Keck A (1995) Distribution and sinking rates of phytoplankton, detritus, and particulate biogenic silica in the Laptev Sea and Lena River (Arctic Siberia). Mar Chem 53:229-245

Hill V, Cota G (2005) Spatial patterns of primary production on the shelf, slope and basin of the Western Arctic in 2002. Deep-Sea Res II 52:3344-3354

Hill V, Cota G, Stockwell D (2005) Spring and summer phytoplankton communities in the Chukchi and Eastern Beaufort Seas. Deep-Sea Res II 52:3369-3385

Hirche H-J (1997) Life cycle of the copepod *Calanus hyperboreus* in the Greenland Sea. Mar Biol 128:607-618

Hirche H-J (1998) Dormancy in three *Calanus* species (*C. finmarchicus*, *C. glacialis* and *C. hyperboreus*) from the North Atlantic. Arch Hydrobiol Spec Issues Advanc Limnol 52:359-369

Hirche H-J, Kosobokova K (2003) Early reproduction and development of dominant calanoid copepods in the sea ice zone of the Barents Sea - need for a change of paradigms? Mar Biol 143:769-781

Hirche H-J, Mumm N (1992) Distribution of dominant copepods in the Nansen basin, Arctic Ocean, in summer. Deep-Sea Res I 39:485-505

Hoppe H-G, Ducklow H, Karrasch B (1993) Evidence for dependency of bacterial growth on enzymatic hydrolysis of particulate organic matter in the mesopelagic ocean. Mar Ecol Prog Ser 93:277-283

Horner R, Schrader GC (1982) Relative contributions of ice algae, phytoplankton and benthic microalgae to primary production in nearshore regions of the Beaufort Sea. Arctic 35:485-503

Hsiao SIC (1987) Sedimentation in Arctic Canada: Species composition and biomass of phytoplankton contributed to the marine sediments in Frobisher Bay. Polar Biol 7:245-251

Hsiao SIC (1992) Dynamics of ice algae and phytoplankton in Frobisher Bay. Polar Biol 12:645-651

IPCC (2007) Climate change 2007: The physical science basis. Contribution of Working Group I to the Fourth Assessment Report of the Intergovernmental Panel on Climate Change. Cambridge University Press, Cambridge and New York

Jakobsson M (2002) Hypsometry and volume of the Arctic Ocean and its constituent seas. Geochem Geophys Geosyst 3, 1028, doi:10.1029/2001GC000302

Johannessen OM, Bengtsson L, Miles MW, Kuzmina SI, Semenov VA, Alekseev GV, Nagurnyi AP, Zakharov VF, Bobylev LP, Pettersson LH, Hasselmann K, Cattle HP (2004) Arctic climate change: observed and modelled temperature and sea-ice variability. Tellus 56:328-341

Juul-Pedersen T, Nielsen TG, Michel C, Møller EF, Tiselius P, Thor P, Olesen M, Selander E, Gooding S (2006) Sedimentation following the spring bloom in Disko Bay, West Greenland, with special emphasis on the role of copepods. Mar Ecol Prog Ser 314:239-255

Kerr RA (1999) Will the Arctic Ocean lose all its ice? Science 286:1828

Kiørboe T (2001) Formation and fate of marine snow: small-scale processes with large-scale implications. Sci Mar 65:57-71

Kiørboe T, Hansen JLS, Allredge AL, Jackson GA, Passow U, Dam HG, Drapeau DT, Waite A, Garcia CM (1996) Sedimentation of phytoplankton during a diatom bloom: Rates and mechanisms. J Mar Res 54:1123-1148

Klein B, LeBlanc B, Mei ZP, Beret R, Michaud J, Mundy C-J, von Quillfeldt CH, Garneau M-È, Roy S, Gratton Y, Cochran JK, Bélanger S, Larouche P, Pakulski JD, Rivkin RB, Legendre L (2002) Phytoplankton biomass, production and potential export in the North Water. Deep-Sea Res II 49:4983–5002

Knap A, Michaels A, Close A, Ducklow H, Dickson A (1996) Protocols for the Joint Global Ocean Flux Study (JGOFS) Core Measurements JGOFS Report Nr. 19. Reprint of the IOC Manuals and Guides No. 29, UNESCO, Bergen

Köberle C, Gerdes R (2007) Simulated variability of the Arctic Ocean freshwater balance 1948-2001. J Phys Oceanogr 37:1628-1644

Lalande C, Grebmeier JM, Wassmann P, Cooper LW, Flint MV, Sergeeva VM (2007) Export fluxes of biogenic matter in the presence and absence of seasonal sea ice cover in the Chukchi Sea. Cont Shelf Res 27:2051-2065

Landry MR, Hassett RP, Fagerness V, Downs J, Lorenzen CJ (1984) Effect of food acclimation on assimilation efficiency of *Calanus pacificus*. Limnol Oceanogr 29:361-364

Lavoie D, Denman K, Michel C (2005) Modelling ice algal growth and decline in a seasonally ice-covered region of the Arctic (Resolute Passage, Canadian Archipelago). J Geophys Res 110, C11009, doi:10.1029/2005JC002922

Lee S, Fuhrman JA (1987) Relationships between biovolume and biomass of naturally derived marine bacterioplankton. Appl Environ Microbiol 53:1298-1303

Lean DRS, Burnison BK (1979) An evaluation of errors in the ^{14}C method of primary measurement. Limnol Oceanogr 24:917-928

Legendre P, Legendre L (1998) Numerical ecology, 2nd edn. Elsevier Science BV, Amsterdam

Legendre L, Ackley SF, Dieckmann GS, Gulliksen B, Horner R, Hoshiai T, Melnikov IA, Reeburgh WS, Spindler M, Sullivan CW (1992) Ecology of sea ice biota. 2 Global significance. Polar Biol 12:429-444

Lorenzen CJ (1968) Carbon/chlorophyll relationships in an upwelling area. Limnol Oceanogr 13:202-204

Long RA, Azam F (1996) Abundant protein-containing particles in the sea. Aquat Microb Ecol 10:213-221

Lovejoy C, Legendre L, Martineau M-J, Bâcle J, von Quillfeldt CH (2002) Distribution of phytoplankton and other protists in the North Water. Deep-Sea Res II 49:5027-5047

Lukovich JV, Barber DG (2005) On sea ice concentration anomaly coherence in the southern Beaufort Sea. Geophys Res Lett 32, L10705, doi:10.1029/2005GL022737

Lund JWG, Kipling C, Le Cren ED (1958) The inverted microscope method of estimating algal numbers and the statistical analysis of estimations by counting. Hydrobiologia 11:143-170

Macdonald RW, Solomon SM, Cranston RE, Welch HE, Yunker MB, Gobeil C (1998) A sediment and organic carbon budget for the Canadian Beaufort Sea. Mar Geol 144:255-273

Madsen SD, Nielsen TG, Hansen BW (2001) Annual population development and production by *Calanus finmarchicus*, *C. glacialis* and *C. hyperboreus* in Disko Bay, western Greenland. Mar Biol 139:75-93

Martin JH, Knauer GA, Karl DM, Broenkow WW (1987) VERTEX: carbon cycling in the northeastern Pacific. Deep-Sea Res 34:267-285

McMahon KW, Ambrose WG Jr, Johnson BJ, Sun M-Y, Lopez GR, Clough LM, Carroll ML (2006) Benthic community response to ice algae and phytoplankton in Ny Ålesund, Svalbard. Mar Ecol Prog Ser 310:1-14

McPhee-Shaw E (2006) Boundary-interior exchange: Reviewing the idea that internal-wave mixing enhances lateral dispersal near continental margins. Deep-Sea Res II 53:42-59

Mei Z-P, Legendre L, Gratton Y, Tremblay J-É, LeBlanc B, Klein B, Gosselin M (2003) Phytoplankton production in the North Water Polynya: size–fractions and carbon fluxes, April to July 1998. Mar Ecol Prog Ser 256:13-27

Melnikov IA (1998) Winter production of sea ice algae in the western Weddell Sea. J Mar Syst 17:195-205

Michel C, Legendre L, Ingram RG, Gosselin M, Levasseur M (1996) Carbon budget of sea-ice algae in spring: Evidence of a significant transfer to zooplankton grazers. J Geophys Res 101:18345-18360

Michel C, Legendre L, Demers S, Therriault J-C (1998) Photoadaptation of sea-ice microalgae in springtime: photosynthesis and carboxylating enzymes. Mar Ecol Prog Ser 50:177-185

Michel C, Gosselin M, Nozais C (2002) Preferential sinking export of biogenic silica during the spring and summer in the North Water Polynya (northern Baffin Bay): Temperature or biological control? J Geophys Res 107, C7, doi:10.1029/2002JC000408

Michel C, Nielsen TG, Nozais C, Gosselin M (2002) Significance of sedimentation and grazing by ice micro- and meiofauna for carbon cycling in annual sea ice (northern Baffin Bay). Aquat Microb Ecol 30:57-68

Michel C, Ingram RG, Harris LR (2006) Variability in oceanographic and ecological processes in the Canadian Arctic Archipelago. Prog Oceanogr 71:379-401

Mundy CJ, Barber DG, Michel C (2005) Variability of snow and ice thermal, physical and optical properties pertinent to sea ice algae biomass during spring. J Mar Syst 58:107-120

Møller EF, Nielsen TG (2001) Production of bacterial substrate by marine copepods: Effects of phytoplankton biomass and cell size. J Plankton Res 23:527-536

Møller EF, Thor P, Nielsen TG (2003) Production of DOC by *Calanus finmarchicus*, *C. glacialis* and *C. hyperboreus* through sloppy feeding and leakage from faecal pellets. Mar Ecol Prog Ser 262:185-191

Nozais C, Gosselin M, Michel C, Tita G (2001) Abundance, biomass, composition and grazing impact of the sea-ice meiofauna in the North Water, northern Baffin Bay. Mar Ecol Prog Ser 217:235-250

O'Brien MC, Macdonald RW, Melling H, Iseki K (2006) Particle fluxes and geochemistry on the Canadian Beaufort Shelf: Implications for sediment transport and deposition. Cont Shelf Res 26:41-81

Olli K, Riser CW, Wassmann P, Rat'kova T, Arashkevich E, Pasternak A (2002) Seasonal variation in vertical flux of biogenic matter in the marginal ice zone and the central Barents Sea. J Mar Syst 38:189-204

Oreskes N (2004) Beyond the ivory tower: The scientific consensus on climate change. Science 306:1686

Pagona M, Gaudy R, Thibault D, Lochet F (1993) Vertical migrations and feeding rhythms of mesozooplanktonic organisms in the Rhone River plume area (North-west Mediterranean Sea). Est Coast Shelf Sci 37:251-269

Parsons TR, Maita Y, Lalli CM (1984) A manual of chemical and biological methods for seawater analysis. Pergamon Press, Toronto

Parsons TR, Webb DG, Dovey H, Haigh R, Lawrence M, Hopky GE (1988) Production studies in the Mackenzie River - Beaufort Sea Estuary. Polar Biol 8:235-239

Parsons TR, Webb DG, Rokeby BE, Lawrence M, Hopky GE, Chiperzak DB (1989) Autotrophic and heterotrophic production in the Mackenzie River/Beaufort Sea Estuary. Polar Biol 9:261-266

Pasternak A, Riser CW, Arashkevich E, Rat'kova T, Wassmann P (2002) *Calanus* spp. grazing affects egg production and vertical carbon flux (the marginal ice zone and open Barents Sea). J Mar Syst 38:147-164

Penry DL, Frost BW (1991) Chlorophyll *a* degradation by *Calanus pacificus*: Dependence on ingestion rate and digestive acclimation to food resources. Limnol Oceangr 36:147-159

Peterson BJ, Holmes RM, McClelland JW, Vörösmarty CJ, Lammers RB, Shiklomanov AI, Shiklomanov IA, Rahmstorf S (2002) Increasing river discharge to the Arctic Ocean. Science 298:2171-2173

Pickart RS (2004) Shelfbreak circulation in the Alaskan–Beaufort Sea: Mean structure and variability. J Geophys Res 109, C04024, doi:10.1029/2003JC001912

Radić T, Ivančić I, Fuks D, Radić J (2006) Marine bacterioplankton production of polysaccharide and proteinaceous particles under different nutrient regimes. FEMS Microbiol Ecol 58:333-342

Ragueneau O, Tréguer P (1994) Determination of biogenic silica in coastal waters: applicability and limits of the alkaline digestion method. Mar Chem 45:43-51

Rat'kova TN, Wassmann P (2002) Seasonal variation and spatial distribution of phyto- and protozooplankton in the central Barents Sea. J Mar Syst 38:47-75

Rat'kova TN, Wassmann P, Verity P, Andreassen IJ (1998) Abundance and biomass of pico-, nano-, and microplankton on a transect across Nordvestbanken, north Norwegian shelf, in 1994. Sarsia 84:213-225

Redfield AC, Ketchum BH, Richards FA (1963) The influence of organisms on the composition of sea water. In: Hill MN (ed) The sea. Wiley, New York, p 26-77

Renaud PE, Morata N, Ambrose WG Jr, Bowie JJ, Chiuchiolo A (2007a) Carbon cycling by seafloor communities on the eastern Beaufort Sea shelf. J Exp Mar Biol Ecol 349:248-260

Renaud PE, Riedel A, Michel C, Morata N, Gosselin M, Juul-Pedersen T, Chiuchiolo A (2007b) Seasonal variation in benthic community oxygen demand: A response to an ice algal bloom in the Beaufort Sea, Canadian Arctic? J Mar Syst 67:1-12

Richter C (1995) Seasonal changes in the vertical distribution of mesozooplankton in the Greenland Sea Gyre (75°N): distribution strategies of calanoid copepods. ICES J Mar Sci 52:533-539

Riebesell U, Schloss I, Smetacek V (1991) Aggregation of algae released from melting sea ice: implications for seeding and sedimentation. Polar Biol 11:239-248

Riebesell U, Reigstad M, Wassmann P, Noji T, Passow U (1995) On the trophic fate of *Phaeocystis pouchetii* (Hariot): VI. Significance of *Phaeocystis*-derived mucus for vertical flux. Neth J Sea Res 33:193-203

Riedel A, Michel C, Gosselin M (2006) Seasonal study of sea-ice exopolymeric substances (EPS) on the Mackenzie Shelf: Implications for the transport of sea-ice bacteria and algae. Aquat Microb Ecol 45:195-206

Riedel A, Michel C, Gosselin M, LeBlanc B (2007) Enrichment of nutrients, exopolymeric substances and microorganisms in newly formed sea ice on the Mackenzie shelf. Mar Ecol Prog Ser 342:55-67

Ringuette M, Fortier L, Fortier M, Runge JA, Bélanger S, Larouche P, Weslawski J-M, Kwasniewski S (2002) Advanced recruitment and accelerated population development in Arctic calanoid copepods of the North Water. Deep-Sea Res II 49:5081-5099

Riser CW, Wassmann P, Olli K, Pasternak A, Arashkevich E (2002) Seasonal variation in production, retention and export of zooplankton faecal pellets in the marginal ice zone and central Barents Sea. J Mar Syst 38:175-188

Riser CW, Reigstad M, Wassmann P, Arashkevich E, Falk-Petersen S (2007) Export or retention? Copepod abundance, faecal pellet production and vertical flux in the marginal ice zone through snap shots from the northern Barents Sea. Polar Biol 30:719-730

Runge JA, Ingram RG (1988) Underice grazing by planktonic, calanoid copepods in relation to a bloom of ice microalgae in southeastern Hudson Bay. Limnol Oceanogr 33:280-286

Sakshaug E (2004) Primary and secondary production in the Arctic Seas. In: Stein R, Macdonald RW (eds) The organic carbon cycle in the Arctic Ocean. Springer, Berlin, p 57-82

Sakshaug E, Skjoldal HR (1989) Life at the ice edge. Ambio 18:60-67

Sampei M, Sasaki H, Hattori H, Fukuchi M, Hargrave BT (2004) Fate of sinking particles, especially fecal pellets, within the epipelagic zone in the North Water (NOW) polynya of northern Baffin Bay. Mar Ecol Prog Ser 278:17-25

Sarmiento JL, Gruber N (2006) Ocean biogeochemical dynamics. Princeton University Press, New Jersey

Schnack-Shiel SB, Isla E (2005) The role of zooplankton in the pelagic-benthic coupling of the Southern Ocean. Sci Mar 69:39-55

Seuthe L, Danis G, Riser CW, Wassmann P, Fortier L (2007) Winter-spring feeding and metabolism of Arctic copepods: insights from faecal pellet production and respiration measurements in the southeastern Beaufort Sea. Polar Biol 30:427-436

Shiklomanov IA (1998) Comprehensive assessment of the freshwater resources of the world: Assessment of water resources and water availability in the world. Stockholm Environment Institute, Stockholm

Simpson KG, Tremblay J-É, Gratton Y, Price NM (ms) An annual study on nutrient distribution in the south-eastern Beaufort Sea, Mackenzie Shelf and Amundsen Gulf

Smith DC, Simon M, Alldredge AL, Azam F (1992) Intense hydrolytic enzyme activity on marine aggregates and implications for rapid particle dissolution. Nature 359:139-142

Smith DC, Steward GF, Long RA, Azam F (1995) Bacterial mediation of carbon fluxes during a diatom bloom in a mesocosm. Deep-Sea Res II 42:75-79

Smith REH, Harrison WG, Harris LR, Herman AW (1990) Vertical fine structure of particulate matter and nutrients in sea ice of the high Arctic. Can J Fish Aquat Sci 47:1348-1355

Sokal RR, Rohlf FJ (1981) Biometry: the principles and practice of statistics in biological research, 2nd edn. WH Freeman, San Francisco

Springer AM, McRoy CP (1993) The paradox of pelagic food webs in the northern Bering Sea. 3. Patterns of primary production. Cont Shelf Res 13:575-599

Stein R, Macdonald RW (2004) The organic carbon cycle in the Arctic Ocean. Springer-Verlag, New York

Stramski D, Sciandra A, Claustre H (2002) Effects of temperature, nitrogen, and light limitation on the optical properties of the marine diatom *Thalassiosira pseudonana*. Limnol Oceanogr 47:392-403

Strass VH, Nöthig E-M (1996) Seasonal shifts in ice edge phytoplankton blooms in the Barents Sea related to the water column stability. Polar Biol 16:409-422

Strom SL, Benner R, Ziegler S, Dagg MJ (1997) Planktonic grazers are a potentially important source of marine dissolved organic carbon. Limnol Oceanogr 42:1364-1374

Subba Rao DV, Platt T (1984) Primary production of Arctic waters. Polar Biol 3:191-201

Suttle CA (2005) Viruses in the sea. Nature 437:356-361

Taguchi S, Saito H, Kasai H (1993) Effect of shape of sediment trap on measurement of vertical flux of particles: Preliminary results. Proc NIPR Symp Polar Biol 6:1-5

Tremblay C, Runge JA, Legendre L (1989) Grazing and sedimentation of ice algae during and immediately after a bloom at the ice-water interface. Mar Ecol Prog Ser 56:291-300

Tremblay J-É, Gratton Y, Carmack EC, Payne CD, Price NM (2002a) Impact of the large-scale Arctic circulation and the North Water Polynya on nutrient inventories in Baffin Bay. J Geophys Res 107, C8, 3112, doi:10.1029/2000JC000595

Tremblay J-É, Gratton Y, Fauchot J, Price NM (2002b) Climatic and oceanic forcing of new, net, and diatom production in the North Water. Deep-Sea Res II 49:4927-4946

Tremblay J-É, Hattori H, Michel C, Ringuette M, Mei Z-P, Lovejoy C, Fortier L, Hobson KA, Amiel D, Cochran K (2006a) Trophic structure and pathways of biogenic carbon flow in the eastern North Water Polynya. Prog Oceanogr 71:402-425

Tremblay J-É, Michel C, Hobson KA, Gosselin M, Price NM (2006b) Bloom dynamics in early opening waters of the Arctic Ocean. Limnol Oceanogr 51:900-912

Turner JT (2002) Zooplankton fecal pellets, marine snow and sinking phytoplankton blooms. Aquat Microb Ecol 27:57-102

Urban JL, McKenzie CH, Deibel D (1992) Seasonal differences in the content of *Oikopleura vanhoeffeni* and *Calanus finmarchicus* faecal pellets: illustrations of zooplankton food web shifts in coastal Newfoundland waters. Mar Ecol Prog Ser 84:255-264

Urban-Rich J, Nordby E, Andreassen IJ, Wassmann P (1999) Contribution by mesozooplankton fecal pellets to the carbon flux on Nordvestbanken north Norwegian shelf in 1994. Sarsia 84:253-264

von Quillfeldt CH (2004) The diatom *Fragilariopsis cylindrus* and its potential as an indicator species for cold water rather than for sea ice. Vie Milieu 54:137-143

von Quillfeldt CH, Ambrose WG Jr, Clough LM (2003) High number of diatom species in first-year ice from the Chukchi Sea. Polar Biol 26:806-818

Vrede K, Heldal M, Norland S, Bratbak G (2002) Elemental composition (C, N, P) and cell volume of exponentially growing and nutrient-limited bacterioplankton. Appl Environ Microbiol 68:2965-2971

Wassmann P (1989) Sedimentation of organic matter and silicate from the euphotic zone of the Barents Sea. Rapp P-v Réun Cons Int Explor Mer 188:108-114

Wassmann P (1998) Retention versus export food chains: processes controlling sinking loss from marine pelagic systems. Hydrobiologia 363:29-57

Wassmann P, Vernet M, Mitchell BG, Rey F (1990) Mass sedimentation of *Phaeocystis pouchetii* in the Barents Sea. Mar Ecol Prog Ser 66:183-195

Wassmann P, Bauerfeind E, Fortier M, Fukuchi M, Hargrave B, Moran B, Noji T, Nöthig E-M, Olli K, Peinert R, Sasaki H, Shevchenko V (2004) Particulate organic carbon flux to the Arctic Ocean sea floor. In: Stein R, Macdonald RW (eds) The organic carbon cycle in the Arctic Ocean. Springer, Berlin, p 101-138

Wassmann P, Reigstad M, Haug T, Rudels B, Carroll ML, Hop H, Gabrielsen GW, Falk-Petersen S, Denisenko SG, Arashkevich E, Slagstad D, Pavlova O (2006) Food webs and carbon flux in the Barents Sea. Prog Oceanogr 71:232-287

Wells LE, Cordray M, Bowerman S, Miller LA, Warwick FV, Deming JW (2006) Archaea in particle-rich waters of the Beaufort Shelf and Franklin Bay, Canadian Arctic: Clues to an allochthonous origin? Limnol Oceanogr 51:47-59

Welschmeyer NA, Lorenzen CJ (1985) Chlorophyll budgets: Zooplankton grazing and phytoplankton growth in a temperate fjord and the Central Pacific Gyres. Limnol Oceanogr 30:1-21

Werner I (2000) Faecal pellet production by Arctic under-ice amphipods – transfer of organic matter through the ice/water interface. Hydrobiologia 426:89-96

White J (1990) The use of sediment traps in high-energy environments. Mar Geophys Res 12:145-152